AD_____

Award Number: W81XWH-**06-1-0303**

TITLE: BATTLE (Biomarker-based Approach of Targeted Therapy for Lung Cancer Elimination)

PRINCIPAL INVESTIGATOR:
Waun Ki Hong, M.D.
Roy Herbst, M.D., Ph.D.
Edward Kim, M.D.

CONTRACTING ORGANIZATION:
The University of Texas M. D. Anderson Cancer Center
Houston, TX 77030

REPORT DATE: April 2010

TYPE OF REPORT: Annual

PREPARED FOR: U.S. Army Medical Research and Materiel Command
Fort Detrick, Maryland 21702-5012

DISTRIBUTION STATEMENT:

X Approved for public release; distribution unlimited

The views, opinions and/or findings contained in this report are those of the author(s) and should not be construed as an official Department of the Army position, policy or decision unless so designated by other documentation.

# REPORT DOCUMENTATION PAGE

*Form Approved*
*OMB No. 0704-0188*

Public reporting burden for this collection of information is estimated to average 1 hour per response, including the time for reviewing instructions, searching existing data sources, gathering and maintaining the data needed, and completing and reviewing this collection of information. Send comments regarding this burden estimate or any other aspect of this collection of information, including suggestions for reducing this burden to Department of Defense, Washington Headquarters Services, Directorate for Information Operations and Reports (0704-0188), 1215 Jefferson Davis Highway, Suite 1204, Arlington, VA 22202-4302. Respondents should be aware that notwithstanding any other provision of law, no person shall be subject to any penalty for failing to comply with a collection of information if it does not display a currently valid OMB control number. **PLEASE DO NOT RETURN YOUR FORM TO THE ABOVE ADDRESS.**

| **1. REPORT DATE** *(DD-MM-YYYY)* | **2. REPORT TYPE** | **3. DATES COVERED** *(From - To)* |
|---|---|---|
| 01-04-2010 | Annual | 1 APR 2009 - 31 MAR 2010 |

**4. TITLE AND SUBTITLE**
BATTLE (Biomarker-based Approach of Targeted Therapy for Lung Cancer Elimination)

**5a. CONTRACT NUMBER**

**5b. GRANT NUMBER**
W81XWH-06-1-0303

**5c. PROGRAM ELEMENT NUMBER**

**6. AUTHOR(S)**
Waun Ki Hong, M.D.

Roy Herbst, M.D., Ph.D.; Edward Kim, M.D.

**5d. PROJECT NUMBER**

**5e. TASK NUMBER**

**5f. WORK UNIT NUMBER**

**7. PERFORMING ORGANIZATION NAME(S) AND ADDRESS(ES)**
The University of Texas M.D. Anderson Cancer Center
Houston, TX 77030

**8. PERFORMING ORGANIZATION REPORT NUMBER**

**9. SPONSORING / MONITORING AGENCY NAME(S) AND ADDRESS(ES)**
U.S. Army Medical Research and Materiel Command
Fort Detrick, Maryland 21702-5012

**10. SPONSOR/MONITOR'S ACRONYM(S)**

**11. SPONSOR/MONITOR'S REPORT NUMBER(S)**

**12. DISTRIBUTION / AVAILABILITY STATEMENT**
Approved for public release; distribution unlimited

**13. SUPPLEMENTARY NOTES**

**14. ABSTRACT**
The Program BATTLE seeks to establish individualized targeted therapy by prospectively examining patients' tumor biomarker profiles and assigning them to corresponding targeted therapies with the expectation to yield a better clinical outcome. Based on common altered signaling pathways in lung cancer, the BATTLE Program proposes to develop four phase II trials for chemorefractory, advanced NSCLC patients: erlotinib, ZD6474, bexarotene with erlotinib, and sorafenib which target, respectively, EGFR, VEGF / VEGFR, retinoid X receptor and cyclin D1, and Ras / Raf signaling pathways. A novel adaptive randomization statistical design will be applied to the clinical trials to accelerate the identification of best-fit treatment for patients. We propose also to study the molecular mechanisms of response or resistance to these targeted agents, identify novel molecular features in tumors and surrogate tissues to correlate with tumor response or resistance to the agents and, finally, explore other novel targeted agents (RAD001 and perifosine) in combination and their mechanisms of action by targeting mTOR and PI3K/Akt signaling, and develop phase I trials to

**15. SUBJECT TERMS**
Lung cancer, biomarker, targeted therapy, ZD6474, erlotinib, Sorafenib, bexarotene.

| **16. SECURITY CLASSIFICATION OF:** | | | **17. LIMITATION OF ABSTRACT** | **18. NUMBER OF PAGES** | **19a. NAME OF RESPONSIBLE PERSON** |
|---|---|---|---|---|---|
| U | | | | | USAMRMC |
| **a. REPORT** | **b. ABSTRACT** | **c. THIS PAGE** | UU | 116 | **19b. TELEPHONE NUMBER** *(include area code)* |
| U | U | U | | | |

## TABLE OF CONTENTS

## INTRODUCTION

Lung cancer is the leading cause of cancer-related death in both men and women in the United States. Chemotherapy has reached its limit in improving the survival of lung cancer patients. Therefore, a different strategy must be waged in the battle against lung cancer. Targeted therapy, a newly emerged therapeutic approach in lung cancer, has succeeded in some cancer types and demonstrated its initial success in the treatment of lung cancer when a class of targeted agents termed epidermal growth factor receptor (EGFR) tyrosine kinase inhibitors, such as gefitinib and erlotinib, improved tumor response rates in patients with advanced non-small cell lung cancer (NSCLC), which was strongly correlated to the presence of *EGFR* mutations in the tumors (Cappuzzo and Hirsch et al., 2004; Cappuzzo and Magrini et al., 2004; Gatzemeier et al., 2004; Herbst and Giaccone et al., 2004; Herbst and Prager et al., 2004; Herbst and Sandler et al., 2004; Lynch et al., 2004; Kobayashi et al., 2005; Miller et al., 2004; Pao et al., 2004; Paez et al., 2004; Shepherd et al., 2004; Shigematsu et al., 2005). This has for the first time demonstrated the importance of selecting patients for individualized targeted therapy in NSCLC.

The Program **BATTLE** (**B**iomarker-integrated **A**pproaches of **T**argeted **T**herapy for **L**ung Cancer **E**limination) seeks to establish individualized targeted therapy by prospectively examining patients' tumor biomarker profiles and assigning them to corresponding targeted therapies with the expectation to yield a better clinical outcome. This novel approach will be a proof-of-principle experiment to test the benefit of molecular-based individualized targeted therapy for lung cancer patients. Specifically, the objectives of the BATTLE program are:

1) To establish a clinical trial program using biomarkers to select individualized targeted therapy for patients with chemorefractory advanced NSCLC through the implementation of molecular classification based on the status of specific targeted biomarkers and adaptive randomization via hierarchical Bayes modeling.
2) To study the molecular mechanisms of response and resistance to targeted agents to discover new signaling pathways for test in future trials.
3) To identify molecular features in tumor tissues to correlate with tumor response or resistance, and identify serum biomarkers as surrogates.
4) To investigate other targeted agents in combination to overcome the resistance due to novel signaling pathways (e.g., mTOR and PI3K/Akt) and improve treatment efficacy.

BATTLE is composed of four Specific Aims with four phase II clinical trials and an umbrella protocol in Aim 1, six research projects in Aims 2 - 4, and two potential phase I trials in Aim 4. Here, we present our scientific progress of the BATTLE program for in this fourth and final funded grant year.

## PROGRESS REPORT

### Aim 1 To establish a clinical trial program using biomarker assessment to select individualized targeted therapy for previously treated chemorefractory advanced NSCLC patients.

(PI, Co-PIs, and Investigators: Drs. Waun Ki Hong, Roy Herbst, Edward S. Kim, George Blumenschein, Anne Tsao, Hai Tran, Marshall Hicks, Rodolfo Morice, Bruce Johnson)

Specific Aim 1 has five clinical trials: one umbrella trial and four Phase II open-label trials. After screening, eligible patients are enrolled in the umbrella trial, and tumor biopsies are taken for

biomarker analysis conducted by the Biomarker Core. (For details, please see the Biomarker Core section of this report.) Biomarker results are analyzed by the Biostatistics and Data Management Core. (For details, please see the Biostatistics and Data Management Core section of this report.) There are two components of this study: 1) an equal randomization phase, where patients are randomized equally to the four trials after biomarker analysis; and 2) an adaptive randomization phase, where patients are enrolled to one of the four clinical trials based on their tumor biomarker characteristics. The four Phase II clinical trials are presented in the four sub-aims of Aim 1 described below and depicted in Figure 1. An update is provided following the list of subaims.

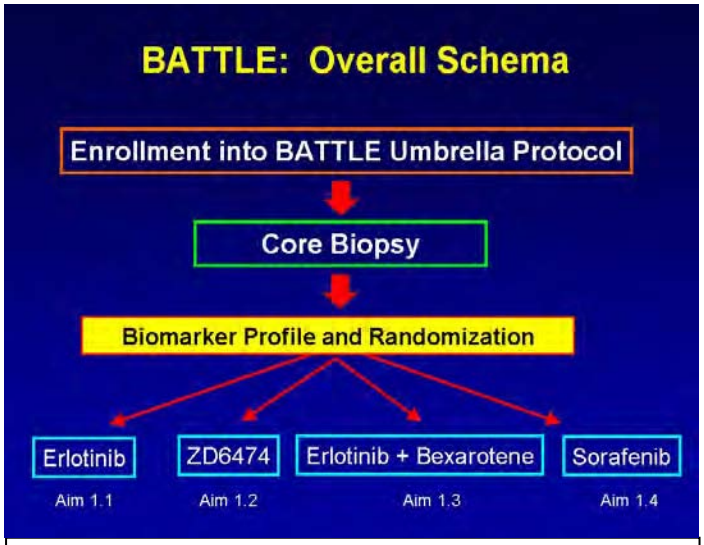


**Figure 1.** Overall Schema for BATTLE Trials.

**Aim 1.1 To conduct a clinical trial with erlotinib in patients with previously treated advanced NSCLC whose tumors have EGFR mutations and / or overrepresentation.**

**Primary objective** is to determine the 8-week progression-free survival (PFS) rate of patients with previously treated advanced NSCLC whose tumors have EGFR mutations and/or overrepresentation who are treated with erlotinib.

**Secondary objectives** are to 1) determine the overall survival rate, response rate, and toxicity profiles of patients with advanced NSCLC whose tumors have EGFR mutations and/or overrepresentation and treated with erlotinib, 2) determine the plasma and (if available) tumor tissue concentrations of erlotinib and their correlation with response and toxicity by using pharmacokinetics and pharmacodynamic modeling.

**Aim 1.2 To conduct a clinical trial with ZD6474 in patients with previously treated advanced NSCLC whose tumors have increased VEGF and / or VEGFR-2.**

**Primary objective** is to determine the 8-week PFS rate in patients with previously treated advanced NSCLC whose tumors have increased VEGF and / or VEGFR-2 who are treated with ZD6474.

**Secondary objectives** are to 1) determine the overall survival rate, response rates, and toxicity profiles of patients with advanced NSCLC whose tumors express increased VEGF and / or VEGFR-2 and treated with ZD6474, and 2) determine the plasma and (if available) tumor tissue levels of ZD6474 and their correlations with response and toxicity by using pharmacokinetics and pharmacodynamic modeling.

**Aim 1.3 To conduct a clinical trial with the combination of bexarotene and erlotinib trial in patients with previously treated advanced NSCLC whose tumors have expressed RXRs and / or increased cyclin D1.**

**Primary objective** is to determine the 8-week PFS rate in patients with previously treated advanced NSCLC whose tumors have expressed RXRs and / or increased cyclin D1 who are treated with the combination of Bexarotene and Erlotinib.

**Secondary objectives** are to 1) determine the overall survival rate, response rate, and toxicity profiles of patients with advanced NSCLC whose tumors have expressed RXRs and / or increased cyclin D1 and treated with the combination of bexarotene and erlotinib, 2) determine the plasma and (if available) tumor tissue concentrations of bexarotene and erlotinib and their correlation with response and toxicity by using pharmacokinetics and pharmacodynamic modeling.

**Aim 1.4 To conduct a clinical trial with sorafenib trial in patients with previously treated advanced NSCLC whose tumors have mutated *K-ras* and / or *B-raf.***

**Primary objective** is to determine the 8-week PFS rate in patients with previously treated advanced NSCLC whose tumors have mutant *K-ras* and / or *B-raf* who are treated with sorafenib.

**Secondary objectives** are to 1) determine the overall survival rate, response rate, and toxicity profiles of patients with advanced NSCLC whose tumors have mutated K-ras and / or B-raf and treated with sorafenib, 2) determine the plasma and (if available) tumor tissue concentrations of sorafenib and their correlation with response and toxicity by using pharmacokinetics and pharmacodynamic modeling.

**Summary of Research Findings**

Considering the highly interactive nature of the clinical trials in the BATTLE program, we will report the progress of the all the clinical trials in an integrated way.

We are pleased to report that we have successfully completed enrollment to the study as of October 2009 and, following sufficient follow-up time to assess the last patients accrued at 8-weeks to determine disease control, the data were unblinded in December 2009 for analysis of the primary and secondary endpoints.

As previously reported, the rates for both enrollment and randomization per month exceeded expectations, allowing completion of accrual in only 35 months. Due to the unexpectedly brisk accrual at the M. D. Anderson site, we deferred activating the trial at the planned second site, the Dana Farber Cancer Institute, and were able complete the study at this single site.

Thus, from November 2006 to October 2009, a total of 341 patients were enrolled on the trial and 255 patients were randomized to the following treatment arms: erlotinib (59 pts), vandetinib (54 pts), erlotinib and bexarotene (37 pts), sorafenib (105 pts). Demographics of the randomized patients are shown in Table 1.

| Table 1. BATTLE Patient Characteristics | |
|---|---|
| Age (Range) | 62 yrs (26-84) |
| Male / Female | 54% / 46% |
| Caucasian | 82% |
| Never / Current Smokers | 22% / 9% |
| ECOG PS 0 / 1 | 9% / 77% |
| Adenocarcinoma / Squamous | 63% / 18% |
| Prior Brain Metastases | 33% |
| Prior EGFR-TKI | 45% |
| Prior Docetaxel / Pemetrexed | 40% / 40% |
| Prior Systemic Therapy | 2 (1-6) |

A total of 244 patients were evaluable for 8-week disease control (DC). A total of 324 biopsies were obtained, and all 11 biomarkers were assessable in 270 (83%) patients. Biopsy sites yielding evaluable tissue included lung (55% of total biopsies), liver/adrenal (19%), and other (26%). Study treatments were generally well tolerated and the toxicities observed were consistent with known treatment toxicities from prior studies, (6.5% of all patients had treatment-related grade 3-4 toxicities). We were particularly concerned regarding the potential for pneumothorax from the lung biopsies; however, pneumothorax incidence in these patients was only 11.5% (16/139).

**Table 2 Biomarker results by marker group.**

| Table 2. Biomarker Results from BATTLE specimens | | | | |
|---|---|---|---|---|
| **Biomarker** | **Positive Cases** | | **Biomarker** | **Positive Cases** |
| *EGFR* mutation (exons 18-21) | 33 (15%) | | VEGF IHC | 191 (89%) |
| | | | VEGFR-2 IHC | 85 (40%) |
| *EGFR* FISH increased copy number: | | | RXR: | |
| -Gene amplification | 34 (16%) | | α (nuc) IHC | 173 (80%) |
| -- High polysomy | 60 (28%) | | α (cyt) IHC | 3 (1%) |
| | | | β (cyt) IHC | 12 (6%) |
| *KRAS* mutation (codons 12, 13, 61) | 42 (20%) | | γ (cyt) IHC | 23 (11%) |
| | | | Cyclin D1: IHC | 114 (54%) |
| *BRAF* mutation (exons 11 and 15) | 5 (2%) | | Cyclin D1 FISH amp | 27 (13%) |

The overall disease control rate (DCR) at 8 weeks was 46%, median overall survival (OS) was 9 months, 1 year survival was 39%, and progression-free survival (PFS) was 1.9 months. The curve shown in Figure 2 illustrates the clinical relevance of DCR and its correlation with OS.

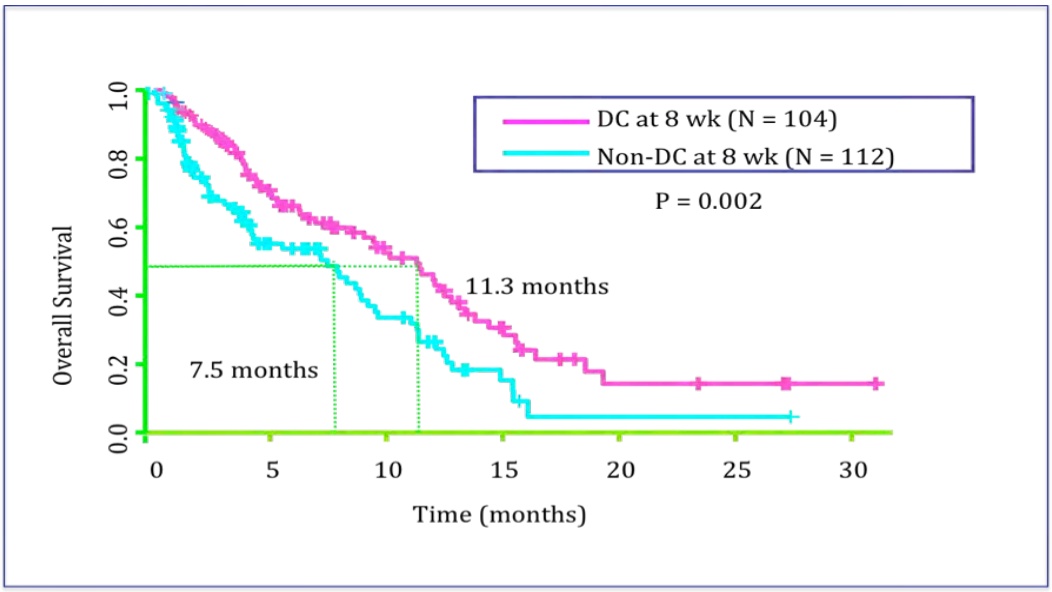


**Figure 2.** 8-week Disease Control Predicts Overall Survival

The DC achieved by marker group is shown in Table 3.

**Table 3.** BATTLE Results: Disease Control in % (n)

| Treatments | Marker Groups: *EGFR* | *KRAS* | VEGF | RXR/ CycD1 | None | Total |
|---|---|---|---|---|---|---|
| Erlotinib | 35% (17) | 14% (7) | 40% (25) | 0% (1) | 38% (8) | 34% (58) |
| Vandetanib | 41% (27) | 0% (3) | 38% (16) | NA (0) | 0% (6) | 33% (52) |
| Erlotinib + Bexarotene | 55% (20) | 33% (3) | 0% (3) | 100% (1) | 56% (9) | 50% (36) |
| Sorafenib | 39% (23) | 79% (14) | 64% (39) | 25% (4) | 61% (18) | 58% (98) |
| Total | 43% (87) | 48% (27) | 49% (83) | 33% (6) | 46% (41) | 46% (244) |

The study also revealed several biomarker associations with treatment outcomes. Better DC was seen in patients with *EGFR* mutations treated with erlotinib (p=0.04); with Cyclin D1 IHC positivity (IHC+) (p=0.011) and *EGFR* (FISH) amplification (p=0.006) treated with erlotinib and bexarotene; with VEGFR2 IHC+ treated with vandetinib (p=0.05); and with the absence of

*EGFR* mutation (p=0.012) or high polysomy (p=0.048) treated with sorafenib. Patients with both EGFR mutation and amplification (FISH) had 100% DC (n=6) when treated with erlotinib; in contrast, patients with these biomarkers had 0% DC (n=6) when treated with sorafenib. Patients with *KRAS* mutations tended to respond better when treated with sorafenib (8-wk DC: 61%) when compared to patients with K mutations treated with the other three regimens (8-wk DC: 32%) (P=0.11). A small exploratory analysis also revealed an intriguing finding, in that the specific type of KRAS mutation may affect the outcome of patients treated with sorafenib. In a small subset analysis, patients with the mutant *KRAS* Cys amino acid (aa) substitution were observed to have worse PFS compared to sorafenib-treated patients with wild-type or all other types of *KRAS* mutations (p=0.038). These hypothesis-generating results, albeit in small numbers, will be further explored in subsequent studies, and additional data analyses are continuing.

Thus, BATTLE is the first completed biopsy-mandated study in pretreated NSCLC. Our pre-specified hypotheses regarding biomarkers and targeted treatment were confirmed. Identifying proper biomarkers for a favorable population is a step towards personalizing therapy. BATTLE establishes a new paradigm to investigate biomarkers and molecularly targeted treatments in lung cancer patients. Discovery biomarker experiments are ongoing in collaboration with the project leaders of the basic and translational research aims as described throughout this annual report.

**Key Research Accomplishments:**

- Completed enrollment of this novel, complex study, resulting in 341 enrolled patients, 255 randomized patients, and more than 320 biopsies for analysis.
- Demonstrated quality tissue specimen acquisition and biomarker evaluation in more than 80% of processed cases.
- Demonstrated highly efficient collaboration of clinical teams, Biostatistics Core, and Biomarker Core.

**Conclusions**

We are excited to report the completion of enrollment to the BATTLE program. Accrual to this ground-breaking study exceeded our goals. We have supported the early efforts in biomarker discovery in collaboration with the other projects and have initiated formal data analysis. A high-profile plenary session presentation was given by the BATTLE PI, Dr. Edward Kim at the 2010 AACR Annual Meeting in Washington, DC, to summarize the BATTLE results.

**Specific Aim 2: To investigate molecular mechanisms of response and resistance to the targeted agents used in the BATTLE program.**

**Specific Aim 2.1. To validate the molecular mechanisms of response and resistance to erlotinib for patients with chemorefractory NSCLC.**

(PI and Co-PI: Bruce Johnson, M.D., and Pasi Jänne, M.D., Ph.D.)

The association between somatic epidermal growth factor receptor (*EGFR*) mutations and clinical response to gefitinib in patients with non-small cell lung cancer (NSCLC) was published in 2004. This proposal builds on previous findings to further characterize *EGFR* mutations in

subjects' tumors and in tumor cell lines and the relationship of these mutations, subject outcome, and *in vitro* behavior to different EGFR inhibitors. The data generated demonstrates that subjects whose NSCLCs have *EGFR* mutations typically respond to single-agent therapy with gefitinib, are treated for a median of 1 year or longer, and achieve a median overall survival duration longer than 2 years. This survival duration is 3-fold longer than that achieved with conventional chemotherapy in previously untreated subjects with NSCLC. The patients treated with gefitinib or erlotinib with increased copy number assessed by fluorescence in situ hybridization (FISH) have a response rate of 20 -30% and the patients live a median of approximately 2 years. The goal of this research is to confirm these initial observations in prospective cohorts of subjects with NSCLC and somatic *EGFR* mutations or increased copy number with erlotinib as the initial therapy. This proposal is generating translational information on somatic mutations and copy number, prospective validation of the outcome of patients with NSCLC and *EGFR* mutations or increased copy number treated with erlotinib, information on activation of the EGFR pathway in NSCLC and NSCLC cell lines, and information about mechanisms of resistance.

**Objective 1: Establish estimates of the response and outcome of previously treated patients with prospectively identified somatic *EGFR* mutations treated with erlotinib.**

**Summary of Research Findings**

During the last project period, the trial entitled, "A Phase II, Open Label Study of Erlotinib (Tarceva®) in Previously Treated Subjects with Advanced Non-Small Cell Lung Cancer" was completed in October 2009, with a total of 58 randomized patients. The baseline analyses for *EGFR* mutations, copy number, and immunohistochemistry were conducted by the Biomarker Core led by Dr. Wistuba. We continue to await further data, patient follow-up, and analysis to correlate the outcome of the patients with *EGFR* mutations compared to those with wild-type *EGFR*; thus, data analysis will take place in the coming months.

The majority of the progress in Specific Aim 2.1 has come from ongoing research to complete Objective 1. Our research focus is on developing noninvasive techniques to monitor the development of resistance to erlotinib, given its impact on the outcome of patients with somatic *EGFR* mutations treated with erlotinib. Studies of DNA on circulating plasma from patients with somatic *EGFR* mutations were published in the past year (see Publications). In addition, techniques to assess the genomic changes in circulating tumors cells have also been developed and the results are in press.

Two different methods, SARMS and WAVE/Surveyor, were used to detect EGFR activation and resistance mutations from plasma DNA. Both SARMS and WAVE/Surveyor technologies are PCR-based methods for mutation detection. SARMS uses a Scorpions primer/probe in a real-time PCR setting. Short probes allow greater allelic specificity and a lower background. The WAVE/Surveyor method combines standard PCR followed by an endonuclease digestion (Surveyor) that targets wild-type/mutant heteroduplexes as before by members of our research group. The resulting products are resolved on the WAVE HS system. The sensitivity and specificity of detecting *EGFR* T790M with the SARMS assay using NSCLC cell lines with known EGFR T790M mutation status (H1975, H820, and H3255 GR, all known to contain an *EGFR* T790M mutation, and A549 that does not contain an *EGFR* T790M mutation). The *EGFR* T790M allele frequencies for each of the cell lines were: H1975 at 55%, H820 at 7%, H3255 GR at 2%, and A549 at 0%. These results were consistent with the previous genotyping results using WAVE/Surveyor and published data. The *EGFR*-activating mutations and the T790M resistance mutation were studied in patient-derived plasma DNA. Based on previous reports and our determination of median patient plasma DNA concentration (0.252 ng/AL, which is

equivalent to a median of 43 genome copies) in our sample cohort, we used 1 microliter of patient plasma DNA in both the SARMS and WAVE/ Surveyor assays. Using the SARMS assay we detected 12 patients with *EGFR* del E746_A750, 7 patients with L858R, and 8 patients with *EGFR* T790M mutations. All plasma DNA samples were also independently PCR-amplified and screened for EGFR exon 19 to 21 mutations using WAVE/Surveyor. At the time of the study, the Scorpions assays were only available to detect two *EGFR*-activating mutations (del E746_A750 and L858R) and the *EGFR* T790M resistance mutation. Thus, we used the WAVE/Surveyor method to evaluate for the remaining *EGFR* mutations and also as a complementary approach to the SARMS assays (Figure 3).

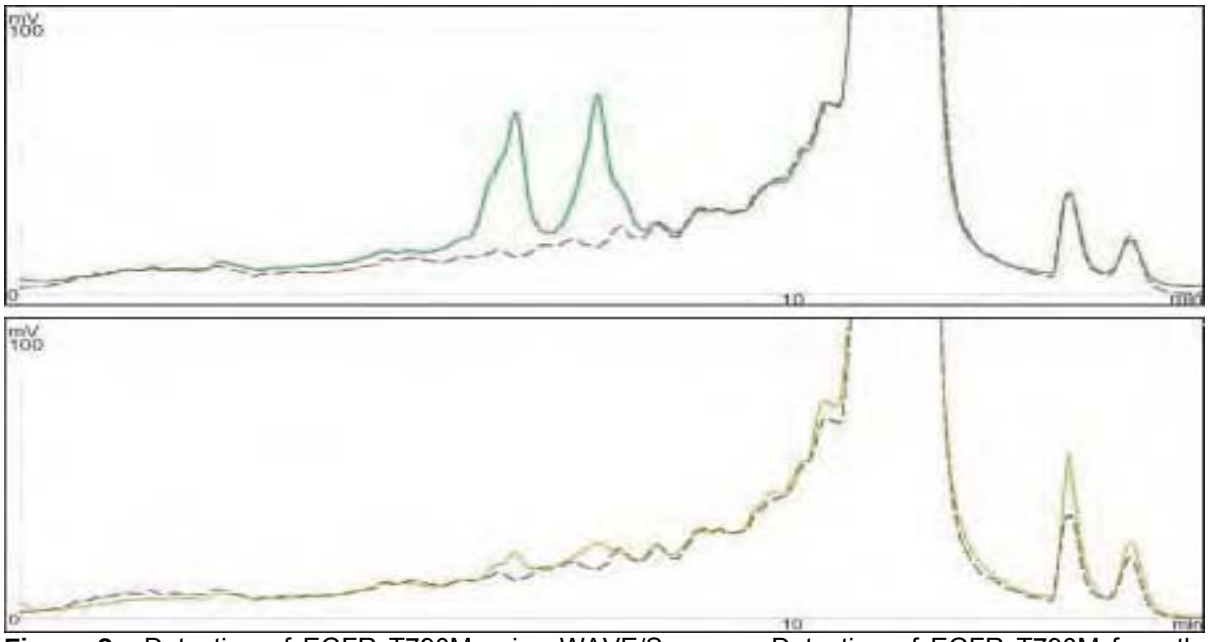


**Figure 3.** Detection of EGFR T790M using WAVE/Surveyor. Detection of EGFR T790M from the H1975 (EGFR L858R/T790M) cell line (top) and plasma DNA from patient 35 (bottom). Exon 20 of EGFR was amplified by PCR, the resulting product digested with Surveyor and analyzed using the WAVE-HS system. In the presence of EGFR T790M, two fragments (asterisk) are generated by Surveyor digestion (solid lines) from the positive control (H1975) and patient 35.The wild-type control (A549; dashed line) is uncut.

Using the WAVE/Surveyor method, we detected EGFR exon 19 deletion mutations in 25 patients, no exon 20 insertion mutations, EGFR L858R mutations in 2 patients, and EGFR T790M mutations in 4 patients. Of the 25 patients with EGFR exon 19 deletion mutations detected by WAVE/Surveyor, 11 were exon 19 deletions other than the del E746_A750 mutation. Such deletions were not a part of the SARMS assay. We compared the findings between these two mutation detection methods. The SARMS and WAVE/Surveyor detected EGFR del E746_A750 in a combined 15 patients, L858R in a combined 7 patients, and T790M in a combined 9 patients, with concordance rates of 73% (11 of 15), 28% (2 of 7), and 33% (3 of 9), respectively.

Circulating tumor cells (CTCs) offer a non-invasive approach to obtain and characterize metastatic tumor cells, but their usefulness has been limited by low CTC yields from conventional isolation methods. The Food and Drug Administration approved the CellSearch Epithelial Kit (CEK) for a simplified CTC capture method, CellSearch Profile Kit (CPK), on paired blood samples from patients with metastatic breast (n=75) and lung (n=71) cancer. The breast

cancer cells were used to provide an established means of genomically characterizing circulating breast cancer cells for *HER2* amplification that could later be used to assess *MET* amplification in circulating lung cancer cells. This approach provides a means of monitoring circulating lung cancer cells for one of the known mechanisms of gefitinib and erlotinib resistance in lung cancer with sensitizing mutations of *EGFR* mediated by *MET* amplification. Molecular markers including *HER2* were evaluated on CTCs by fluorescence *in situ* hybridization (FISH) and compared to patients' primary and metastatic cancer. The median cell count from patients with breast cancer using the CPK was 117 vs 4 for CEK (P<0.0001) in 7.5 mls of blood. Lung cancer samples were similar; CPK: 145 cells vs CEK: 4 cells (P<0.0001). Recovered CTCs were relatively pure (60–70%) and were evaluable by FISH and immunofluorescence. A total of 10 of 30 (33%) breast cancer patients with *HER2*-negative primary and metastatic tissue had *HER2*-amplified CTCs. The CPK method provides a high yield of relatively pure CTCs, facilitating their molecular characterization. Circulating tumor cells obtained using CPK technology demonstrate that a significant discordance exists between HER2 amplification of a patient's CTCs and that of the primary and metastatic tumor.

**Objective 2: Determine effects of TGF-α, EGF, and AR on the growth of *EGFR*-mutant and wild-type cell lines.**

**Summary of Research Findings**

Studies reported in 2009 in our yearly report and published last year showed that head and neck and NSCLC cell lines that produced 20 or more pmol/L of amphiregulin were significantly more likely to be growth-inhibited by both gefitinib and cetuximab than those that produced minimal or no amphiregulin.

**Objective 3: Determine effects of TGF-α, EGF, and AR on the cell cycle and apoptosis of *EGFR*-mutant and wild-type cell lines.**

**Summary of Research Findings**

Studies reported in 2009 and published last year showed gefitinib and cetuximab at concentrations are achievable in the plasma of cancer patients led to $G_1$-S arrest without any evidence of apoptosis in cell lines producing amphiregulin. In contrast, in the low amphiregulin cell lines, cetuximab and gefitinib lead to either no significant increases or only minor changes in the $G_1$-S phase of the cell cycle consistent with the lack of growth inhibition in this group of cell lines.

**Objective 4: Determine effects of different *EGFR* mutations and EGFR inhibitors on phosphorylation of EGFR and downstream signaling intermediates.**

**Summary of Research Findings**

The results from this objective were reported in the publication along with the findings of objectives 2 and 3.

**Key Research Accomplishments:**

- Completed accrual of the phase II erlotinib trial as part of the BATTLE Program.
- Published studies that show *EGFR* T790M can be detected using plasma DNA from gefitinib- or erlotinib-resistant patients.
- Developed a technique to identify more than 100 circulating breast cancer and lung cancer cells in 7.5 mls of blood from patients with these cancers.

- Demonstrated the ability to detect gene amplification (*HER2*) in circulating tumor cells. This finding provides a proof-of-concept for studying the circulating tumor cells from patients with lung cancer and sensitizing mutations of *EGFR* as a mechanism of erlotinib resistance.

## Conclusions

Both *EGFR* activating and *EGFR* T790M can be identified in 70% of patients with known tumor *EGFR*-activating (21/30) or T790M (5/7) mutations. The secondary acquired resistance T790M EGFR mutation was identified from plasma DNA in 15 of the 28 (54%) patients with prior clinical response to gefitinib/erlotinib, 4 of 14 patients (29%) with prior stable disease, and in 0 of 12 patients with primary progressive disease or were untreated with gefitinib/erlotinib**:**

The median cell count from patients with breast cancer using the CPK was 117 vs 4 for CEK (P<0.0001). Lung cancer samples were similar; CPK: 145 cells vs CEK: 4 cells (P<0.0001). Recovered CTCs were relatively pure (60–70%) and were evaluable by FISH and immunofluorescence. A total of 10 of 30 ( 33%) breast cancer patients with HER2-negative primary and metastatic tissue had HER2-amplified CTCs. These data provide evidence that we will likely be able to detect *MET* amplification in circulating lung cancer cells in patients with *EGFR* sensitizing mutations.

### Specific Aim 2.2. Insulin-like Growth Factor Receptor Signaling Pathways and Resistance to Gefitinib in Non Small-Cell Lung Cancer Cells

(PI: Ho-Young Lee, Ph.D.)

Non-small cell lung cancer (NSCLC) accounts for about 75%-80% of lung cancer cases and its dismal survival rate has not improved in the past 2 decades. The lack of effective therapy, the high proportion of patients with advanced disease at the time of diagnosis, and the rapidity of tumor progression are major contributors to lung cancer mortality, and raises the urgent need for novel strategies to treat this disease. Of many potential targets in adult solid tumors, the epidermal growth factor receptor (EGFR) has been extensively studied because overexpression of EGFR has been observed in a number of other common solid tumors including 40–80% of NSCLC (Jemal et al, 2003). Therefore, one therapeutic strategy was to use the agents targeting the EGFR pathway. However, negative results from several large-scale phase III clinical trials in lung cancer have been reported (Giaccone et al, 2002; Johnson, 2002), indicating the need for understanding the mechanisms that induce resistance to EGFR inhibitors. Accumulating evidence has implicated insulin-like growth factor receptor-I (IGF-IR) pathways in resistance to chemotherapy, radiation therapy, and molecularly targeted agents (Kulik et al, 1997; Lin et al, 1999; DiGiovanni et al, 2000; Porras et al, 1998; Toker and Newton, 2000). Our objective is to investigate whether IGF-IR and downstream signaling mediators, such as PI3K/Akt and MAPK, are involved in the resistance to anti-EGFR therapies in NSCLC.

**Objective 1: Determine whether inhibition of the IGF-1R–mediated signaling pathway augments the antiproliferative effects of erlotinib on NSCLC cells *in vitro,* and investigate the mechanism by which erlotinib leads NSCLC cells to activate the IGF-1R signaling pathway.**

Objective 1 and 2 have been completed and reported on in previous reports. In the past year, we investigated whether inhibition of the IGF-1R-mediated signaling pathway augments the

antiproliferative effects of IGF-1R antibody, either individually or in combination with EGFR antibodies on NSCLC cells *in vitro* to confirm our findings reported in prior years. By the MTT analysis, we have not been able to detect any effects from the treatments. We plan to analyze the anchorage-independent growth of a subset of NSCLC cells after treatment.

**Objective 2:** **Determine whether inhibition of the IGF-1R–mediated signaling pathway augments effects of erlotinib on the growth of human NSCLC xenograft tumors established in nude mice.**

See above.

**Objective 3:** **Investigate whether IGF-1R activity influences the therapeutic activity of erlotinib in patients with NSCLC.**

**Summary of Research Findings**

We previously found that IGF-1R TKI was not effective in NSCLC cells harboring the K-ras mutation. Our objectives in this study are to determine the efficacy of the IGF-IR neutralizing antibody, MK0646, on inhibition of NSCLC cell growth. Treatment with MK0646 at doses ranging from 5, 10 and 25 µg/mL exhibited a range of sensitivities after 3-day treatment (Figure 4).

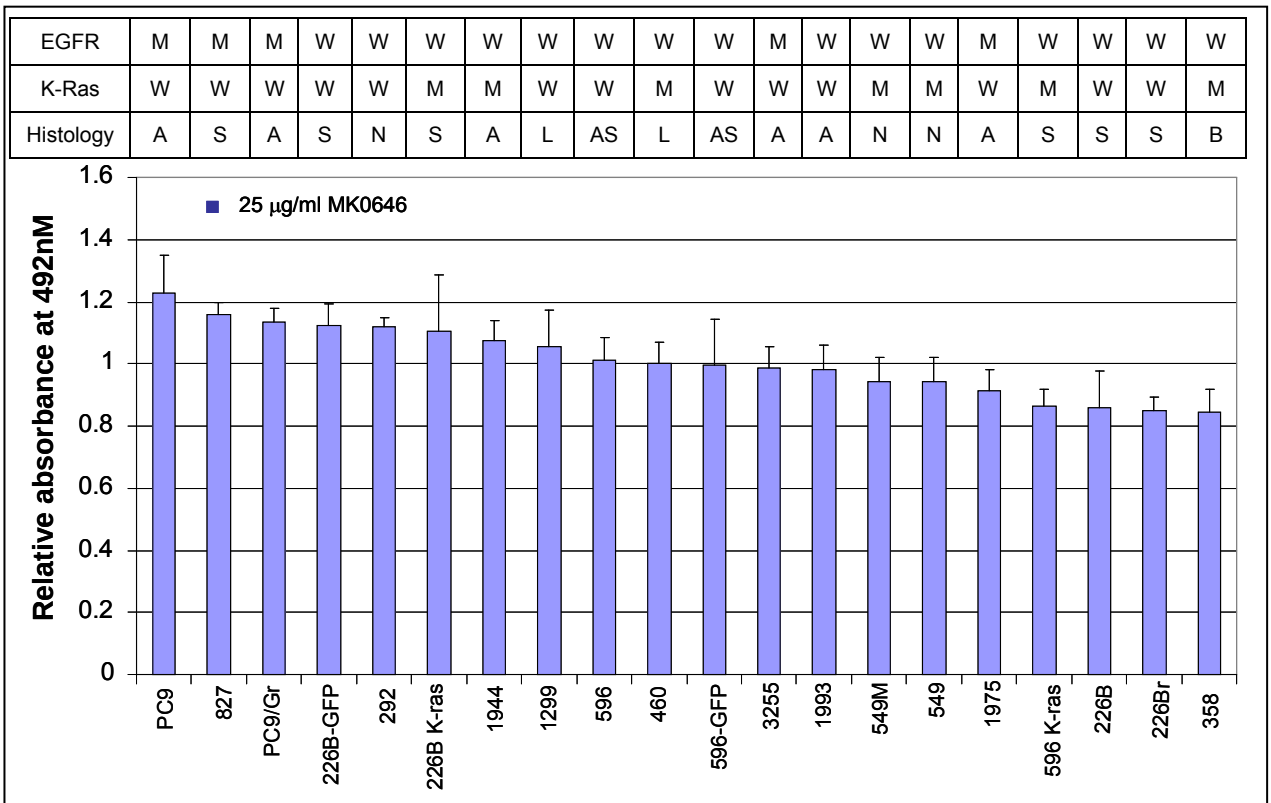


**Figure 4.** Characterization of MK0646 response in human NSCLC cell lines. The response of a panel of 20 NSCLC cells to MK0646-based treatment was measured on ultra-low attaching condition by MTS assay. Three independent experiments were performed with similar results; representative results of one experiment are presented. Mutational status and histological information were obtained from COSMIC (http://www.sanger.ac.uk/genetics/CGP/CellLines/). Abbreviation: W: wt. M: mt, S: squamous, AS: adenosquamous,. L: large cell, A: adenocarcinoma, B: Bronchioloalveolar carcinoma.

The behavior, growth, and response to internal and external signals of cells grown on tissue culture plates are largely different from those of cells grown *in vivo* (three-dimensional), so we performed soft agar colony-forming assays to further understand the clustering of cells. When the relative number of colonies were calculated by dividing the colony number of the control (no treatment) and arranged by the decreasing order, the five resistant cells were again observed to be clustered in the resistant group (Figure 5).

Response to MK0646 and erlotinib in EGFR mutant and K-Ras mutant/EGFR mutant cells (H3255 and H1975, respectively) and K-ras mutant cells (H226B-KRas) showed persistent phospho-AKT levels regardless of MK0646 treatment (Figure 6). In contrast, H226B-GFP cells showed de-phosphorylation of AKT in response to MK0646 treatment (Figure 7).

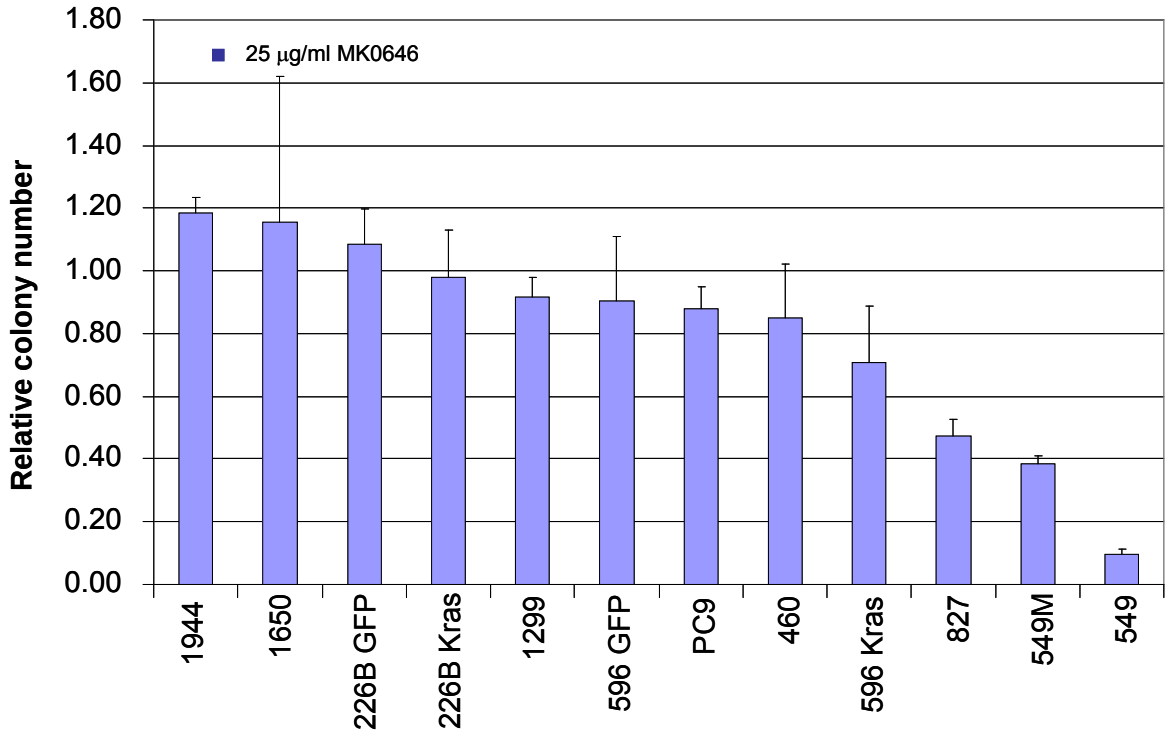


**Figure 5.** Soft agar colony forming assay: Relative colony number in MK0646 25μg/mL. NSCLC cell lines were assessed for the ability to form colonies in soft agar. Results are expressed as percent colony number on 25ug/mL of MK0646 relative to the number of PBS-treated controls for each cell lines and arranged by decreasing order.

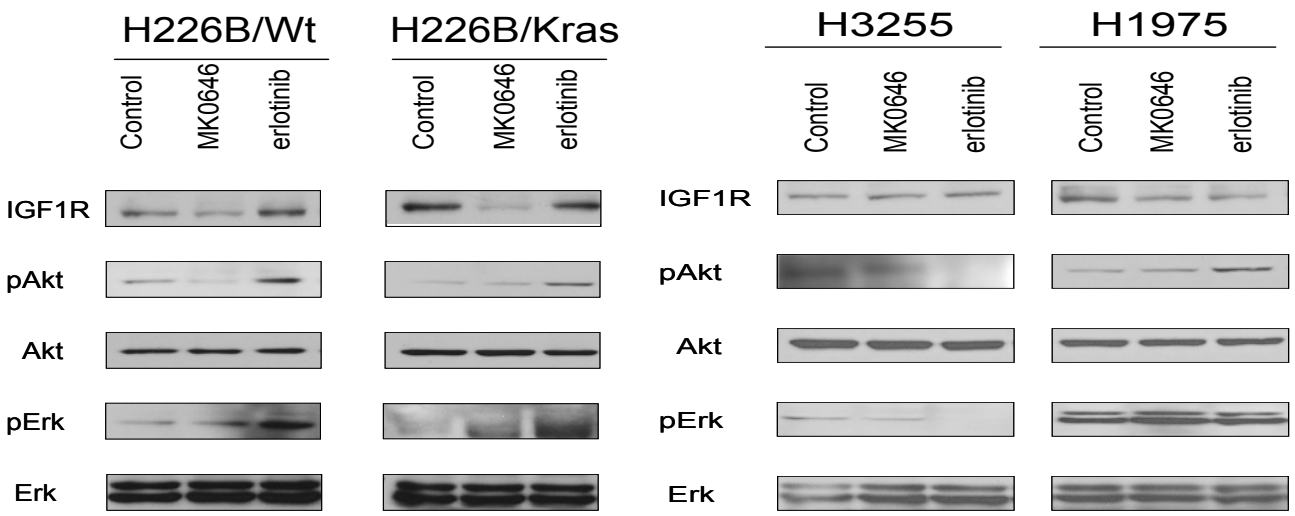


**Figure 6.** Response to MK0646 and erlotinib according to EGFR and K-ras mutation status. Cells were cultured on poly-HEMA coated plates in complete medium and exposed to the indicated drugs for 72 hours. Doses for each drug were as follows: MK0646 25µg/mL, and erlotinib 5µM.

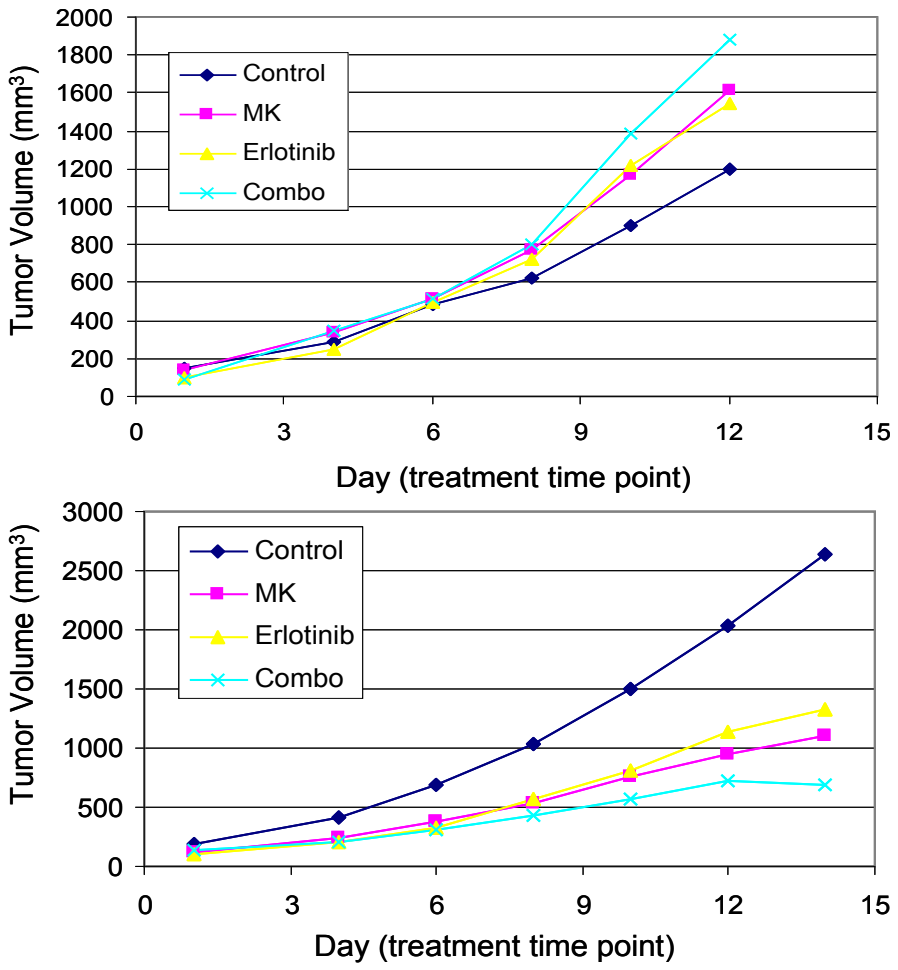


**Figure 7.** Combination of MK0646 and erlotinib inhibit xenograft growth in nude mice with H226B-GFP tumors (upper panel), but not in H226B-K-ras tumors (bottom panel). H226B-GFP and H226B-KRas cell lines were implanted on t he back of nude mice by subcutaneous injection. The mice were treated twice a week with MK0646 (15 mg/kg), erlotinib (mg/kg) or their combination by intraperitoneal (IP) injection.

**Key Research Accomplishments:**

- Demonstrated that the resistance to IGF-1R antibody MK0646 is independent of the mutational status of EGFR or K-ras *in vitro.*
- Demonstrated that treatment with MK0646 delayed tumor growth in H226B-GFP xenografts.

**Conclusions**

Our results suggested that (a) resistance to IGF-1R antibody MK0646 does not seem to depend on the mutational status of EGFR or K-ras *in vitro* and (b) treatment with MK0646 delayed tumor growth in H226B-GFP xenograft, while that treatment did not affect tumor growth in H226B-KRas xenograft. Response to MK0646 *in vitro* was not consistent to that in *in vivo* with H226B-GFP cells, and this discordance should be further investigated.

**Specific Aim 2.3. To investigate the molecular mechanisms of resistance to and biomarkers of the biologic activity of inhibitors of the VEGF pathway**

(PI: John Heymach, M.D., Ph.D.)

The primary goals of this Aim were to develop biomarkers for the activity of VEGF inhibitors and investigate potential markers of therapeutic resistance. Substantial progress has been made towards these goals. The focus of our effort thus far has been in the identification of potential mechanisms of resistance to VEGF inhibitors and development of our methodologies for identification of blood-based biomarkers, in large part because of specimen availability. Notable advances over the past year, detailed below, include the following: 1) Identification of potential mechanisms of resistance to VEGF inhibitors in preclinical models 2) Identification of tumor endothelial markers (TEM) and development of techniques for assessing circulating TEM+ endothelial cells; 3) Analyzing the various platforms for plasma profiling of angiogenic factors to achieve CLIA certification; and 4) Identification of circulating VEGF as a marker of response to vandetanib.

The objectives of this aim have not been modified since the project began. Progress on these objectives is detailed below.

**Objective 1: Quantitatively assess VEGFR phosphorylation, downstream signaling, and biomarkers of angiogenesis in pre- and post-treatment tumor biopsy samples.**

**Summary of Research Findings**

The goal of this objective is to quantitatively analyze tumor specimens pre- and post-treatment from patients enrolled in the BATTLE clinical trial to detect angiogenesis, endothelial apoptosis, and VEGF receptor phosphorylation. Using preclinical models, we have refined our methods for this analysis and made great progress in identifying models of resistance to VEGF inhibitors.

Resistance to VEGF inhibitors can occur through changes in the tumor itself, the stroma, or a combination of the two. To determine the effect of these compartments on VEGF inhibitor resistance, we performed RNA microarray analyses comparing lung cancer H1975 control and bevacizumab (BV)-resistant xenograft (N=3 samples in each group) using Illumina mouse (WG-6 v2) and human (WG-6 v3)-specific expression arrays. We found that a larger number of

stromal mouse genes (1385) were significantly modulated in BV-resistant (BV progression) vs. control xenografts (vehicle progression) compared to human tumor genes (98). We observed significant changes in the expression of genes involved in angiogenesis-, lymphangiogenesis-, and hypoxia-related signaling pathways between the BV-resistant and control xenografts. Specifically, the fibroblast growth factor receptor-2 (Fgfr2) gene was upregulated in the stromal compartment, but not in tumor cells, of H1975 BV-resistant tumors compared with controls. Additionally, upregulation of other stromal molecules and ligands associated with this signaling pathway (e.g., Fgf13, Fgfbp1) were detected (Figure 8). We further validated the stromal expression of Fgfr2, which we noted to be upregulated in BV-resistant H1975 tumors in the microarray analysis. A significant increase in mouse Fgfr2 mRNA expression, but not human FGFR2, was observed in H1975 resistant xenografts compared with controls ($p<0.05$).

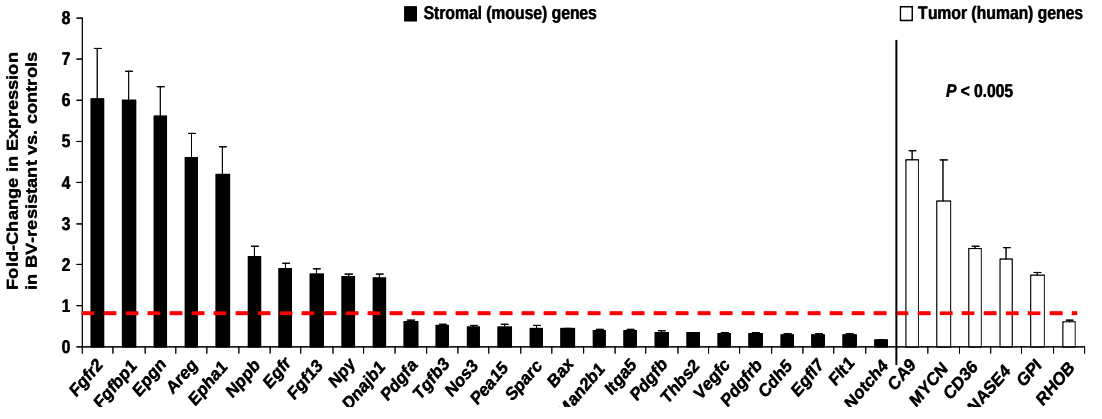


**Figure 8.** Stromal factors are involved in developing resistance to the anti-VEGF inhibitor bevacizumab. Stromal angiogenic genes found to be modulated in bevacizumab-resistant vs. -sensitive H1975 xenografts.

Based on our observation that mouse Fgfr2 gene expression was increased in the stromal compartment of BV-resistant H1975 tumors, we performed immunofluorescent co-localization studies on H1975 vehicle and BV-treated xenografts at progression (n=4, each group) using CD31 (red) and FGFR2 (green) antibodies (Figure 9A). We observed a significant increase in total FGFR2 expression in resistant tumors compared with controls ($p<0.001$, Figure 9B). Furthermore, to assess changes in the FGFR2 ligand, we next measured the plasma concentration (pg/mL) and the expression levels of basic FGF (bFGF). We found a 1.5 fold increase in the levels of the circulating cytokine in BV-resistant tumors compared with controls ($p=0.058$; Figure 9C). The immunohistochemical analysis of H1975 vehicle and BV-treated xenografts at progression (n=4, each group) suggested that BV-resistance is associated with increased expression of bFGF compared with controls (Figure 9D).

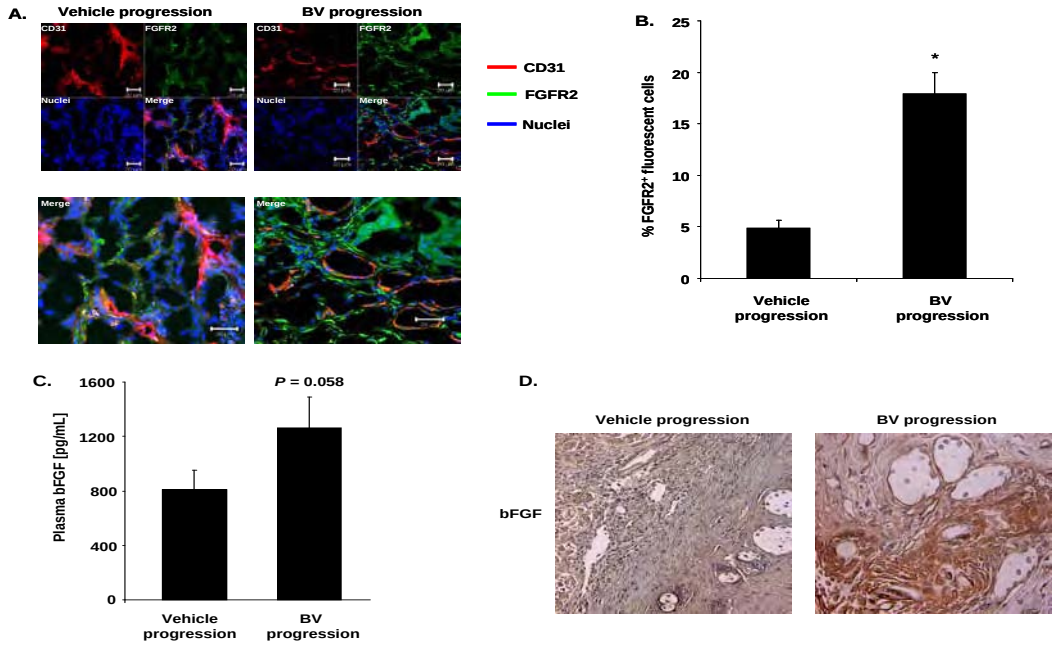


**Figure 9.** Stromal basic FGF/FGFR is associated with bevacizumab resistance in xenograft models **A)** Colocalization of FGFR and CD31 detected by immunoflorescence in bevacizumab-treated H1975 tumors: CD31 (red), FGFR2 (green); **B)** Increased quantification of FGFR2 in bevacizumab-resistant tumors; **C)** Increased bFGF in bevacizumab-treated xenografts; **D)** Increased expression of bFGF in tumors at the time of progression during treatment with bevacizumab.

These results highlight the importance of the contribution of the stroma in developing resistance to anti-VEGF therapies. We will further investigate the role of stromal FGFR signaling in resistance mechanisms utilizing samples from the completed BATTLE trial (Aim 1) that may provide important insights into stromal changes contributing the VEGF inhibitor resistance.

**Objective 2: Investigate the utility of circulating endothelial cells (CECs), monocytes, and other cells in peripheral blood as biomarkers for antiangiogenic activity and inhibition of the VEGF pathway.**

**Summary of Research Findings**

Our previous work focused on identifying tumor endothelial markers (TEMs) in preclinical models that would identify a new subset of circulating TEM+ positive endothelial cells (CTECs) derived from tumor endothelium sloughed into the circulation. This sloughing is known to increase after antiangiogenic therapy and therefore, we hypothesized that this population of detectable CTECs may increase after antiangiogenic therapy. Identification of the tumor endothelium specific CECs would provide a more accurate measure of response to antiangiogenic therapy and would be used in the analysis of samples from the BATTLE clinical study. This work led to the investigation of these CTECs in a set of clinical samples.

**Objective 3: Systematically examine changes in the plasma and serum angiogenic profiles consisting of a panel of proangiogenic cytokines, targeted receptors, and potential biomarkers of endothelial damage.**

## Summary of Research Findings

We have completed analysis of 185 baseline samples from patients whom consented to the optional blood collection for cytokine and an giogenic factor (CAF) analysis. This analysis incorporated a total of 65 anal ytes, including newly available markers of the E GFR axis including Amphiregulin, Betacellulin, EGF, EGFR, Epiregulin, FGF-basic, HB-EGF, PDGF-BB, PlGF, Tenascin C, and TGF-α (Table 4). With these additional markers, we will be able to evaluate the potential correlation of the data from Specific Aim 2.1 on marker of response/resistance to erlotinib. Data was sent to send to Biostatistics/Bioinformatics Core for analysis, and a report will be forthcoming on results of this analysis. We are also in the process of evaluating available post-treatment samples as well to determine treatment effects on CAFs.

**Table 4.** Cytokines and Angiogenic Factors Analyzed in the BATTLE Study

| **Pro/antiangiogenic factors** | **EGF axis** | **Chemokines** | **Interleukins** |
|---|---|---|---|
| VEGF, FGF-basic | EGF, EGFR, TGF-a | MCP-1, -3 | IL-1a, -1b, -1RA |
| HGF, PDGF-bb | Amphiregulin, Betacellulin | MIP-1a, b | IL-2, -2Ra |
| MMP-9, PlGF | HB-EGF | RANTES (CCL5) | IL3 - IL10 |
| | | MIP-2 | IL-12 – IL18 |
| | | MIG (CXCL-9) | |
| **Endothelial function/damage** | **Hypoxia** | Eotaxin (CCL11) | **Growth factors** |
| sVEGFR-2 | Osteopontin* | IP-10 (CXCL10) | GM-CSF |
| sE-selectin | CA-9* | SDF-1a (CXCR4) | G-CSF |
| VCAM-1 | IGF axis | KC (CXCL1) | M-CSF |
| | IGF-I*, -II* | GRO-a | SCGF-b |
| **Inflammation/ adhesion** | IGF-BP3* | CTACK (CCL27) | SCF |
| sICAM-1 | | | Beta-NGF |
| IFN- a, g | | | |
| TNF-a, b | | | |
| MIF, LIF | | | |

*ELISA assays (R&D Systems)

**Key Research Accomplishments:**

- Demonstrated one mechanism of resistance to VEGF inhibitors that involves activation of the stromal FGFR pathway, and proved that the stromal compartment may be a key player in the development of resistance.
- Identified a new population of circulating TEM+ endothelial cells (CTECs) that offers a specific biomarker for evaluating the effect of angiogenesis inhibitors and was evaluated in a set of clinical samples.
- Explored multiple platforms for determining CAF signatures has brought us closer to the goal of reaching CLIA certification for this method.
- Quantified CAFs in all samples from BATTLE study and are currently analyzing the data.

**Conclusions**

Our preclinical studies have identified a number of potential markers that predict response to VEGFR inhibitors. We are interested to see if further testing proves these same markers can be used to predict response in patient samples. In addition, our studies have identified a new population of cells that can be detected that identify circulating endothelial cells derived from tumor endothelium. Analysis of this population of cells in patients treated with angiogenesis inhibitors is likely to be a better prognostic marker of response to treatment.

Several plasma CAFs are associated with specific tumor-derived pathway activation. Our preliminary study suggests that broad-based plasma profiling of cytokines and angiogenic factors may be a feasible approach for identifying markers of activation of tumor signaling pathways. In addition to the evaluation of pathway activation using plasma samples, we will be evaluating modulation of CAFs by each treatment arm and searching for potential predictive plasma signatures with clinical outcome measures such as progression-free survival (PFS). The final step will be to validate the plasma predictive signature derived from BATTLE with other randomized clinical studies. These studies can also validate our results that identify circulating VEGF as a predictive marker of response to angiogenic therapies in other clinical studies.

**Specific Aim 2.4. To investigate the molecular mechanisms of the effects of the combination of bexarotene and erlotinib on NSCLC cells**

(PI: Reuben Lotan, Ph.D.)

The need to discover and introduce more effective treatment agents and combinations is urgent, as is the need to improve the selection of the right agent or combination of agents for each patient on the basis of our understanding of the molecular targets. The combination of the retinoid X receptor (RXR)-selective ligand Bexarotene and the epidermal growth factor receptor (EGFR) tyrosine kinase (TK) inhibitor erlotinib appears to be a promising approach, and it will be tested in patients with NSCLC in the BATTLE program. Some aspects of the mechanisms of action of these two agents are not fully resolved. Therefore, we propose to investigate how they exert their effects on NSCLC cells so as to improve their usefulness in future clinical trials.

The objectives of this project have not changed.

**Objective 1: To determine by immunohistochemical analysis the expression of nuclear receptors (retinoic acid receptors [RAR]-α, -β, and -γ; RXR-α, -β, and -γ; and PPAR-γ1 and PPAR-γ2) and cyclin D1 in NSCLC specimens obtained from patients to be enrolled in the BATTLE umbrella trial and from patients whose cancer progresses on treatment.**

**Summary of Research Findings**

This objective was a collaborative work with Dr. Ignacio Wistuba (Director of the Biomarker Core) on the analysis of NSCLC samples from the clinical trial patients continued, facilitated by the robust patient accrual. The progress is detailed in his report (see Biomarker Core).

**Objective 2: Examine the effects of bexarotene, erlotinib, and rosiglitazone alone and in combination on the growth and apoptosis of NSCLC cells, cyclin D1 and PPAR-γ levels, and gene expression profiles.**

**Summary of Research Findings**

This aim was completed as reported in the previous annual report.

**Objective 3: Determine whether RXRs, EGFR, and PPAR-γ are required to mediate the effects of bexarotene, erlotinib, and rosiglitazone, respectively, on cell growth control and apoptosis, and examine the functional significance of changes in gene expression induced by receptor agonists used singly or in combinations.**

**Summary of Research Findings**

In previous reports, we have shown that the gene GPRC5A, which had been found by gene expression microarray analysis to be induced by bexarotene, can be induced in human lung adenocarcinoma cells *in vitro*. We studied the functions of this bexarotene-inducible gene and found that it is phosphorylated in cells treated with EGF but not when cells were co-treated with EGF and EGFR inhibitor AG1478, suggesting that GPRC5A can be a substrate for a kinase in the EGF/EGFR signaling pathway. We found that EGFR and GPRC5A form a new type of interaction between bexarotene and EGF/EGFR signaling; thus, our research during the past year has focused on elucidating the role of EGFR-mediated phosphorylation of GPRC5A with respect to its tumor suppressor functions. First, we determined whether some NSCLCs express both GPRC5A and EGFR or its family member HER-2. Figure 10 shows that 4/11 NSCLC cell lines analyzed expressed high levels of GPRC5A, whereas 8/11 expressed EGFR and 4/11 expressed HER-2. All cell lines that expressed GPRC5A also expressed EGFR, and 2 of these cell lines also expressed HER-2. This finding is important because previous reports state that GPRC5A can be tyrosine phosphorylated in human normal mammary epithelial cells treated with EGF (which activates EGFR) or heregulin (which activates HER-2), and our studies identified lung cancer cell lines that express GPRC5A as well as EGFR and HER-2.

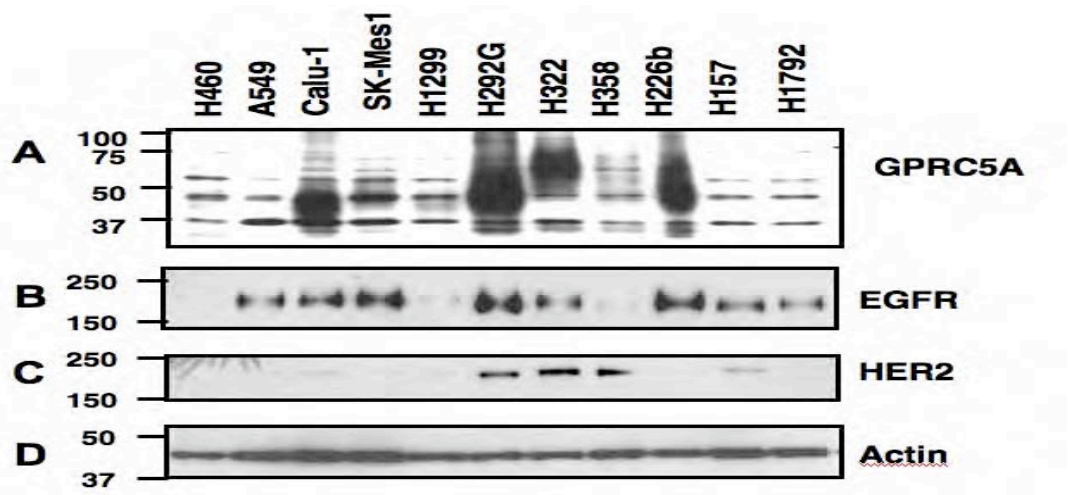


**Figure 10**. The NSCLC cell lines (indicated above each lane) were cultured in DMEM/F12 medium with 10% serum and subconfluent cultures were harvested, lysed, and processed for SDS-polyacrylamide gel electrophoresis and immunoblotting using antibodies against GPRC5A **(A)**, EGFR **(B)**, HER2 **(C)**, and actin **(D)**. The actin blotting was used to assess the loading of proteins in each lane.

Next, we used the cell line H292G, which expresses both GPRC5A and EGFR, to determine whether the activation of EGFR by EGF induces tyrosine phosphorylation of GPRC5A. Figure 2 shows that treatment of the H292G cells with EGF increases the tyrosine phosphorylation of EGFR as revealed by immunoblotting with anti-phosphotyrosine antibodies (PY99) (two left lanes in panel A), indicating that the EGFR signaling can be activated by EGF in these cells. The figure also shows that GPRC5A (protein bands of 40 to 50 kda) as well as its C-terminus-containing fragment of 20 kda immunoprecipitated from EGF-treated cells are more tyrosine phosphorylated than the corresponding proteins from untreated cells (third and fourth lanes in panel A). Panel B in the same figure shows that similar amounts of GPRC5A were immunoprecipitated from untreated and EGF-treated cells. The immunoglobulin controls (IgG) indicate that the immunoprecipitation with anti-GPRC5A was specific. These results clearly demonstrated that GPRC5A is a substrate for EGFR in lung cancer cells; however, it is not known if GPRC5A is a direct substrate of EGFR itself (as presented schematically in the bottom of Figure 11) or one of the downstream kinases activated by EGFR.

To test the hypothesis that GPRC5A is a direct substrate of EGFR, we performed experiments to determine whether GPRC5A and EGFR are positioned in very close proximity in the cell membrane so that they can be crosslinked by a bifunctional cleavable Sulfo-NHS-ester crosslinker called DTSSP (3,3′-dithiobis [sulfosuccinimidylpropionate]). Figure 12 shows that immunoprecipitation of GPRC5A from lysates of cells treated with DTSSP (labeled as D) or with EGF followed by DTSSP (labeled as E+D) co-precipitates EGFR. These results prove that GPRC5A and EGFR are close enough in the cell to support the notion that GPRC5A is a direct substrate of EGFR.

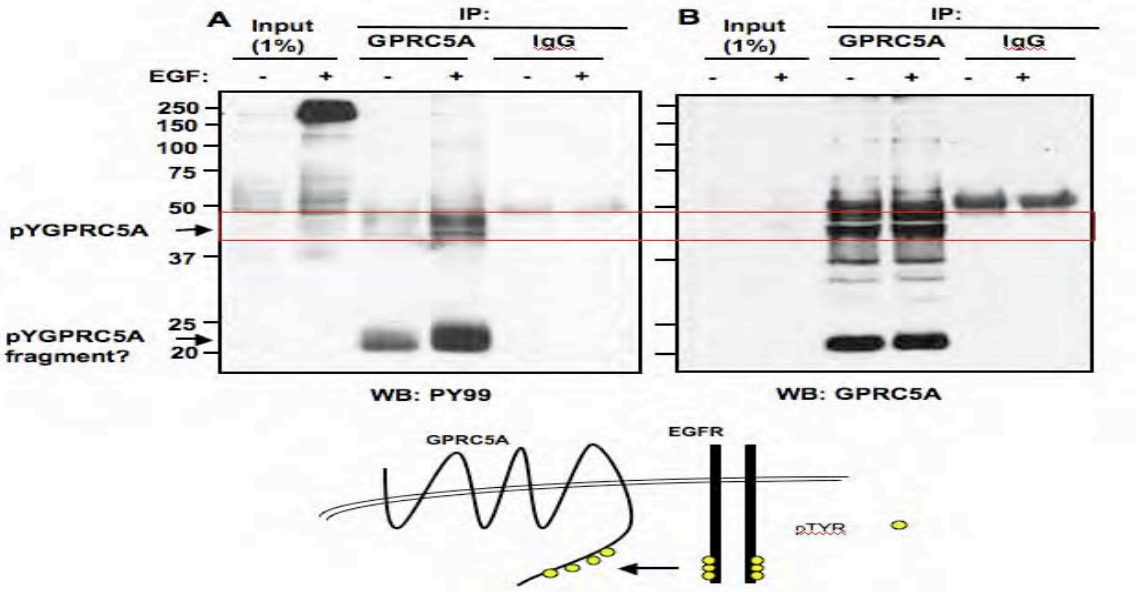


**Figure 11.** The NSCLC cell line H292G was cultured in serum-free medium overnight in several tissue culture dishes and then some of the cultures received fresh serum-free medium with EGF (100 ng/ml) whereas the other dishes received fresh medium without EGF. After 5 minutes, the cells were harvested and total cell lysates were prepared and subjected to immunoprecipitation (IP) with either anti-GPRC5A antibodies or control IgG followed by Western blotting using sequentially pY99 anti-phosphotyrosine antibodies **(A)** and antibodies against GPRC5A **(B)**.The two leftmost lanes in each panel represent cell lysate (1% of total) before immunoprecipitation (input).

Several groups have analyzed global tyrosine phosphorylated peptides in cells treated with EGF and our mining of their data indicated that GPRC5A can be phosphorylated on tyrosine residues (Y) located in the cytoplasmic domain at positions 317, 320, 340, and 347. Since we have demonstrated previously that GPRC5A is a tumor suppressor, our results did not suggest that it would be activated by the mitogenic/oncogenic EGFR signaling. As a result, we hypothesized that its phosphorylation by activated EGFR leads to inactivation of GPRC5A. To test this idea, we prepared a mutant GPRC5A (4F) and we replaced tyrosine residues 317, 320, 340, and 347 with phenylalanine (F); therefore, this mutant should not be phosphorylated by EGFR. If our hypothesis is valid, then the 4F mutant should be more active as a tumor suppressor than the normal (wild type) GPRC5A. First, we examined whether the generated 4F mutant is indeed resistant to EGFR-mediated tyrosine phosphorylation. We transfected the wild-type (WT) GPRC5A and the 4F mutant into HEK293 cells that express transfected EGFR. After treating the cells with EGF for 0 to 360 minutes, we found that the WT GPRC5A undergoes phosphorylation after 5 minutes of EGF treatment, whereas the 4F mutant does not undergo phosphorylation at any time (Figure 13).

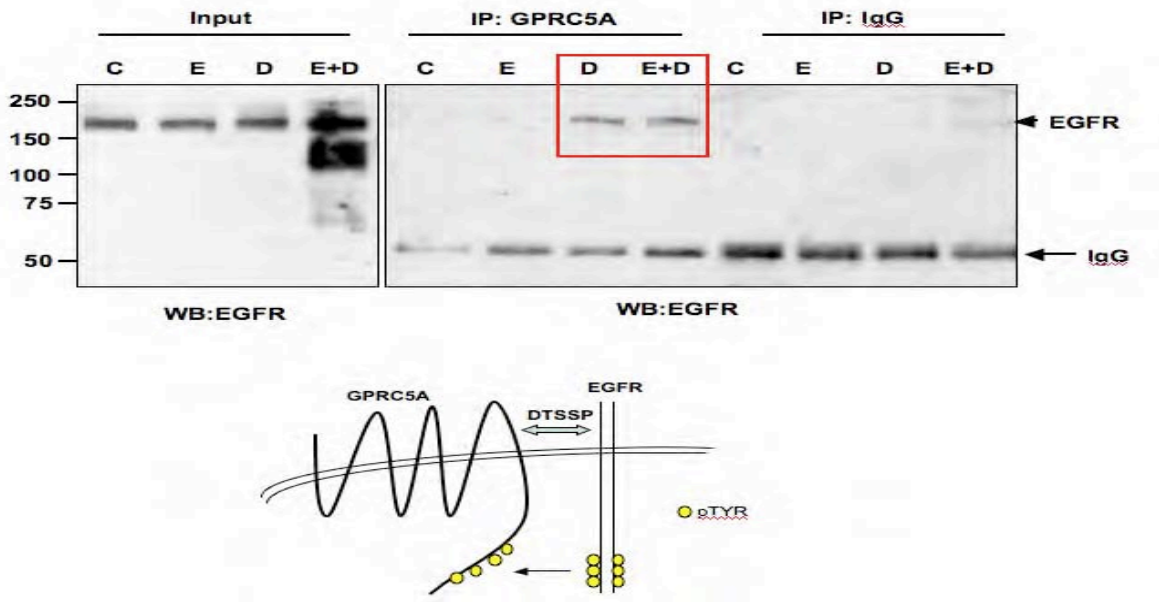


**Figure 12.** H292G Cells were cultured overnight in serum-free medium in several tissue culture dishes. The cultures treated with control serum-free medium **(C)**, or EGF (100 ng/ml) **(E)**. After 5 minutes, the crosslinking reagent DTSSP was added to some of the cultures in control medium **(D)** or those pre-treated with EGF **(E+D)**. After 5 minutes, the cells were lysed and a portion of the lysate was analyzed by immunoblotting with antibodies against EGFR (left panel labeled as input). The remaining lysate was divided in two aliquots one of which was incubated with antibodies against GPRC5A and the other with control IgG. After immunoprecipitation (IP), the precipitates were subjected to western blotting using anti-EGFR antibodies.

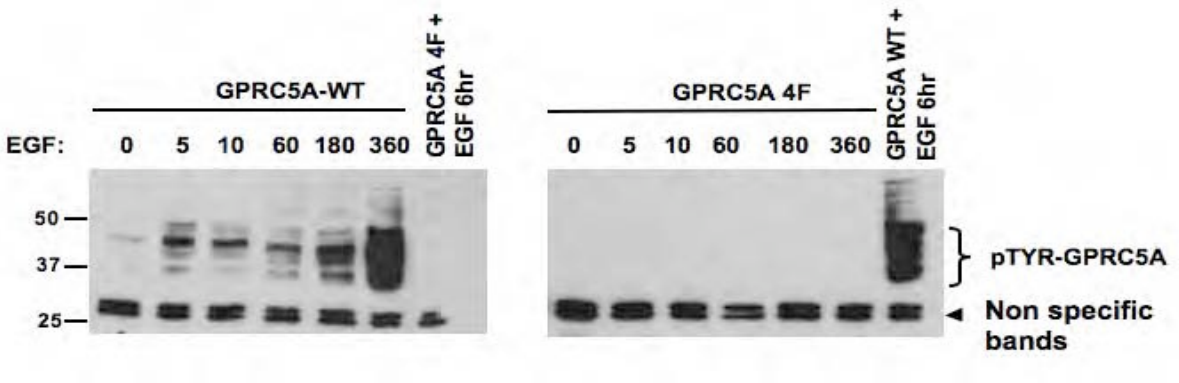


**Figure 13.** HEK293T cells expressing transfected EGFR were transiently transfected with normal GPRC5a-WT or mutant GPRC5A-4F. The cells were cultured in serum-free medium overnight and then they were treated with EGF (100 ng/ml) for the indicated times (minutes). Cell cultures were harvested after these times and the cells were analyzed by Western blotting using anti-phosphotyrosine antibodies.

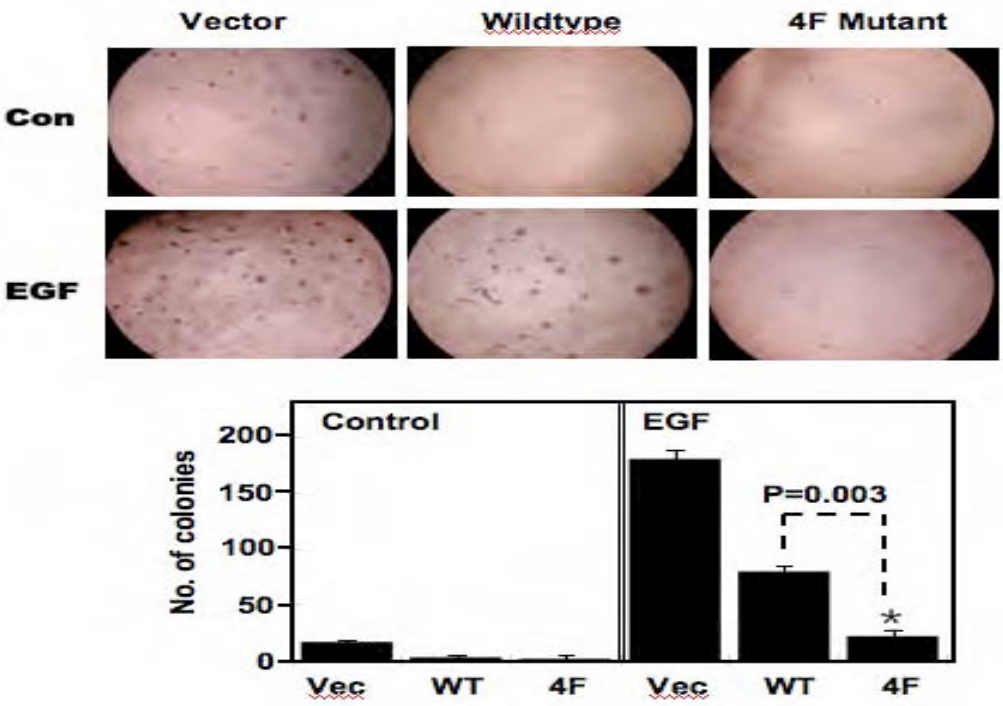


**Figure 14**. H1792 cells were transfected with empty vector, or GPRC5A WT, or 4F and treated with control medium of EGF, plated in agarose and analyzed for colony numbers after 18 days. The upper panels show photographic examples of such colonies and the bar graph shows the mean number of colonies per plate ± SE of triplicate plates.

After confirming that the 4F mutant is resistant to EGFR-mediated tyrosine phosphorylation, we wanted to compare the activities of the WT and 4F GPRC5A proteins in cells. To do so, we used the lung cancer cell line H1792, which expresses a low level of constitutive EGFR and a negligible level of GPRC5A, as shown in Figure 10. H1792 cells transfected with WT GPRC5A exhibited lower suppression of anchorage-independent colony formation, an *in vitro* more characteristic of transformed cells than cells transfected with the phosphorylation-resistant 4F mutant (Figure 14). These preliminary results support the hypothesis that phosphorylation of GPRC5A may decrease its tumor suppressive effects; however, additional studies beyond the scope of this project are required to establish the phosphorylation of GPRC5A in H1792 with and without EGF treatment.

**Objective 4: Evaluate the growth inhibitory effects and mechanisms of action of novel RXR ligands AGN194204 and 9cUAB30 alone or combined with erlotinib and rosiglitazone on NSCLC cells.**

**Summary of Research Findings**

This aim was closed as reported in the previous annual report.

**Key Research Accomplishments:**

- Demonstrated that GPRC5A interacts with EGFR at the cell membrane and serves as a substrate for the phosphorylation of tyrosine residues in the cytoplasmic domain.

- Demonstrated that the phosphorylation of tyrosine may decrease the activity of GPRC5A.

**Conclusions**

This finding is consistent with the increased disease control rate observed in patients treated with erlotinib plus bexarotene, compared to that achieved in patients receiving erlotinib alone, in the BATTLE clinical trial (see Aim 1). Our finding explains at least in part the biological basis for the enhanced efficacy of the combination.

**Specific Aim 3: To identify biomarkers as novel predictors of clinical end points and potential therapeutic targets**

(PI: Ignacio Wistuba, M.D.)

**Objective 1: Identify molecular features in tumor tissues that correlate with patients' responses to individual regimens used in the clinical trials of the proposed program.**

**Summary of Research Findings**

The BATTLE clinical trial completed accrual in October 2009, and subsequent follow-up achieved the goal of 200 evaluable patients in December 2009. Because the patient response data to individual regimens in the clinical trial has only been recently unblinded, these recently initiated analyses will be finalized during the next unfunded year of the grant (our request for a no-cost extension is pending review by the DoD).

A total of 324 patients were biopsied in the clinical trial, and tumor tissue was detected in 270 cases. Of these, frozen tissue specimens from 257 patients were made available for RNA extraction and for global gene expression analysis. Only 8 patients who consented to a second biopsy eight weeks after treatment ended had frozen tissue available before and after treatment. RNA quality was measured using the Nanodrop and Agilent Bioanalyzer, and a total of 187 RNA samples were found to be suitable for amplification using the NuGEN RNA pico amplification system. Of these, histology quality control was performed in 175 frozen tissues samples, and malignant cells were detected in 143 (82%) of cases.

A total of 50 qualified RNA samples from the first set of extractions were used for gene expression analysis through the Affymetrix GeneChip array (Human gene U 133 plus 2.0 array). Among the RNA samples tested, 32 (64%) showed acceptable gene expression profiles and the remaining 18 samples (36%) were labeled as of poor quality and not suitable for analysis. We subsequently adapted a new RNA amplification protocol (WT-Ovation RNA pico amplification systems) developed by NuGEN and a new generation of Affymetrix GeneChips (Human gene ST 1.0 Array) and analyzed the newly extracted 173 RNA samples. The new strategy generated high quality expression profiles from 139 samples suitable for bioinformatics analyses (Table 5). Both the yield and the quality of gene expression profiles obtained from the recent 139 samples were significantly higher than the profiles from the previous 50 samples.

**Table 5:** Quality expression profiles per GeneChip array

| Affymetrix Chips | Qualified RNA | Passed Array QC |
|---|---|---|
| U133 plus 2.0 | 50/84 (60%) | 32/50 (64%) |
| Human ST 1.0 | 139/173 (80%) | 139/139 (100%) |

To assess potential differences in signatures between refractory treatment (our study) and treatment-naïve tumors (Table 6), we compared gene expression profiling from the BATTLE clinical trial (pretreated, resistant tumors, stage III/IV, N=32) and a control group from two independent publicly available datasets (never-treated tumors, stage III/IV, N=45) (Table 6).

**Table 6:** Description of the different sets used to compare pretreated refractory and treatment-naïve NSCLC

| | BATTLE | Duke University | International Genomics Consortium |
|---|---|---|---|
| Platform (Affymetrix) | HG-U133 Plus 2.0 | HG-U133 Plus 2.0 | HG-U133 Plus 2.0 |
| Sample size | 32 | 23 | 22 |
| Treatment-naive | No | Yes | Yes |
| Sample source | NSCLC | NSCLC | NSCLC |
| Stage | III-IV | III-IV | III-IV |
| Number of probesets | 54,675 | 54,675 | 54,675 |

*IGC: International Genomics Consortium; NSCLC: Non-small-Cell Lung Cancer

Gene expression profiling was generated using the same platform (U133 Plus 2.0 Array). A total of 3,963 probesets were found to be differentially expressed between BATTLE samples and the control group with a p-value < 0.001 ( two-tailed t-test). Pathway and gene set analyses were used to define networks and pathways associated with resistance (Figure 15). DNA repair gene sets were upregulated in BATTLE samples compared to never-treated-tumors (1). Network analysis found that MYC as well as many of its downstream-regulated genes were significantly downregulated in BATTLE samples. In particular, a high proportion of MYC target genes associated with apoptosis were downregulated. For validation, we used: i) an independent set of 38 never treated NSCLC stage III/IV; ii) a set of 53 NSCLC cell lines tested for cisplatin sensitivity with proteomic profiling generated by Reverse Phase Protein Array (RPPA) technology using 177 well-characterized antibodies; iii) the comparison of two pairs of NSCLC cell lines (H1437, H460) that were made resistant by iterative exposure to cisplatin, and iv) transfection experiments. Using real-time PCR, MYC gene expression was significantly lower in 15 BATTLE samples compared with an independent set of 38 never-treated, stage III/IV NSCLC (p-value=0.01). The proteomic profiling of 53 NSCLC cell lines showed that MYC expression was one of the top proteins associated with sensitivity to cisplatin. An inverse correlation was observed between sensitivity to cisplatin (IC50) and MYC protein expression evaluated by RPPA (total MYC: r=-0.41, p-value=0.003; phosphorylated MYC: r=-0.30, p-value=0.03). MYC gene expression by real-time PCR was lower in resistant H1437 and H460 cell lines compared to parental cell lines. Finally, transfection of H226 cell lines with a vector expressing MYC improved sensitivity to cisplatin compared to the control. In conclusion, MYC downregulation may play an important role in NSCLC resistance to platinum-based chemotherapy, and the role of MYC targeting agents in lung cancer therapy should be re-evaluated for future cancer treatment. This work was presented in a poster session at the 101 AACR Annual Meeting, April 17-22, Washington, DC.

Using the primary end-point of the trial and available gene expression profiles, we are now in the process of identifying potential biomarkers of response, and testing gene expression signatures developed in independent studies. Three gene expression signatures representing activation of important molecular pathways were developed, and they are currently being tested in the BATTLE specimens. Briefly, an *EGFR* signature has been developed and trained using 95 treatment-naïve adenocarcinoma and validated in both cell lines and surgically resected lung cancer independent tumor sets (2)(3)(4)(5). A *KRAS* signature was developed using a publicly available set of lung adenocarcinoma (6), and validated in the two independent tumor sets (1), including the BATTLE set. Finally, an epithelial-mesenchymal transition (EMT) signature has been generated by comparing epithelial-like and mesenchymal-like NSCLC cell lines, validated in the same lines on an Illumina platform (v3) and in an independent set of lung cancer tumors (4) and HNSCC cell lines (on Illumina V2). All of these three mRNA expression signatures are being currently tested in the BATTLE profiled samples. The development of the EGFR activation signature was presented at the AACR-IASLC Joint Conference Molecular Origins of Lung Cancer: Prospects for Personalized Prevention and Therapy, Coronado, CA, January 17, 2010, and to the 10th Annual Targeted Therapies of the Treatment of Lung Cancer (sponsored by IASLC), Santa Monica, February 10, 2010.

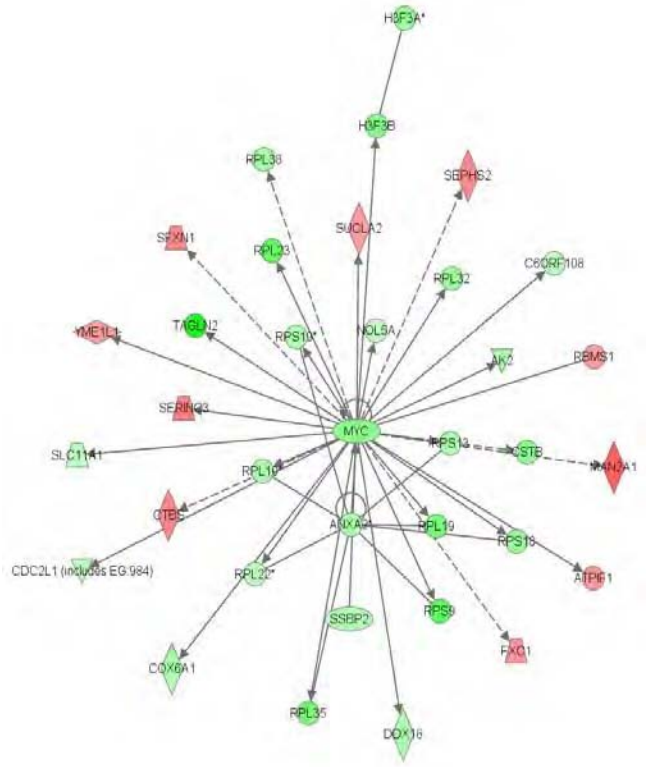


**Figure 15.** Pathway analysis by differentially expressed genes between treatment naïve and refractory NSCLC showed a downregulation of *MYC* and its downstream regulated genes

**Objective 2: Determine the effect of targeted agents in tumor tissues, and identify novel molecular mechanisms of tumor response or progression.**

**Summary of Research Findings**

We have successfully adapted a new strategy to obtain high-quality gene expression profiles from the small quantity of tissue present in core needle biopsies that will significantly improve the yield rate and allow for improved bioinformatic analyses. The high-quality gene expression profiles found in our recently profiled tissue specimens are now ready to be used for analyses comparing these data with clinical and molecular parameters obtained in our clinical trial, including response of patients in each treatment group. This analysis is currently being performed in conjunction with the Biomarker Core and it will be completed during the next unfunded year of this program (no-cost extension request pending DoD review).

**Key Research Accomplishments:**

- Obtained biopsies from 324 patients in the clinical trial, with tumor tissue detected in 270 cases. Of these, frozen tissue specimens from 257 patients were made available for RNA extraction and for global gene expression analysis.
- Optimized a new RNA amplification protocol developed by NuGEN to generate high quality expression profiles suitable for bioinformatic analysis from core needle biopsies from lung cancer patients with chemorefractory tumors (BATTLE).
- Obtained high-quality mRNA expression signatures from fresh core needle biopsies from 171 BATTLE patients that will be correlated with tumors' genetic abnormalities identified by the Biomarker Core and with patients' outcome based on the targeted therapy treatment received.

**Conclusions**

During this project period, we demonstrated that global gene expression profiles can be successfully obtained using residual tumor biopsies after fulfilling required biomarker analysis. We optimized new RNA amplification protocols to produce high quality gene expression mRNA profiles for correlative analysis with tumors' genetic and patients' clinical parameters, including response and outcome after treatment.

**Specific Aim 4: To explore new preclinical combinations and their mechanisms of action by targeting mTOR signaling and develop phase I trials to test these combinations.**

(PI and Co-PIs: Suresh Ramalingam, M.D., Shi-Yong Sun, Ph.D., Haian Fu, Ph.D.)

The overall objective of Aim 4 is to study the efficacy of mTOR inhibitor combination therapies that co-target mTOR and PI3K/Akt signaling. Following is a summary of our research progress for Year 3:

**Objective 1: To study the efficacy of mTOR inhibitor combination therapies that co-target mTOR and PI3K/Akt signaling.**

**Summary of Research Findings**

We previously had shown that the combination of an mTOR inhibitor (e.g., RAD001) and a PI3K inhibitor (e.g., LY294002) exerts enhanced antitumor effects both in cell cultures and in mouse xenografts (Wang et al., Cancer Res 2008). However, we do not know if the sequence of the treatment impacts the therapeutic efficacy of the combination without conducting an experiment to address this issue. We found that the concurrent treatment with rapamycin and LY294002 was far more potent than both sequential treatments: rapamycin followed by LYT294002 and LY294002 followed by rapamycin in inhibiting the growth of cancer colonies (Figure 16). We recommend using the concurrent combination of an mTOR inhibitor and a PI3K inhibitor as a potential cancer therapeutic regimen based on our results.

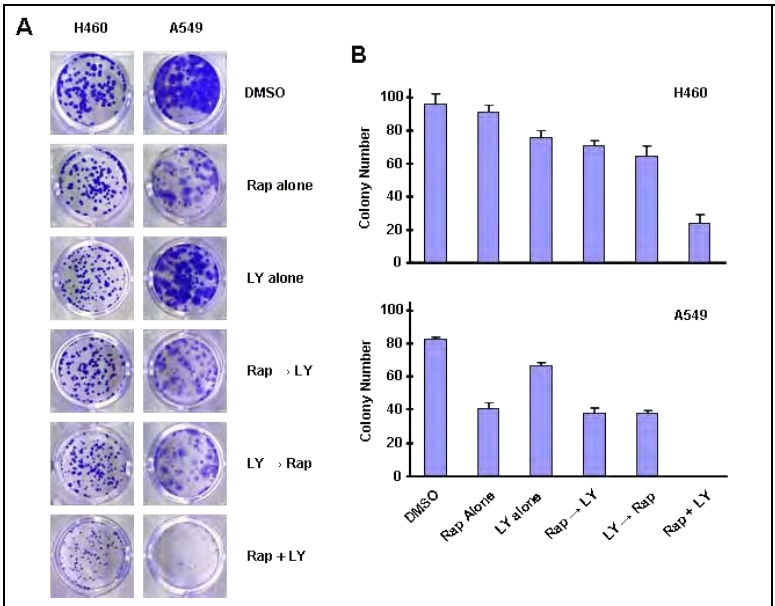


**Figure 16.** Impact of sequential combinations of rapamycin and LY294002 on inhibition of lung cancer growth. The indicated cell lines were seeded in 24-well plates and next day treated with rapamycin (Rap) alone, LY294002 (LY) alone, or the indicated combinations. The treatments were repeated every 3 days with fresh medium. After 12 days, the colonies were fixed, photographed **(*A*)** and counted **(*B*).** Each column represents a mean ± SD of triplicate determinations.

We further investigated the effects of rapamycin or RAD001 in combination with the PI3K/mTOR dual inhibitor, BEZ235, on the growth of human lung cancer cells both in cell culture and in animal xenograft models. The combination of RAD001 and BEZ235 was much more potent than each single agent in inhibiting the growth of human lung cancer cells, including induction of apoptosis and G1 cell cycle arrest. Similar results were also generated in a long-term colony formation assay. Again, we found that the concurrent combination of RAD001 and BEZ235 worked better than sequential treatments in inhibiting the growth of colonies (Figure 17), reinforcing our hypothesis that the concurrent combination of an mTOR inhibitor and a PI3K inhibitor is a potential cancer therapeutic regimen.

We conducted animal experiments to confirm our observations made from the RAD001 and BEZ235 combination treatments described previously. Similar to the cell culture results, the combination of RAD001 and BEZ235 was significantly more potent than each single agent in inhibiting the growth of lung cancer xenografts with minimal toxicity (Figure 18). Thus, this *in vivo* data supports the combination of an mTOR inhibitor and a PI3K inhibitor as a potential cancer therapeutic strategy.

Interestingly, we found that the combination did not inhibit the RAD001-induced p-Akt increase in cell culture. The work is ongoing to analyze p-Akt levels in various groups presented in Figure 18 to demonstrate if the combination inhibits RAD001-induced Akt phosphorylation *in vivo*.

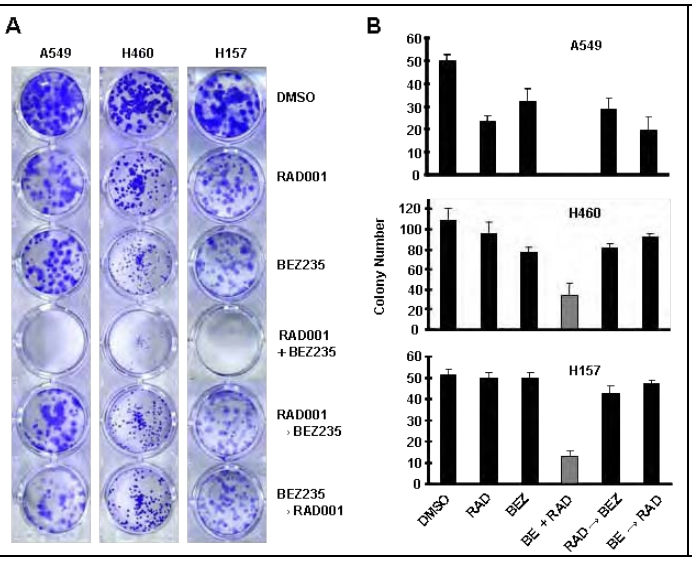


**Figure 17.** Effects of the combination of RAD001 and BEZ235 on the growth of cancer colonies. The indicated cell lines were seeded in 24-well plates and next day treated with RAD001 alone, BEZ235 alone, or the indicated combinations. The treatments were repeated every 3 days with fresh medium. After 12 days, the colonies were fixed, photographed **(*A*)** and counted **(*B*).** Each column represents a mean ± SD of triplicate determinations.

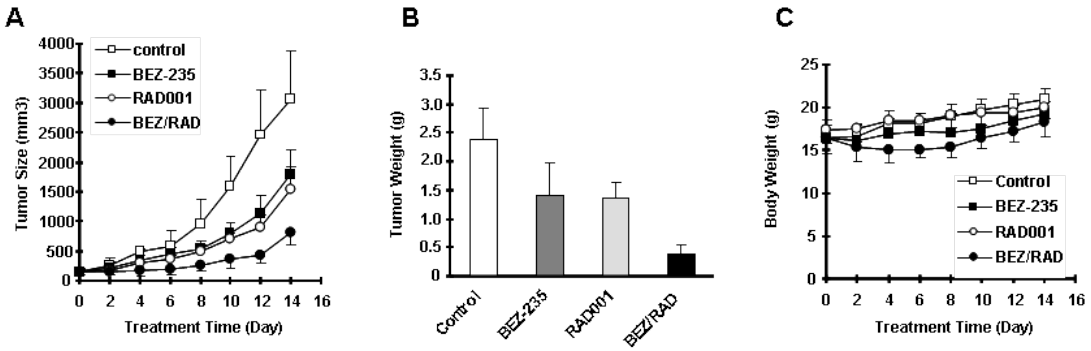


**Figure 18.** Effect of the RAD001 and BEZ235 combination on the growth of A549 xenograft. The tumors were treated with 3 mg/kg RAD001 (og), 20 mg/kg BEZ235 (og) or their combination for a consecutive 14 day treatment. The data are means ± SD (n = 6).

**Objective 2: To examine whether rapamycin-induced Akt activation suppresses ASK1-mediated apoptosis and leads to decreased therapeutic efficacy.**

**Summary of Research Findings**

Our previous annual report indicated a critical role of ASK2 in regulating ASK1 through recruiting 14-3-3 into the ASK1 protein complex. We have completed this study by demonstrating that phosphorylation of ASK2 at S964 induces 14-3-3 binding, which subsequently relays a survival signal to ASK1 through binding to phosphorylated ASK1 at S967. This work has been published in *Oncogene*.

In order to understand how Akt upregulation suppresses the ASK1 function in cells after rapamycin treatment, we examined the functional interaction between Akt and ASK1 as ASK1 is known to be regulated by Akt directly through phopshorylation at S83 site. Interestingly, we discovered that activated Akt induces phosphorylation of ASK1 at S967, a 14-3-3 binding site associated with cell survival. In support of this finding, treatment of cells with IGF1, which activate Akt, triggers ASK1 phosphorylation at S967 and an pS967-mediated 14-3-3 association. On the other hand, inhibition of PI3K, an upstream activator of Akt, reduces S967

phosphorylation. Thus, Akt may exert its impact on ASK1 through a dual mechanism through S83 and S967. We are currently exploring the mechanistic details.

mTOR inhibition by rapamycin induces Akt activation, which not only provides a feedback survival mechanism, but also releases an inhibitory mechanism through phosphorylation of PRAS40. PRAS40 is an Akt substrate, which in its unphosphorylated state can suppress mTOR function. Our recent studies reveal that PRAS40 is upregulated in lung cancer cells. In particular, the phosphorylated form of PRAS40 is present in lung cancer cells and tumor tissues as demonstrated by immunohistochemistry studies. We propose that phosphorylation of upregulated PRAS40 allows mTOR signaling and promotes tumorigenesis; we are currently testing this hypothesis. Together, our research suggests that Akt activation suppresses mTOR inhibitor's therapeutic efficacy, possibly through multiple mechanisms including ASK1 suppression and PRAS40 phosphorylation.

**Objective 3: To conduct two phase I clinical trials to test the efficacy of the combination of an mTOR inhibitor with an Akt or an EGFR inhibitor in advanced NSCLC patients resistant to the front and second line therapy, and assess the modulation of targeted biomarkers from tumor tissues before and after the treatment.**

**Summary of Research Findings**

A phase I study of the combination of everolimus and erlotinib in advanced NSCLC was conducted by our collaborators and led by Dr. Bruce Johnson at the Dana Farber Cancer Institute. We participated in a multi-institution randomized phase II study of erlotinib alone or in combination with everolimus for patients with advanced NSCLC following progression with prior platinum-based chemotherapy. Erlotinib was administered at the dose of 150 mg/day and everolimus was given at 5 mg/day PO. The primary endpoint of the study was to compare the disease control rate between the two treatment arms. A total of 133 patients were enrolled, and the disease control rate at 3 months was 40% for the combination and 28% for erlotinib monotherapy. The median progression-free survival also favored the combination of the two agents (2.9 m vs. 2.0 m), which was tolerated well by our patients. Overall, the study documented a modest efficacy advantage for the combination of erlotinib and everolimus. The next phase of this project is to evaluate the baseline tumor tissues collected from these patients to study the expression of various mTOR-related biomarkers and to correlate these results with the documented patient outcomes.

**Key Research Accomplishments:**

- Demonstrated that concurrent combination of an mTOR inhibitor and a PI3K inhibitor is a potential cancer therapeutic strategy.
- Discovered a new mechanism by which Akt induces ASK1 phosphorylation at S967.
- Revealed dysregulated PRAS40 in the mTOR complex in lung cancer cells and tumor tissues, which may represent a new biomarker for future studies.

**Conclusions**

Concurrent combination of an mTOR inhibitor and a PI3K inhibitor is a potential cancer therapeutic strategy as demonstrated by our research findings. Since the combination of an EGFR inhibitor and an mTOR inhibitor only demonstrated modest improvement in efficacy, our future plans will include the evaluation of predictive biomarkers for this combination and may

lead to the evaluation of a new combination consisting of an mTOR inhibitor and a PI3K inhibitor based on our preclinical observations.

**Biostatistics and Data Management Core**

(Core Director: J Jack Lee, Ph.D.)

In close collaboration with the Biomarker Core, the clinical research team, and each of the basic science research components, the Biostatistics and Data Management Core (BDMC) for the Department of Defense (DoD) BATTLE lung cancer research program is a comprehensive, multi-lateral resource for designing clinical and basic science experiments; developing and applying innovative statistical methodology, data acquisition and management, and statistical analysis; and publishing translational research generated by this research proposal.

The main objectives of the BDMC are as follows:

1. Develop and implement a novel adaptive randomization scheme for assigning patients into the treatment arms with the highest probability of success.
2. Provide the statistical design, sample size, and power calculations for each project.
3. Develop a secure, internet-driven, web-based database network between UTMDACC and other research centers, including Emory University and the Dana-Farber Cancer Center, that integrates the clinical data generated by the five proposed clinical trials and relating basic science research efforts of the BATTLE research project.
4. Develop a comprehensive, Web-based database management system for tissue specimen tracking and distribution and for a central repository of all biomarker data.
5. Provide all statistical data analyses, including descriptive analysis, hypothesis testing, estimation, and modeling of prospectively generated data.
6. Provide prospective collection, entry, quality control, and integration of data for the basic science, pre-clinical, and clinical studies in the BATTLE grant.
7. Provide study monitoring and conduct that ensures patient safety by timely reporting of toxicity and interim analysis results to various institutional review boards (IRBs), the UTMDACC data monitoring committee, the DoD, and other regulatory agencies.
8. Generate statistical reports for all projects.
9. Collaborate with all project investigators and assist them in publishing scientific results.
10. Develop and adapt innovative statistical methods pertinent to biomarker-integrated translational lung cancer studies.

**Summary of Research Findings**

In the fourth and last funded year, the Biostatistics and Data Management Core continued to work with all project investigators and provide biostatistics and database management support for all projects and cores in the BATTLE program. The clinical trial operations, including patient registration, randomization, clinical visits, and outcome evaluation, have progressed as planned. We have completed the clinical trial enrollment and the evaluation of the primary endpoint.

(A) Biostatistics

We have implemented a novel study design incorporating the hierarchical Bayesian model and adaptive randomization to identify the best treatment for each patient's biomarker profile and to adaptively randomize more patients into more effective treatments accordingly. We have worked with clinical investigators on protocol amendments. We provided statistical reports for

our monthly project meetings to update the accrual, randomization, and demographic data of the patients on trial. We designed and implemented the adaptive randomization phase of the trial, and the adaptive randomization program was written in a statistical package "R." Web-based services were applied to integrate the adaptive randomization program with the main Web-interfaced database application. The study has a steady accrual rate of 9.5 patients registered and 7.1 patients randomized per month. The study accrual and randomization were completed in October 2009. We registered a total of 341 patients and randomized 255. From November to December 2009, our Core facilitated a systematic, blinded review of the primary endpoint (i.e., 8-week disease control status) for all randomized patients. We reported the most updated interim results to the Data Safety and Monitoring Board (DSMB) in December 22, 2009, and requested to unblind the data for the analysis of primary data. The DSMB approved the unblinding of the study and concluded the monitoring of this trial. The main results based on the analysis of the primary endpoint were submitted to the late-breaking sessions of the Annual Meeting of the American Associations for Cancer Research (AACR) and was presented to the External Advisory Board on February 12, 2010 (see also Aim 1 for clinical results). The abstract was presented at the Opening Plenary Session of the AACR Annual meeting on April 18, 2010. Based on extensive data analysis, the following reports were generated.

*Statistical Reports Generated*

- Patient characteristics report on the main medical demographical information.
- Main efficacy report on 8-week disease control status, progression-free survival, and overall survival. Analyses were performed for each treatment by marker group and by each individual biomarker.
- Biopsy report on the sites and complications of the biopsy.
- Biomarker report for the distribution of each of the 11 markers measured and the marker groups.
- Toxicity report by patient and by incidence for each treatment.
- Compliance report for drug compliance.
- Randomizing report detailing the probability of randomization for each patient during the adaptive randomization phase.
- Discovery biomarker report on the analysis of microarray data and CAF data.

(B) Data Management

*Database tasks*

- The On Study EKG Form now allows for non-numeric study weeks.
- Added support for "inevaluable" and "too early" overall tumor measurement responses in data entry as well as the protocol summary report.
- Tissue Inventory has additional enhancements to fix some potential data entry issues.
- The comment fields now allow additional text input in several forms.
- The "Patients on a protocol" report includes the umbrella protocol patients.
- The administrative tool was enhanced to allow for easier removal of duplicate data.
- Changes to the reporting tool were made to correct some minor bugs.

*Database programming effort*

- Generated Blood Sample Inventory Reports to get an accurate inventory as well as an updated sample storage location.
- Updated the patient evaluable status and the 8-week disease control status once patient enrollment closed,

- Data dumps were generated, both independently and with research nurses, on most forms to spot check data for accuracy and to improve data accuracy.
- Generated reports to analyze the adaptive randomization results based on previous observed and posterior treatment responses.

**Key Research Accomplishments:**

- Developed and implemented a novel adaptive randomization design for the BATTLE program.
- Performed extensive statistical analysis on the study findings including treatment efficacy, toxicity, compliance, pre-specified biomarkers, and discovery biomarkers, etc.
- Developed and maintained a secured, web-based database application to assist with the data collection and analysis.
- A web-based database application is developed, deployed, and maintained at: https://insidebiostat/DMI_BATTLE/Common/Login.aspx.

**Conclusions**

In collaboration with clinical investigators, research nurses, the Biomarker Core, and basic scientists, the Biostatistics and Data Management Core has continued to deliver the biostatistics and data management support as proposed.

**Biomarker Core: Perform biomarker assessment to stratify patients into a particular arm of clinical trials and coordinate the distribution of clinical samples.**

(Core Director: Ignacio Wistuba, M.D.)

The Biomarker Core, in close collaboration with the Biostatistics and Data Management Core, the Clinical Trial team, and Research Project Investigators, has played an important role in achieving the objectives proposed in the aims of the proposed BATTLE program by acquiring and processing lung cancer tissue specimens and performing the biomarker analysis for the stratification of patients into the clinical trials. In addition, the Core has collected and banked tissue specimens to support mechanistic studies of response or resistance to targeted agents used in the BATTLE trials.

The Biomarker Core has successfully combined standard methods of histopathology processing and assessment of lung cancer tissue specimens with more advanced tools of molecular and genetic biomarker analyses.

**Objective 1: To acquire, bank, process, and distribute tumor and blood specimens obtained from BATTLE enrolled patients for biomarker analyses and molecular mechanistic studies of targeted agents.**

**Summary of Research Findings**

The Biomarker Core completed the collection and processing of all patients enrolled in the BATTLE clinical trial in December 2009. The Core collected and processed NSCLC tumor tissue specimens from 324 patients for biomarker analysis. Of the 324 specimens collected, 270 (83%) cases yielded enough tumor cells to examine and report a complete set of biomarkers as

proposed (see Objective 2 - Table 1). We were not able to detect enough viable tumor cells (higher that 50 cell/slide) for biomarker analysis in 54 (17%) patients; in these specimens, the most frequent findings were necrotic tumor tissue and dense fibrosis. We obtained 171 tissue specimens from lung tumor sites, and the remaining specimens were collected from metastatic sites (including 45 lymph nodes, 36 liver, 30 adrenal glands, 26 soft tissues/skin, 8 mediastinum, and 8 pleura). NSCLC histology types included 197 adenocarcinoma (61%), 30 squamous cell carcinoma (9%), and 40 NSCLC not otherwise specified (12%).

At least one fresh tumor tissue core obtained from 257/270 (95%) cases was snap-frozen, and those specimens were distributed to Dr. Wistuba's lab for mRNA and protein profiling. Of these, histology quality control was performed in 175 frozen tissues samples, and malignant cells were detected in 143 (82%) of cases.

The residual tissue specimens of formalin-fixed and paraffin-embedded (FFPE) tissues of all the evaluated biopsies were banked in the Biomarker Core, and they represent 588 tissue blocks from 266 cases (2.2 block/case; range 1-4) and 3,965 unstained histology sections from 246 cases (16 slides/case; range 1-36).

In addition, in close collaboration with the Biostatistics Core and the Clinical Trial team, we collected diagnostic, pre-chemotherapy tissue specimens from over 120 BATTLE patients; this collection is still in progress. We will use these diagnostic tissue specimens to compare the expression of molecular markers before and after chemotherapy treatments.

**Objective 2: To perform biomarker analyses and report results in a timely fashion for patient stratification in the BATTLE trials and molecular mechanistic studies of the targeted agents.**

**Summary of Research Findings**

Tissue specimen workflow for biomarker analysis

We completed the tissue processing and histology assessment of all 324 tumors biopsied 24 hours after specimen collection. We performed the analysis of the 11 molecular markers from the 270 tumors with adequate malignant cells, and recorded the results in the Web-based clinical trial database within 14 days in more than 99% of cases.

Biomarker analyses

Biomarkers examined using the formalin-fixed and paraffin-embedded tissues in the lung tumor specimens are listed in Table 7. DNA for mutation analyses of *EGFR*, *KRAS* and *BRAF* genes was extracted from microdissected tissue obtained under direct microscope observation from hematoxylin-eosin (H&E) stained tissue sections.

**Table 7.** Biomarkers examined in lung cancer biopsy samples and for patient stratification in the clinical trial.

| Molecular Pathway | Biomarkers | Type of Analysis |
|---|---|---|
| EGFR | *EGFR* Mutation (exons 18 to 21)<br>*EGFR* Increased Copy Number (polysomy/amplification) | DNA sequencing<br>DNA FISH[1] |
| K-Ras/B-Raf | *K-RAS* Mutation (codons 12,13, 61)<br>*B-RAF* Mutations (exons 11 and 15) | DNA sequencing<br>DNA sequencing |
| Angiogenesis | VEGF Expression<br>VEGFR-2 Expression | Protein IHC[2]<br>Protein IHC |
| RXRs/Cyclin D1 | RXR $\alpha$, $\beta$, $\gamma$ Expression<br>Cyclin D1 Expression<br>Cyclin D1 Amplification | Protein IHC<br>Protein IHC<br>DNA FISH |

Summary of biomarker data

As stated above, we reported the complete set of biomarker results for the 270 patients enrolled in the clinical trial that had sufficient tissue for analysis of all 11 markers (Table 8).

**Table 8.** Summary of biomarker results in 270 NSCLC cases.

| Biomarker Group | Positive Cases |
|---|---|
| *EGFR* markers | 113 (42%) |
| *EGFR* mutation (exons 18-21) | 46 (17%) |
| *EGFR* FISH increased copy number | 105 (39%) |
| High polysomy | 60 (22%) |
| Gene amplification | 45 (17%) |
| | |
| KRas/BRaf | 51 (19%) |
| *KRAS* mutation (codons 12, 13 and 61) | 48 (18%) |
| *BRAF* mutation (exons 11 and 15) | 8 (3%) |
| | |
| Angiogenesis | 228 (84%) |
| VEGFR IHC expression (score >100) | 223 (83%) |
| VEGFR-2 IHC expression (score >100) | 97 (36%) |
| | |
| RXRs/CyclinD1 | 227 (84%) |
| RXR $\alpha$ nuclear IHC expression (score >30) | 213 (79%) |
| RXR $\alpha$ cytoplasmic IHC expression (score >200) | 3 (1%) |
| RXR $\beta$ cytoplasmic IHC expression (score >200) | 18 (7%) |
| RXR $\beta$ membrane IHC expression (score >200) | 0 |
| RXR $\gamma$ cytoplasmic IHC expression (score >200) | 24 (9%) |
| Cyclin D1 IHC Expression (score >10%) | 143 (53%) |
| Cyclin D1 FISH amplification | 26 (10%) |

**Key Research Accomplishments:**

- Established and maintained a system for tissue processing and molecular biomarker analysis of core biopsy tissue specimens from lung cancer patients in timely fashion (within 14 days).
- Collected, processed, and reported tissue histology in all biopsies obtained.
- Completed the tissue collecting, processing, and biomarker analysis of tissue specimens from all patients enrolled in the clinical trial and biopsied (N=324).

## Conclusions

The Biomarker Core has successfully combined standard methods of histopathology processing and assessment of lung cancer tissue samples while using more advanced tools of molecular and genetic biomarker analyses to prospectively examine molecular biomarkers for individualized targeted therapy in all 324 NSCLC patients enrolled and biopsied. We will continue to compare the pathology and biomarker expression of diagnostic tumor tissue specimens before chemotherapy with the specimens obtained in the BATTLE clinical trial. In addition, we will examine novel molecular abnormalities obtained in the mRNA profiling analysis of frozen tissue specimens using the residual tissue specimens banked.

## KEY RESEARCH ACCOMPLISHMENTS

**Specific Aim 1: To establish a clinical trial program using biomarker assessment to select individualized targeted therapy for previously treated chemorefractory advanced NSCLC patients.**

- Completed enrollment of this novel, complex study, resulting in 341 enrolled patients, 255 randomized patients, and more than 320 biopsies for analysis.
- Demonstrated quality tissue specimen acquisition and biomarker evaluation in more than 80% of processed cases.
- Demonstrated highly efficient collaboration of clinical teams, Biostatistics Core, and Biomarker Core.

**Specific Aim 2.1. To validate the molecular mechanisms of response and resistance to erlotinib for patients with chemorefractory NSCLC.**

- Completed accrual of the phase II erlotinib trial as part of the BATTLE Program.
- Published studies that show *EGFR* T790M can be detected using plasma DNA from gefitinib- or erlotinib-resistant patients.
- Developed a technique to identify more than 100 circulating breast cancer and lung cancer cells in 7.5 mls of blood from patients with these cancers.
- Demonstrated the ability to detect gene amplification (*HER2*) in circulating tumor cells. This finding provides a proof-of-concept for studying the circulating tumor cells from patients with lung cancer and sensitizing mutations of *EGFR* as a mechanism of erlotinib resistance.

**Specific Aim 2.2. To investigate whether the resistance to erlotinib is mediated by the activation of type I insulin-like growth factor receptor (IGF-1R) signaling pathway**

- Demonstrated that the resistance to IGF-1R antibody MK0646 is independent of the mutational status of EGFR or K-ras *in vitro.*
- Demonstrated that treatment with MK0646 delayed tumor growth in H226B-GFP xenografts.

**Specific Aim 2.3. To investigate the molecular mechanisms of resistance to and biomarkers of the biologic activity of inhibitors of the VEGF pathway**

- Demonstrated one mechanism of resistance to VEGF inhibitors that involves activation of the stromal FGFR pathway, and proved that the stromal compartment may be a key player in the development of resistance.
- Identified a new population of circulating TEM+ endothelial cells (CTECs) that offers a specific biomarker for evaluating the effect of angiogenesis inhibitors and was evaluated in a set of clinical samples.
- Explored multiple platforms for determining CAF signatures has brought us closer to the goal of reaching CLIA certification for this method.
- Quantified CAFs in all samples from BATTLE study and are currently analyzing the data.

**Specific Aim 2.4. To investigate the molecular mechanisms of the effects of the combination of bexarotene and erlotinib on NSCLC cells**

- Demonstrated that GPRC5A interacts with EGFR at the cell membrane and serves as a substrate for the phosphorylation of tyrosine residues in the cytoplasmic domain.
- Demonstrated that the phosphorylation of tyrosine may decrease the activity of GPRC5A.

**Specific Aim 3: To identify biomarkers as novel predictors of clinical end points and potential therapeutic targets**

- Obtained biopsies from 324 patients in the clinical trial, with tumor tissue detected in 270 cases. Of these, frozen tissue specimens from 257 patients were made available for RNA extraction and for global gene expression analysis.
- Optimized a new RNA amplification protocol developed by NuGEN to generate high quality expression profiles suitable for bioinformatic analysis from core needle biopsies from lung cancer patients with chemorefractory tumors (BATTLE).
- Obtained high-quality mRNA expression signatures from fresh core needle biopsies from 171 BATTLE patients that will be correlated with tumors' genetic abnormalities identified by the Biomarker Core and with patients' outcome based on the targeted therapy treatment received.

**Specific Aim 4: To explore new preclinical combinations and their mechanisms of action by targeting mTOR signaling and develop phase I trials to test these combinations.**

- Demonstrated that concurrent combination of an mTOR inhibitor and a PI3K inhibitor is a potential cancer therapeutic strategy.
- Discovered a new mechanism by which Akt induces ASK1 phosphorylation at S967.
- Revealed dysregulated PRAS40 in the mTOR complex in lung cancer cells and tumor tissues, which may represent a new biomarker for future studies.

**Biostatistics and Data Management Core:**

- Developed and implemented a novel adaptive randomization design for the BATTLE program.
- Performed extensive statistical analysis on the study findings including treatment efficacy, toxicity, compliance, pre-specified biomarkers, and discovery biomarkers, etc.
- Developed and maintained a secured, web-based database application to assist with the data collection and analysis.
- A web-based database application is developed, deployed, and maintained at: https://insidebiostat/DMI_BATTLE/Common/Login.aspx.

**Biomarker Core:**

- Established and maintained a system for tissue processing and molecular biomarker analysis of core biopsy tissue specimens from lung cancer patients in timely fashion (within 14 days).
- Collected, processed, and reported tissue histology in all biopsies obtained.

- Completed the tissue collecting, processing, and biomarker analysis of tissue specimens from all patients enrolled in the clinical trial and biopsied (N=324).

## REPORTABLE OUTCOMES:

**Publications** (Attached in Appendix A)

Cockrell LM, Puckett MC, Goldman EH, Khuri FR, Fu H. Dual engagement of 14-3-3 proteins controls signal relay from ASK2 to the ASK1 signalosome. *Oncogene,* 2010 Feb 11;29(6):822-30. PMID: 19935702.

Fan S, Ramalingam SS, Kauh J, Xu Z, Khuri FR, Sun S-Y. Phosphorylated eukaryotic translation initiation factor 4 (eIF4E) is elevated in human cancer tissues. *Cancer Biology & Therapy.* 2009 Aug;8(15):1463-9. PMCID: PMC2804981.

Fu L, Kim YA, Wang X, Wu X, Yue P, Lonial S, Khuri FR, Sun S-Y. Perifosine inhibits mTOR signaling through facilitating degradation of major components in the mTOR axis and induces autophagy. *Cancer Research.* 2009 Dec 1;69(23):8967-76. PMCID: PMC2789206.

Hanrahan EO, Ryan AJ, Mann H, Kennedy SJ, Langmuir P, Natale RB, Herbst RS, Johnson BE, Heymach JV. Baseline vascular endothelial growth factor concentration as a potential predictive marker of benefit from vandetanib in non-small cell lung cancer. *Clinical Cancer Research*. 2009 May 15;15(10):3600-9. PMID: 19447868.

Kuang Y, Rogers A, Yeap BY, Wang L, Makrigiorgos M, Vetrand K, Thiede S, Distel RJ, Janne PA. Noninvasive Detection of EGFR T790Min Gefitinib or Erlotinib Resistant Non Small Cell Lung Cancer. *Clinical Cancer Research.* 2009 Apr 15;15(8):2630-6. PMCID: PMC2727796.

Mino-Kenudson M, Chirieac LR, Law K, Hornick JL, Lindeman N, Mark EJ, Cohen DW, Johnson BE, Jänne PA, Iafrate AJ, Rodig SJ. A novel, highly sensitive antibody allows for the routine detection of ALK-rearranged lung adenocarcinomas by standard immunohistochemistry. *Clinical Cancer Research.* 2010 Mar 1;16(5):1561-71. PMCID: PMC2831135.

**Manuscripts submitted, in revision, or in review** (Attached in Appendix A)

Cascone T, Herynk MH, Du D, Kadara H, Oborn CJ, Nilsson M, Park YY, Lee JS, Ciardiello F, Langley RR, Heymach JV. A role for stromal EGFR activation in resistance to VEGF blockade in human non-small cell lung cancer (NSCLC) xenograft models. *Submitted.*

Flores LM, Kindelberger DW, Ligon AH, Capelletti M, Fiorentino M, Loda M, Cibas ES, Janne PA, Krop IE, Improved yields of circulating tumour cells facilitates molecular characterization and recognition of discordant HER2 amplification in breast cancer. *British Journal of Cancer*, In Press.

**Abstracts** (Attached in Appendix A)

Cascone T, Herynk M, Du D, Kadara H, Hanrahan EO, Nilsson MB, Lin HY, Lee JJ, Park YY, Lee JS and Heymach JV (2009) Stromal HGF and VEGFR-1 are associated with acquired resistance to VEGFR tyrosine kinase inhibitors in non-small cell lung cancer (NSCLC). IASLC 13th World Conference on Lung Cancer, San Francisco, CA, 2009. 7956.

Cascone T, Herynk MH, Xu L, Kadara H, Hanrahan EO, Y-H F, Saigal B, Y-Y P, Lee J J, Langley RR, Jurgensmeier JM, Ryan AJ and Heymach JV. Increased HGF is associated with resistance to VEGFR tyrosine kinase inhibitors (TKIs) in non-small cell lung cancer (NSCLC).

Proceedings of the 101 st Annual Meeting of the A merican Association for Cancer Research; 2010 Apr 17-21; Washington, DC. Philadelphia (PA): AACR; 2010.1981. 376.

Kim ES, Herbst RS, Lee JJ, Blumenschein Jr. GR, Tsao A, Alden CM, Tang X, Liu S, Stewart DJ, Heymach JV, Tran HT, Hicks ME, Erasmus Jr. J, Gupta S, Powis G, Lippman SM, Wistuba II, Hong WK. The BATTLE trial (Biomarker-integrated Approaches of Targeted Therapy for Lung Cancer Elimination): personalizing therapy for lung cancer Proceedings of the 1 01st Annual Meeting of the American Association for Cancer Research; 2010 Apr 17-21; Washington, DC. Philadelphia (PA): AACR; 2010. LB-1.

Soria JC, Bennouna J, Leighl N, Khuri FR, Traynor AM. Johnson BE, Blais, N, Kay A, Jehl V, Papadimitrakopoulou V. Phase 2 study of everolimus plus erlotinib in previously treated patients with advanced non-small cell lung cancer. 34th Congress of the E uropean Society for Medical Oncology (ESMO), September 2009. P-9174.

Saintigny P, Zhang L, Girard L, Fan YH, Lee JJ, Herbst RS, Kim ES, Coombes K, Blumenschein G, Tsao A, Lam DC, Gerald WL, Beer DG, Tang X, Lippman SM, Mao L, Hong WK, Wistuba I, Minna J, Heymach JV. Development and testing of a m RNA expression signature correlated with the pr esence of *EGFR* mutations in non-small cell lung cancer. Presented as poster at the AACR-IASLC Joint Conference Molecular Origins of Lung Cancer: Prospects for Personalized Prevention and Therapy, Coronado, CA; and, 10th Annual Targeted Therapies of the Treatment of Lung Cancer, Santa Monica, CA.

Saintigny P, Byers LA, Zhang L, Yordy JS, Tang X, Girard L, Lang W, Fan YH, Ji L, Lee JJ, Kim ES, Hong WK, Lippman SM, Herbst RS, Minna J, Wistuba I, Heymach JV, Mao L. MYC down regulation and chemoresistance: evidence from the Biomarker-Based Approaches of Targeted Therapy for Lung Cancer Elimination (BATTLE) program. Proceedings of the 10 1st Annual Meeting of the American Association for Cancer Research; 2010 Apr 17-21; Washington, DC. Philadelphia (PA): AACR; 2010.1981.

## CONCLUSIONS

**Aim 1:** We are excited to report the completion of enrollment to the BATTLE program. Accrual to this ground-breaking study exceeded our goals. We have supported the early efforts in biomarker discovery in collaboration with the other projects and have initiated formal data analysis. A high-profile plenary session presentation was given by the BATTLE PI, Dr. Edward Kim at the 2010 AACR Annual Meeting in Washington, DC, to summarize the BATTLE results.

**Aim 2.1:** Both *EGFR* activating and *EGFR* T790M can be identified in 70% of patients with known tumor *EGFR*-activating (21/30) or T790M (5/7) mutations. The secondary acquired resistance T790M EGFR mutation was identified from plasma DNA in 15 of the 28 (54%) patients with prior clinical response to gefitinib/erlotinib, 4 of 14 patients (29%) with prior stable disease, and in 0 of 12 patients with primary progressive disease or were untreated with gefitinib/erlotinib**:**

The median cell count from patients with breast cancer using the CPK was 117 vs 4 for CEK (P<0.0001). Lung cancer samples were similar; CPK: 145 cells vs CEK:4 cells (P<0.0001). Recovered CTCs were relatively pure (60–70%) and were evaluable by FISH and immunofluorescence. A total of 10 of 30 ( 33%) breast cancer patients with HER2-negative primary and metastatic tissue had HER2-amplified CTCs. These data provide evidence that we will likely be able to detect *MET* amplification in circulating lung cancer cells in patients with *EGFR* sensitizing mutations.

**Aim 2.2:** Our results suggested that (a) resistance to IGF-1R antibody MK0646 does not seem to depend on the mutational status of EGFR or K-ras *in vitro* and (b) treatment with MK0646 delayed tumor growth in H226B-GFP xenograft, while that treatment did not affect tumor growth in H226B-KRas xenograft. Response to MK0646 *in vitro* was not consistent to that in *in vivo* with H226B-GFP cells, and this discordance should be further investigated.

**Aim 2.3:** Our preclinical studies have identified a number of potential markers that predict response to VEGFR inhibitors. We are interested to see if further testing proves these same markers can be used to predict response in patient samples. In addition, our studies have identified a new population of cells that can be detected that identify circulating endothelial cells derived from tumor endothelium. Analysis of this population of cells in patients treated with angiogenesis inhibitors is likely to be a better prognostic marker of response to treatment.

Several plasma CAFs are associated with specific tumor-derived pathway activation. Our preliminary study suggests that broad-based plasma profiling of cytokines and angiogenic factors may be a feasible approach for identifying markers of activation of tumor signaling pathways. In addition to the evaluation of pathway activation using plasma samples, we will be evaluating modulation of CAFs by each treatment arm and searching for potential predictive plasma signatures with clinical outcome measures such as progression-free survival (PFS). The final step will be to validate the plasma predictive signature derived from BATTLE with other randomized clinical studies. These studies can also validate our results that identify circulating VEGF as a predictive marker of response to angiogenic therapies in other clinical studies.

**Aim 2.4:** This finding is consistent with the increased disease control rate observed in patients treated with erlotinib plus bexarotene, compared to that achieved in patients receiving erlotinib alone, in the BATTLE clinical trial (see Aim 1). Our finding explains at least in part the biological basis for the enhanced efficacy of the combination.

**Aim 3:** During this project period, we demonstrated that global gene expression profiles can be successfully obtained using residual tumor biopsies after fulfilling required biomarker analysis. We optimized new RNA amplification protocols to produce high quality gene expression mRNA profiles for correlative analysis with tumors' genetic and patients' clinical parameters, including response and outcome after treatment.

**Aim 4**: Concurrent combination of an mTOR inhibitor and a PI3K inhibitor is a potential cancer therapeutic strategy as demonstrated by our research findings. Since the combination of an EGFR inhibitor and an mTOR inhibitor only demonstrated modest improvement in efficacy, our future plans will include the evaluation of predictive biomarkers for this combination and may lead to the evaluation of a new combination consisting of an mTOR inhibitor and a PI3K inhibitor based on our preclinical observations.

**Biostatistics and Data Management Core:** In collaboration with clinical investigators, research nurses, the Biomarker Core, and basic scientists, the Biostatistics and Data Management Core has continued to deliver the biostatistics and data management support as proposed.

**Biomarker Core:** The Biomarker Core has successfully combined standard methods of histopathology processing and assessment of lung cancer tissue samples while using more advanced tools of molecular and genetic biomarker analyses to prospectively examine molecular biomarkers for individualized targeted therapy in all 324 NSCLC patients enrolled and biopsied. We will continue to compare the pathology and biomarker expression of diagnostic tumor tissue specimens before chemotherapy with the specimens obtained in the BATTLE clinical trial. In addition, we will examine novel molecular abnormalities obtained in the mRNA profiling analysis of frozen tissue specimens using the residual tissue specimens banked.

**References:**

1. Bild AH, Yao G, Chang JT, et al. Oncogenic pathway signatures in human cancers as a guide to targeted therapies. Nature 2006;439:353-7.
2. Lam DC, Girard L, Ramirez R, et al. Expression of nicotinic acetylcholine receptor subunit genes in non-small-cell lung cancer reveals differences between smokers and nonsmokers. Cancer Res 2007;67:4638-47.
3. Shedden K, Taylor JM, Enkemann SA, et al. Gene expression-based survival prediction in lung adenocarcinoma: a multi-site, blinded validation study. Nat Med 2008;14:822-7.
4. Zhou BB, Peyton M, He B, et al. Targeting ADAM-mediated ligand cleavage to inhibit HER3 and EGFR pathways in non-small cell lung cancer. Cancer Cell 2006;10:39-50.
5. Chitale D, Gong Y, Taylor BS, et al. An integrated genomic analysis of lung cancer reveals loss of DUSP4 in EGFR-mutant tumors. Oncogene 2009;28:2773-83.
6. Bhattacharjee A, Richards WG, Staunton J, et al. Classification of human lung carcinomas by mRNA expression profiling reveals distinct adenocarcinoma subclasses. Proc Natl Acad Sci U S A 2001;98:13790-5.
7. Han JY, Oh SH, Morgillo F, Myers JN, Kim E, Hong WK, et al. Hypoxia-inducible factor 1alpha and antiangiogenic activity of farnesyltransferase inhibitor SCH66336 in human aerodigestive tract cancer. J Natl Cancer Inst. 2005 Sep 7;97(17):1272-86.
8. Lee HY, Moon H, Chun KH, Chang YS, Hassan K, Ji L, et al. Effects of insulin-like growth factor binding protein-3 and farnesyltransferase inhibitor SCH66336 on Akt expression and apoptosis in non-small-cell lung cancer cells. J Natl Cancer Inst. 2004 Oct 20;96(20):1536-48.

# APPENDIX

# Abstracts and Publications

Oncogene (2010) 29, 822–830
© 2010 Macmillan Publishers Limited All rights reserved 0950-9232/10 $32.00
www.nature.com/onc

ORIGINAL ARTICLE

# Dual engagement of 14-3-3 proteins controls signal relay from ASK2 to the ASK1 signalosome

LM Cockrell[1,2,4], MC Puckett[1,2,4], EH Goldman[1,2], FR Khuri[3] and H Fu[1,2,3]

[1]*Program in Molecular and Systems Pharmacology of the Graduate Division of Biological and Biomedical Sciences, Emory University, Atlanta, GA, USA;* [2]*Department of Pharmacology, Emory University, Rollins Research Center, Atlanta, GA, USA and* [3]*Department of Hematology and Medical Oncology, Winship Cancer Institute, Emory University, Atlanta, GA, USA*

**Faithful and efficient transmission of biological signals through mitogen-activated protein kinase (MAPK) pathways requires engagement of highly regulated cellular machinery in response to diverse environmental cues. Here, we report a novel mechanism controlling signal relay between two MAP3Ks, apoptosis signal-regulating kinase (ASK) 1 and ASK2. We show that ASK2 specifically interacts with 14-3-3 proteins through phosphorylated S964. Although a 14-3-3-binding defective mutant of ASK1 (S967A) has no effect on the ASK2/14-3-3 interaction, both overexpression of the analogous ASK2 (S964A) mutant and knockdown of ASK2 dramatically reduced the amount of ASK1 complexed with 14-3-3. These data suggest a dominant role of ASK2 in 14-3-3 control of ASK1 function. Indeed, ASK2 S964A-induced dissociation of 14-3-3 from ASK1 correlated with enhanced phosphorylation of ASK1 at T838 and increased c-Jun N-terminal kinase phosphorylation, the two biological readouts of ASK1 activation. Our results suggest a model in which upstream signals couple ASK2 S964 phosphorylation to the ASK1 signalosome through dual engagement of 14-3-3.**
*Oncogene* (2010) **29,** 822–830; doi:10.1038/onc.2009.382; published online 23 November 2009

**Keywords:** ASK1; ASK2; 14-3-3; apoptosis; mitogen-activated protein kinase

## Introduction

The evolutionarily conserved mitogen-activated protein kinase (MAPK) cascades consist of tiered protein kinases that undergo sequential phosphorylation and activation, allowing specific signal amplification to elicit a corresponding cellular response (Kyriakis and Avruch, 2001; Winter-Vann and Johnson, 2007). Each cascade module consists of an MAPK, an MAPK kinase (MAP2K), and an MAPK kinase kinase (MAP3K). MAPK cascades are activated by diverse stimuli to mediate multiple signaling pathways, resulting in a crucial impact on cell fate processes such as cell growth, differentiation and death. Among the MAPK cascades, those triggered by the MAP3K apoptosis signal-regulating kinase 1 (ASK1) are critical determinants of apoptosis (Wang *et al*., 1996; Ichijo *et al*., 1997; Takeda *et al*., 2008). ASK1 activation leads to phosphorylation and activation of MAP2K4/7 or MAP2K3/6 and the resulting MAPKs c-Jun N-terminal kinase (JNK) and p38 activation, respectively. A variety of intrinsic and extrinsic cellular stress stimuli induce ASK1 activation. For example, ASK1 relays signals from death receptors, such as those activated by tumor necrosis factor $\alpha$ (Chang *et al*., 1998). ASK1 is also activated by unfolded protein response-induced endoplasmic reticulum stress (Nishitoh *et al*., 2002). Recently, important physiological and pathological roles of ASK1 have emerged to include the regulation of innate immunity, cellular differentiation, and various human diseases such as cardiac hypertrophy and remodeling, insulin resistance, neurodegeneration and tumorigenesis (Izumiya *et al*., 2003; Matsuzawa *et al*., 2005; Imoto *et al*., 2006; Osaka *et al*., 2007; Iriyama *et al*., 2009). Because of its importance as a central mediator of diverse developmental and stress signals, ASK1 activation is tightly controlled. The newly defined ASK1 signalosome reflects the numerous phosphorylation and protein interaction events critical to maintain ASK1 regulation (Takeda *et al*., 2007).

One important ASK1 regulatory protein is 14-3-3, a phosphoserine/threonine-recognition protein (Fu *et al*., 2000; Yaffe, 2002; Mackintosh, 2004; Muslin and Lau, 2005; Aitken, 2006; Gardino *et al*., 2006; Morrison, 2009). 14-3-3 is a multifunctional regulatory protein that is important in maintaining a multitude of cellular processes, including cell cycle control, cell proliferation and inhibition of apoptosis. Seven mammalian isoforms of 14-3-3 have been identified and are denoted by Greek lettering ($\gamma$, $\tau$, $\zeta$, $\sigma$, $\beta$, $\varepsilon$, $\eta$). 14-3-3 binds to the majority of its cellular ligands through a phosphorylated motif. The canonical 14-3-3 recognition motif has been identified as RSXpSXP, in which phosphorylation of the second serine is critical for 14-3-3 recognition (Muslin *et al*., 1996; Yaffe *et al*., 1997). Binding of 14-3-3 to ASK1 through a phosphorylated S967 motif (RSIS$^{967}$LP) has been shown to decrease ASK1 kinase activity and inhibit ASK1-induced apoptosis (Zhang *et al*., 1999a, 2003; Goldman *et al*., 2004).

Correspondence: Dr H Fu, Department of Pharmacology, Emory University, 5111 Rollins Research Center, 1510 Clifton Road, Atlanta, GA 30322, USA.
E-mail: hfu@emory.edu
[4]These authors contributed equally to this work.
Received 2 September 2008; revised 20 July 2009; accepted 30 September 2009; published online 23 November 2009

Recently, another MAP3K, ASK2, was found to bind with ASK1 (Wang *et al*., 1998b). ASK2 has been shown to function as a tumor suppressor in combination with ASK1, and ASK2 levels are reduced in human gastrointestinal cancers (Iriyama *et al*., 2009). The heteromeric complex of ASK1 and ASK2 is thought to have reciprocal functionality, which means that ASK1 and ASK2 function to activate each other (Osaka *et al*., 2007). ASK2 activation of ASK1 is mediated by phosphorylation of T838 within the activation loop of the human ASK1 kinase domain, whereas ASK1 activation of ASK2 seems to occur through a phosphorylation-independent mechanism. Thus, dissection of ASK1-associated protein interactions may offer opportunities to gain further understanding of the general mechanisms controlling signal transmission through MAP3Ks.

Here we describe a novel mechanism by which ASK2 suppresses ASK1 function through the induced recruitment of 14-3-3 proteins. Our work establishes a new signaling complex consisting of ASK2, ASK1 and 14-3-3, suggests an inhibitory function of ASK2 for ASK1, and reveals a dynamic signal-relay function for the family of 14-3-3 proteins.

## Results

*ASK2 specifically interacts with 14-3-3 proteins*

In our mechanistic study of the ASK1 signalosome, we noticed the presence of a putative 14-3-3 recognition motif surrounding S916 (RSPS$^{916}$SP) in the C-terminus of ASK2. This motif fits well with the defined consensus 14-3-3 binding motif, RSXpSXP, and raises the possibility of ASK2 as a new 14-3-3 target protein (Gardino *et al*., 2006). To test whether ASK2 interacts with 14-3-3, we carried out a series of affinity pulldown assays using $Ni^{2+}$-charged resin to isolate hexahistidine (6xHis) tagged 14-3-3γ protein complexes from COS7 cell lysates. 14-3-3γ K50E, a ligand-binding defective mutant, was used as a control (Thorson *et al*., 1998; Zhang *et al*., 1999b). As revealed by western blot, glutathione *S*-transferase (GST)-ASK2 was found within the 14-3-3γ wild-type (WT) complex, but was absent in the K50E complex (Figure 1a), suggesting a specific interaction of ASK2 with 14-3-3γ. Consistent with a potential role of ASK2 S916 in 14-3-3 binding, a truncated ASK2 lacking the sequence N-terminal to the kinase domain (ASK2–KC: 638–1288 aa) was still capable of binding with 14-3-3γ (Figure 1a). To confirm this interaction, a reciprocal experiment was performed. When Flag-ASK2–KC was isolated from COS7 cell lysates using co-immunoprecipitation (co-IP), 14-3-3γ WT, but not K50E, was found in the resulting ASK2 protein complex (Figure 1b). In further support of these results, 14-3-3γ was also able to pull down endogenous ASK2 (Figure 1c). Together, the above data suggest that ASK2 specifically interacts with 14-3-3γ through a binding site mapped to the KC fragment of the ASK2 protein. Therefore, ASK2–KC was used to further characterize binding with 14-3-3 in subsequent experiments.

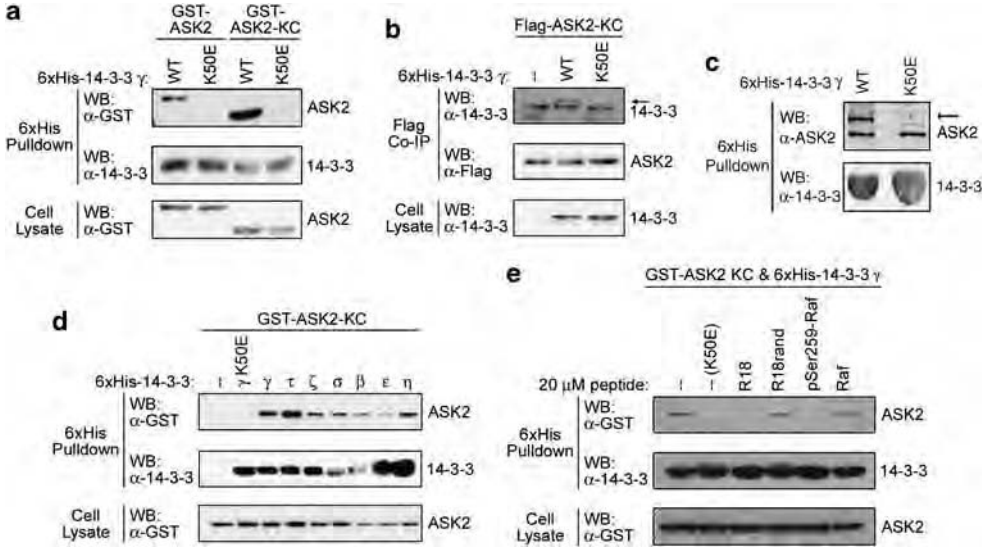


**Figure 1** Interaction of apoptosis signal-regulating kinase 2 (ASK2) with 14-3-3 proteins. (**a**) ASK2 is in complex with 14-3-3γ. COS7 cells were co-transfected with either glutathione *S*-transferase (GST)-ASK2 or GST-ASK2–KC and hexahistidine (6xHis)-14-3-3γ wild type (WT) or K50E. The 14-3-3 protein complex was isolated 40 h after transfection with $Ni^{2+}$-charged resin and bound ASK2 was visualized by western blot. (**b**) 14-3-3 binds to ASK2 in a reverse co-immunoprecipitation (co-IP) assay. COS7 cell lysates overexpressing Flag-ASK2–KC and 6xHis-14-3-3γ WT or K50E were used to isolate the ASK2–KC complex with an anti-Flag antibody. The resulting ASK2 protein complex was used for the detection of 14-3-3 by western blot. (**c**) 14-3-3 specifically binds endogenous ASK2. COS7 cells were transfected with 6xHis-14-3-3γ (WT or K50E). The 14-3-3 γ complex was isolated with $Ni_2^+$-charged resin, and endogenous ASK2 was detected by western blot. (**d**) Interaction of ASK2 with multiple 14-3-3 isoforms. The isolation of the 14-3-3 isoform complex and the detection of ASK2 in each 14-3-3 complex were determined as in (**a**). (**e**) Competitive binding of ASK2 to 14-3-3 with defined 14-3-3 peptide antagonists. The 14-3-3/ASK2 complexes were isolated with an affinity pulldown assay as in (**a**), either in the presence or in the absence of antagonistic peptides (pSer259Raf and R18). Non-phosphorylated Raf peptide (Raf) or a randomized R18 peptide (R18rand) was used as control.

There are seven 14-3-3 isoforms in mammalian cells (γ, τ, ζ, σ, β, ε, η). 14-3-3 interaction with ASK2 is not unique to the γ isoform, as ASK2 was found in complex with all seven 14-3-3 isoforms (Figure 1d). These data imply that ASK2 may use a common binding site within 14-3-3 proteins, such as the conserved amphipathic groove within the 14-3-3 structure (Gardino *et al*., 2006). To test this possibility, we used two approaches: peptide competition assay and mutational analysis. Indeed, two well-defined 14-3-3 groove-binding peptides, a phosphorylated Raf peptide (pSer259-Raf) and an unphosphorylated antagonist peptide (R18), effectively competed away ASK2's interaction with 14-3-3γ (Figure 1e) (Muslin *et al*., 1996; Petosa *et al*., 1998; Wang *et al*., 1999). Conversely, inclusion of the respective peptide controls, unphosphorylated Raf peptide (Raf) or randomized R18 peptide (R18rand), showed no competitive effect. In further support of the involvement of the amphipathic groove in ASK2 binding, several charge-reversal mutations of 14-3-3ζ amino acid residues within the groove (K49E, R56E, R60E, V176D) greatly diminished interaction with ASK2 (data not shown; Wang *et al*., 1998a, b; Zhang *et al*., 1999b). These data show how the amphipathic groove of 14-3-3 proteins is used as an ASK2 docking site, allowing common and specific binding between 14-3-3 and ASK2.

*ASK2 requires phosphorylation for 14-3-3 binding*

We found that incubation of cell lysates at 37 °C led to a decrease in ASK2's interaction with 14-3-3γ (Figure 2a). This decrease is likely due to the increased action of an endogenous protein phosphatase(s), as the presence of a consensus motif (RSPS$^{916}$SP) within ASK2 predicts a phosphorylation requirement for recognition by 14-3-3. In support of this notion, the inclusion of general phosphatase inhibitors during this incubation prevented the dissociation (Figure 2a). The phosphorylation dependence of the interaction was further confirmed in a separate assay, in which calf intestinal phosphatase was shown to accelerate the dissociation of ASK2 from 14-3-3 (data not shown). This phenomenon allowed the use of more specific phosphatase inhibitors to validate the requirement of phosphorylation for the interaction and to define the class of protein phosphatases involved. At lower concentrations, okadaic acid is more specific for inhibition of the PP1/PP2A phosphatase family, whereas cyclosporine A is specific for inhibition of PP2B, or calcineurin (Cohen *et al*., 1989). Treatment of cells with okadaic acid, but not cyclosporine A, led to a dramatic increase in the amount of the ASK2/14-3-3γ complex (Figure 2b). From these data, we conclude that ASK2's interaction with 14-3-3 is negatively regulated by the PP1/PP2A phosphatase family, supporting the importance of a regulated phosphorylation dictating the ASK2/14-3-3 interaction.

*14-3-3 binds ASK2 through a novel S964-mediated motif*

Both the phosphorylation dependence of the ASK2/14-3-3 interaction and the presence of a putative 14-3-3 binding motif within the ASK2 sequence (RSPS$^{916}$SP) predict the importance of S916 as the critical phosphoacceptor mediating 14-3-3 interaction (Figure 3a). To test whether the S916-containing motif is indeed an essential determinant of 14-3-3 interactions, we performed a competitive binding assay using a phosphorylated peptide representing the residues surrounding S916 (pSer916-ASK2). Unexpectedly, this peptide failed to compete with ASK2 for 14-3-3 binding, even at concentrations up to 100 μM (Figure 3b). Intriguingly, this peptide also did not disrupt the interaction of 14-3-3 with Raf-1, another well-defined 14-3-3 client protein. However, it remained possible that this peptide did not have the correct conformation for effective competition. To specifically test whether ASK2 S916 was necessary for 14-3-3 binding, we performed site-directed mutagenesis to generate a nonphosphorylatable GST-ASK2 S916A mutant. GST-ASK2 S916A was fully capable of binding to 14-3-3γ (Figure 3c). We also mutated the serines within and around this predicted 14-3-3 binding motif in ASK2, generating S912A, S914A and S917A. However, none of these mutations showed any effect on the ASK2/14-3-3 association (Figure 3c). The failure of these mutations to inhibit ASK2 binding with 14-3-3, together with the lack of peptide competition using the putative phosphorylated motif, suggests that 14-3-3 targets a structure other than the S916-mediated motif for binding.

In search of the 14-3-3 binding site, we generated a series of deletion mutants within GST-ASK2–KC to further narrow down the binding region (depicted in

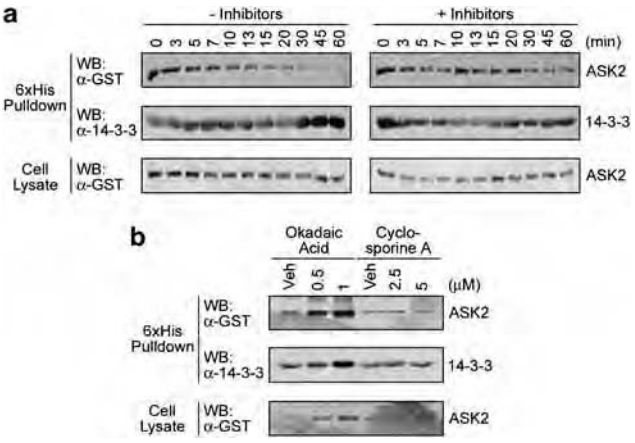


**Figure 2** The apoptosis signal-regulating kinase 2 (ASK2)/14-3-3 interaction requires phosphorylation. (**a**) Phosphatase inhibition increased the amount of ASK2/14-3-3 interaction. Cell lysates with co-expressed glutathione *S*-transferase (GST)-ASK2–KC and hexahistidine (6xHis)-14-3-3γ were divided into two samples, and incubated at 37 °C either in the presence or in the absence of 50 mM phosphatase inhibitors ($Na_4P_2O_7$, NaF, $Na_3VO_4$). The lysate was removed at the indicated times and subjected to affinity pulldown and western blot as in Figure 1a. (**b**) An inhibitor of the protein phosphatase 2A family blocks ASK2's dissociation from 14-3-3. Cells co-expressing GST-ASK2–KC and 6xHis-14-3-3γ were treated with increasing concentrations of either okadaic acid or cyclosporine A (Sigma), or vehicle (ethanol or methanol, respectively), for 1 h. Cell lysates were used in an affinity pulldown assay as described in Figure 1a.

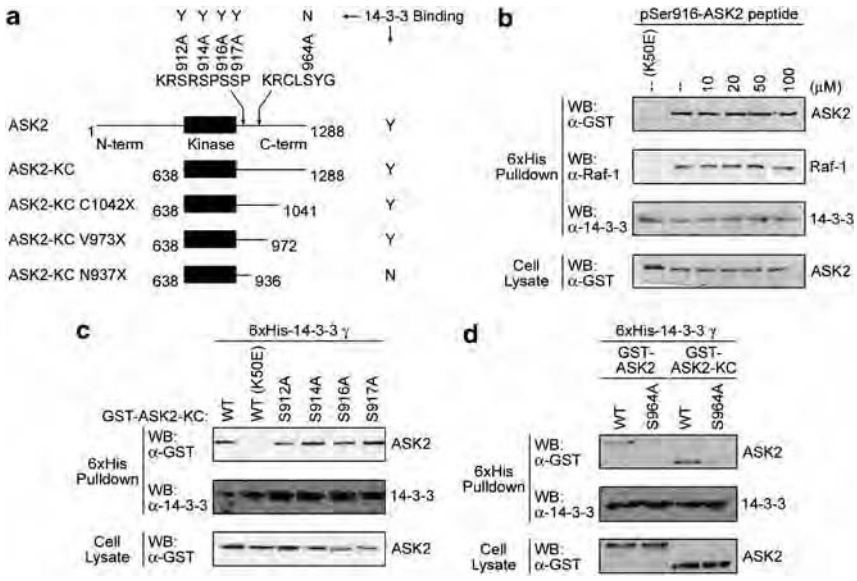


**Figure 3** Determination of the 14-3-3 binding site within apoptosis signal-regulating kinase 2 (ASK2). (**a**) Schematic of the predicted 14-3-3 recognition motifs within ASK2. Amino acid sequences surrounding the tested 14-3-3 binding motifs within ASK2 are shown, along with truncations and Ser to Ala mutations used in (**c**) and (**d**). Binding results summarized as positive (Y) or negative (N). (**b**) Competition with a pSer916-ASK2 peptide (NH2-CQPGKRSRSPpSSPRH-COOH) has no effect on the interaction of ASK2 with 14-3-3. Experiments were performed as in Figure 1d, and the 14-3-3/Raf-1 interaction was used as a control. (**c**) Mutations in the S916 motif of ASK2 fail to disrupt 14-3-3 binding. Point mutations were generated as shown, and the presence of mutated ASK2 in the 14-3-3 complex was determined as in Figure 1a. (**d**) ASK2 S964A abolishes binding to 14-3-3. COS7 cells were co-transfected with 6xHis-14-3-3γ and glutathione *S*-transferase (GST)-ASK2 and GST-ASK2–KC wild-type (WT) or S964A mutants. After transfection, cells were lysed and used in the previously described 14-3-3 affinity pulldown assay.

Figure 3a). Using these truncations, we localized the binding site within the ASK2 sequence between N937 and V973 (data not shown). Examination of the amino acid sequence within this region revealed that the most likely site for 14-3-3 recognition was a motif surrounding serine 964 (RCLS$^{964}$YG; Figure 3a). We then mutated the S964 residue to alanine (S964A), and used this mutant in an affinity pulldown assay. Mutation of this site did not affect the autokinase activity of ASK2 (Supplementary Figure S1). However, the single S964A point mutation alone was sufficient to diminish ASK2's interaction with 14-3-3 (Figure 3d), suggesting that phosphorylation at S964 has an essential function in 14-3-3 binding. Although minimal 14-3-3 binding was still seen to the S964A mutant, the significant loss of binding indicates that S964 is a critical 14-3-3 binding site. Thus, this study identifies S964 as the primary 14-3-3 recognition site within the ASK2 protein, and defines a novel, noncanonical 14-3-3 motif that may be present in other 14-3-3 client proteins.

### *14-3-3 is present in a ternary complex with ASK1 and ASK2*

It is interesting to note that 14-3-3 interacts with both ASK2 and ASK1 (Zhang *et al*., 1999a) (Figure 1). This suggests the possibility of the formation of an ASK2/ASK1/14-3-3 ternary complex within the ASK1 signalosome. To test this model, affinity pulldown assays were performed with COS7 cell lysates transfected with HA-ASK1, GST-ASK2 and 6xHis-14-3-3γ. Indeed, both ASK1 and ASK2 were present in the resulting 14-3-3 protein complex (Figure 4a). This complex occurred independently of the expression of either the full-length or the KC versions of GST-ASK2. Further, this ternary complex was confirmed with reverse pulldown assays, which showed that 14-3-3 and ASK1 were found in the GST–ASK2 complex, and 14-3-3 and ASK2 were in the HA–ASK1 complex (data not shown). Neither ASK1 nor ASK2 was present in the 6xHis-14-3-3γ K50E pulldown, suggesting that the ternary complex was mediated specifically by the amphipathic groove of 14-3-3. However, the above results did not rule out the possibility that ASK1/14-3-3 and ASK2/14-3-3 may be present in separate binary protein complexes. We therefore set out to test the specificity and functional significance of this ternary complex.

### *ASK2/14-3-3 interaction dictates ASK1/14-3-3 interaction*

The interaction of 14-3-3 with both ASK2 and ASK1 is dynamically regulated by phosphorylation through S964 of ASK2 and S967 of ASK1 (Zhang *et al*., 1999a) (Figure 3d). Point mutation of these sites to alanine allows the generation of ASK1 or ASK2 proteins that are specifically defective in 14-3-3 binding, permitting the examination of 14-3-3's contribution to the ASK1/ASK2 complex. We used 14-3-3-binding defective mutants of ASK1 (S967A) and ASK2 (S964A) to establish the interplay among 14-3-3, ASK2 and ASK1 in the ternary protein complex. These point mutations

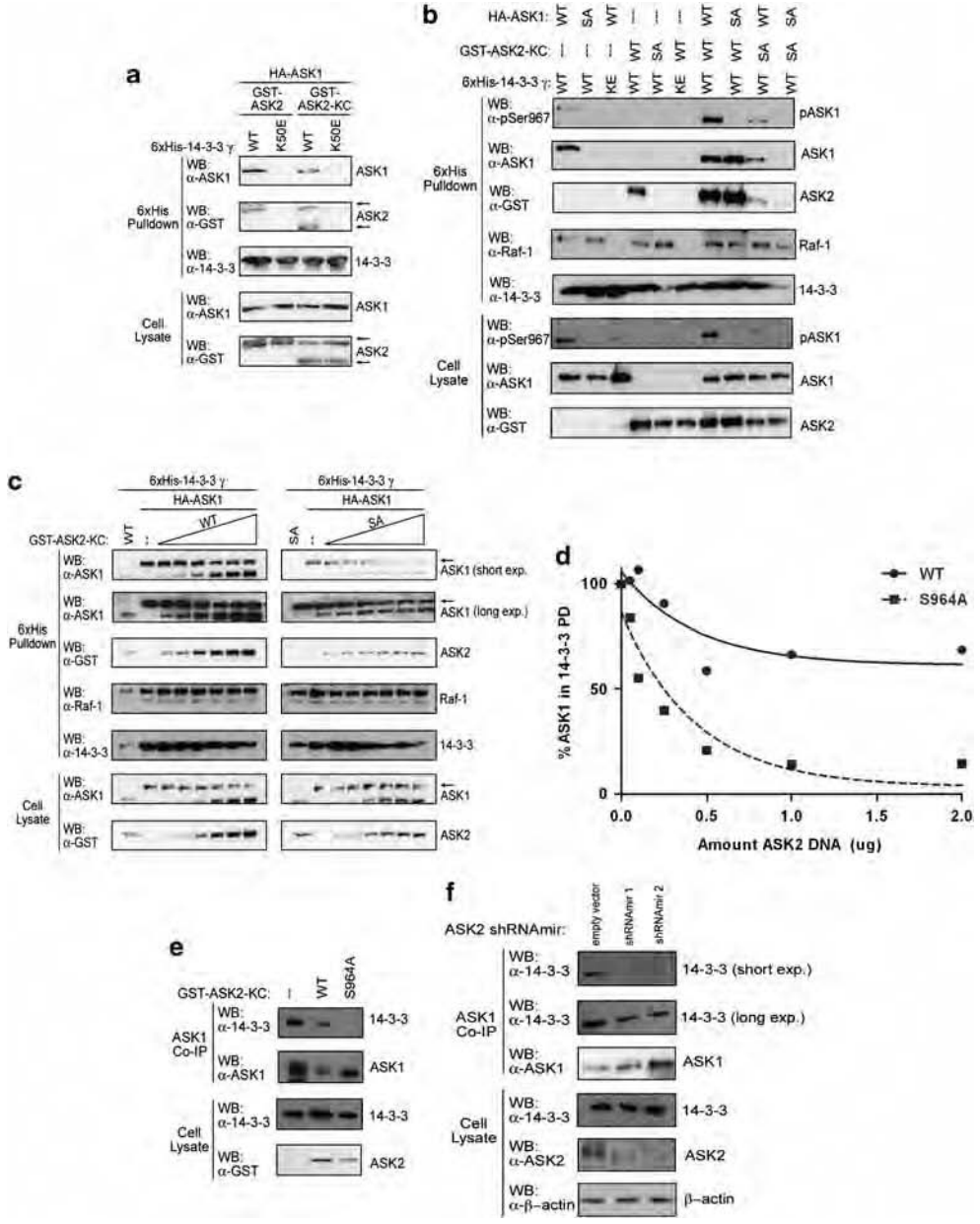


**Figure 4** Association of apoptosis signal-regulating kinase 2 (ASK2) with ASK1 and 14-3-3 in a ternary complex. (**a**) ASK2, ASK1 and 14-3-3 exist in a multi-protein complex. HA-ASK1 and glutathione *S*-transferase (GST)-ASK2 were co-transfected into COS7 cells with either hexahistidine (6xHis)-14-3-3γ wild type (WT) or K50E. Cell lysates were used in a 14-3-3 affinity pulldown assay, and the presence of ASK1 and ASK2 was revealed by anti-HA and anti-GST antibodies in a western blot. (**b**) Phosphorylation status of ASK2 S964 controls the association of 14-3-3 with ASK1. COS7 cells were transfected with the expression plasmids for 6xHis-14-3-3γ (WT or K50E), HA-ASK1 (WT or S967A) and GST-ASK2–KC (WT or S964A). 14-3-3γ protein complexes were isolated by affinity pulldown and associated ASK1, ASK2 and Raf-1, and the phosphorylation status of ASK1 at S967 was detected using the respective antibodies by western blot. (**c**) Increased expression of ASK2 S964A is correlated with decreased association of ASK1 from 14-3-3. COS7 cells were co-transfected with HA-ASK1 WT and 6xHis-14-3-3γ, along with increasing amounts of expression vectors for either GST-ASK2–KC WT or S964A. The amount of ASK1 in the resulting 14-3-3 affinity pulldown complex from each sample was determined as in Figure 1a. (**d**) Quantification of data from (**c**). The relative percentage of ASK1 in each 6xHis-14-3-3γ pulldown sample is shown. Lysates containing GST-ASK2–KC WT and S964A are indicated by solid circles (●) and squares (■), respectively. (**e**) ASK2 S964A mutation diminishes the association between endogenous ASK1 and 14-3-3. HeLa cells were transfected with pcDNA or GST-ASK2–KC (WT or S964A). Following transfection, endogenous ASK1 was immunoprecipitated from the cell lysates using a specific anti-ASK1 antibody. Endogenous 14-3-3 in the ASK1 co-immunoprecipitation (co-IP) was detected with a pan anti-14-3-3 antibody by western blot. (**f**) ASK2 knockdown diminishes endogenous ASK1/14-3-3 binding. HeLa cells were transfected with shRNAmir constructs targeting ASK2 or pGIPz empty vector control. Cells were selected with puromycin, and endogenous ASK1 was immunoprecipitated from lysates using a specific anti-ASK1 antibody. Endogenous 14-3-3 in the ASK1 co-IP was detected with a pan anti-14-3-3 antibody by western blot.

did not affect the interaction between ASK1 and ASK2 (Supplementary Figure S2). The ASK2/14-3-3 interaction seems to be independent of the ASK1/14-3-3 interaction, as overexpression of neither ASK1 WT nor S967A induced any detectable change in ASK2/14-3-3 binding (Figure 4b). However, the ability of ASK2 to bind 14-3-3 showed a dramatic impact on 14-3-3's interaction with ASK1. As previously shown, ASK1 WT is associated with 14-3-3, whereas ASK1 S967A has diminished 14-3-3 binding (Zhang *et al*., 1999a). Unexpectedly, when ASK2–KC WT was overexpressed along with ASK1 S967A and 14-3-3γ, ASK1 S967A was found in the 14-3-3γ complex (Figure 4b). One explanation for these results is that enhanced ASK2 WT expression increased the amount of ASK1 S967A in the ASK2/ASK1 protein complex, which was then pulled down with 14-3-3. However, overexpression of mutated ASK2 (S964A) dramatically decreased the amount of ASK1 WT in the 14-3-3 complex, lending strong support to a functional and regulated ternary protein association (Figure 4b). Importantly, the effect of ASK2 S964A could be recapitulated with endogenous 14-3-3/ASK1 interaction as well (Figure 4e). To further validate the ASK2 effect, dose–response experiments were carried out. Increasing amounts of ASK2 S964A, but not WT, led to a corresponding decrease in the amount of ASK1 appearing within the 14-3-3 complex (Figures 4c and d).

We further explored the specificity of the ASK2/ASK1/14-3-3 ternary complex formation by probing the effect of ASK2 or ASK1 on the interaction of 14-3-3 with Raf-1, another well-characterized MAP3K that binds 14-3-3. Interestingly, endogenous Raf-1 binding to 14-3-3 was unaffected by the overexpression of either WT or mutated ASK1 or ASK2 (Figures 4b and c). These data suggest that the ASK2/ASK1/14-3-3 ternary complex is distinct from the 14-3-3/Raf-1 complex.

To further support the hypothesis that ASK2 regulates the ASK1/14-3-3 interaction, we performed ASK2 silencing experiments and examined the effect of reducing ASK2 on endogenous ASK1/14-3-3 binding (Figure 4f). When ASK2 expression was knocked down, endogenous 14-3-3 binding to ASK1 was greatly reduced, indicating that ASK2 has a substantial role in regulating the interaction between these two proteins. Together, these results show that ASK2, ASK1 and 14-3-3 form a specific and unique ternary complex, in which the interaction between ASK2 and 14-3-3 determines the extent of ASK1 binding to 14-3-3.

*ASK2/14-3-3 interaction controls ASK1 function*

Previous studies have shown that 14-3-3 binding suppresses ASK1 activity by maintaining S967 in a phosphorylated state, inhibiting ASK1-mediated JNK pathway activation (Zhang *et al*., 1999a, 2003; Min *et al*., 2008). We reasoned that ASK2 might exert control over ASK1 by dictating the action of 14-3-3 within this ternary complex. To probe the functional consequence of the dynamically regulated ASK2/14-3-3 interaction, we examined the effect of the 14-3-3-binding defective mutant of ASK2 (S964A) on the phosphorylation status of ASK1 at S967 and the activation state of ASK1. Indeed, co-expression of ASK2 S964A resulted in a decrease in ASK1 S967 phosphorylation, an effect not observed on ASK2 WT expression (Figure 4b). Although ASK1 S967A showed enhanced ASK1 activity (T838 phosphorylation) over ASK1 WT, the ASK1 WT activity was also stimulated on co-expression with ASK2 S964A, supporting an ASK2-mediated inhibitory role of 14-3-3 in the ternary complex (Figure 5a).

As an additional biological readout of ASK1 activity, we monitored JNK activation. As we have previously shown, dephosphorylation of ASK1 at S967 is correlated with an increase in ASK1 kinase activity and ASK1-induced apoptotic signaling (Zhang *et al*., 1999a; Goldman *et al*., 2004). After co-expression of ASK1 with ASK2 (WT or S964A), JNK activation was determined by western blot with an antibody directed against phosphorylated T183/Y185 of JNK (Figures 5b and c). Co-expression of ASK2–KC S964A showed a statistically significant increase in JNK activation ($P = 0.028$) compared with ASK1 expression plus control pcDNA. No statistically significant increase in JNK activation was seen with expression of ASK2–KC S964A alone ($P = 0.130$). These results indicate that ASK2's interaction with 14-3-3 is critical to allow 14-3-3 to engage and suppress ASK1, leading to a reduction in ASK1-mediated JNK signaling. Further evidence in support of a physiological role of an ASK2/14-3-3 connection in the regulation of the ASK1–JNK axis is provided by our peptide inhibitor study, in which disruption of the ASK2/ASK1 interaction was correlated with decreased ASK1/14-3-3 interaction and $H_2O_2$-induced JNK activation (M Puckett, L Cockrell and H Fu, unpublished data).

## Discussion

Our data suggest a novel mechanism of ASK1 signalosome regulation, through ASK2-mediated recruitment of 14-3-3 proteins under certain physiological conditions, such as cells receiving survival signals (Figure 5d). Our proposed model predicts an ASK2 kinase that phosphorylates S964 in response to a survival-promoting signal, which in turn induces association of ASK2 with 14-3-3 and recruits 14-3-3 to the ASK2/ASK1 complex. This allows 14-3-3 to bind to and suppress ASK1 through phosphorylated S967. Conversely, signals that promote dephosphorylation of ASK2 at S964 are expected to disengage 14-3-3 from ASK2, triggering 14-3-3's dissociation from the ASK1 complex. Once removed, the ASK1 signalosome is free of 14-3-3-imposed inhibition, allowing activation of downstream effector pathways, such as JNK stimulation. In this way, ASK2 functions as a dual regulator in the ASK1 signalosome: serving as an ASK1 activator under stress conditions (Takeda *et al*., 2007) while acting as an ASK1 suppressor by recruiting 14-3-3 under other conditions such as cell survival. Thus, ASK2 provides a signal integration point by which external or internal

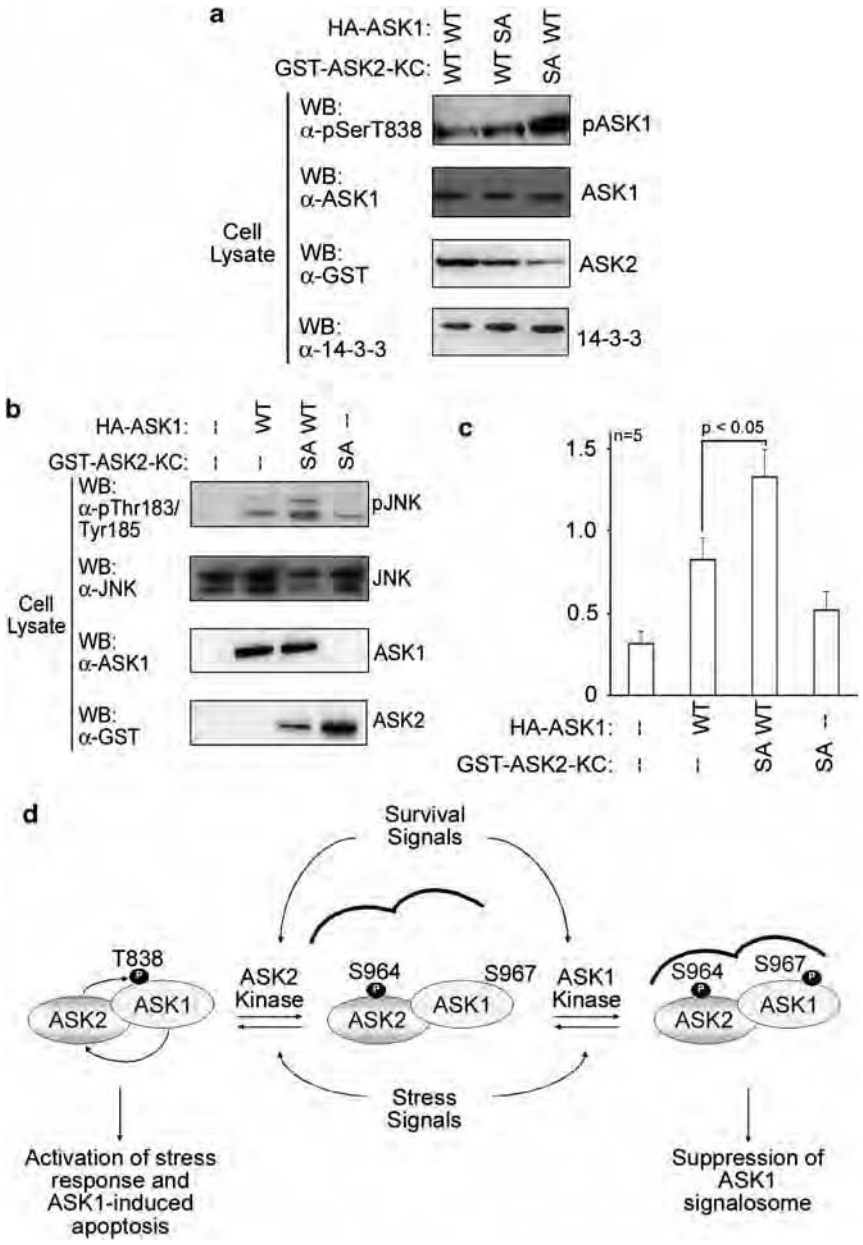


**Figure 5** Effect of apoptosis signal-regulating kinase 2 (ASK2)/14-3-3 association on ASK1 function. (**a**) The phosphorylation state of ASK2 at S964 affects ASK1 activation. COS7 cells were co-transfected with HA-ASK1 (wild type (WT) or S967A) and glutathione *S*-transferase (GST)-ASK2–KC (WT or S964A). Activation of ASK1 was assessed by phosphorylation of T838 determined by western blot with a phospho-T838 specific antibody. (**b**) Expression of ASK2 S964A enhances ASK1–c-Jun N-terminal kinase (JNK) signaling. COS7 cells were transfected with HA-ASK1 and either GST-ASK2–KC S964A or a control pcDNA vector. JNK activation status in the resulting cell lysates was revealed by western blot with an anti-pT183/Y185 JNK specific antibody. (**c**) Quantification of pJNK to JNK ratio. Values given are mean ± standard error ($n = 5$). (**d**) Working model. Under stress conditions, ASK1 and ASK2 exist in a heteromeric complex, and are dephosphorylated at S967 and S964, respectively. In this complex, ASK2 facilitates ASK1 activation through phosphorylation of T838, whereas ASK1 exhibits positive feedback regulation on ASK2 through stabilization of the ASK2 protein (Osaka *et al*., 2007). These activities culminate in the activation of ASK1 downstream signals, leading to ASK1-induced apoptosis. Conversely, under conditions of cell survival, ASK2 S964 is phosphorylated through a pro-survival kinase-signaling cascade, generating a high-affinity 14-3-3 docking site. On phosphorylation at S964, ASK2 recruits 14-3-3 to the ASK2/ASK1 complex, leading to an interaction with ASK1 through phosphorylated S967 and subsequent suppression of the ASK1 signalosome.

environmental signals are faithfully transmitted to ASK1 through engaging the phospho-binding protein 14-3-3, leading to either activation or suppression of ASK1 signaling. Even though 14-3-3 also interacts with another MAP3K Raf-1, the interaction status of ASK2 with 14-3-3 showed no obvious effect on the 14-3-3/Raf-1 association, suggesting a functionally distinct ASK2/14-3-3/ASK1 signaling complex. Because 14-3-3 proteins bind most members of the MAP3K family, this may represent a general mechanism by which 14-3-3

regulates signal relay among MAP3Ks to ensure signaling integrity in various physiological processes.

## Materials and methods

*Cell culture, DNA transfection and plasmids*
COS7 and HeLa cells were maintained in Dulbecco's modified Eagle's medium and plasmid transfections were performed using FuGene6 or Fugene HD (Roche, Boulder, CO, USA) as previously described (Ichijo *et al*., 1997; Zhang *et al*., 1999a; Subramanian *et al*., 2004). ASK2–KC and full-length ASK2 were amplified by PCR and cloned into the pDEST27 GST mammalian expression vector (Invitrogen, Carlsbad, CA, USA). Primer sequences are available in Supplementary data.

*ASK2 knockdown*
Plasmids encoding ASK2 shRNAmir constructs (RH54430-98513431 and RH54430-98903615) were purchased from Open Biosystems (Huntsville, AL, USA). HeLa cells were transfected with shRNAmir plasmid using Fugene HD (Roche) (Ichijo *et al*., 1997; Zhang *et al*., 1999a; Subramanian *et al*., 2004). Transfected cells were selected with puromycin (2 mg/ml) for 3 days.

*Protein interaction assays*
*Affinity pulldown assay.* Cells were lysed in 200 µl of pulldown lysis buffer (Goldman *et al*., 2004). HexaHis-tag fusion proteins in the clarified cell lysates were isolated with $Ni^{2+}$-charged resin (Novagen, Madison, WI, USA) as described (Subramanian *et al*., 2004).

*Co-IP assay.* Cells were lysed in either 200 µl (COS7) or 1000 µl (HeLa) of co-IP lysis buffer (Goldman *et al*., 2004). Cleared cell lysates were incubated with Protein A or G conjugated sepharose (GE Healthcare, Piscataway, NJ, USA) and the appropriate antibody for 2 h to overnight at 4 °C. Following incubation, the resin was washed three times with lysis buffer and protein samples were eluted by boiling in 6 × SDS sample buffer for western blot analysis.

*Phosphatase assay*
Cleared lysates of COS7 cells were divided into two samples, a 'plus inhibitors' sample with added phosphatase inhibitors ($Na_4P_2O_7$, NaF, $Na_3VO_4$), and a 'minus inhibitors' control sample. Time-course experiments were carried out as indicated. Lysates were then subjected to affinity pulldown as described above.

*Western blotting*
Proteins were separated on 8% or 12.5% SDS–PAGE gels and transferred to a nitrocellulose membrane, which were blocked with 5% milk. Membranes were probed overnight with anti-GST, anti-14-3-3 K19, anti-6xHis, anti-Raf anti-ASK1 (Santa Cruz Biotechnology, Santa Cruz, CA, USA), anti-Flag M2 (Sigma, St Louis, MO, USA), anti-ASK2 (Abnova, Taipei, Taiwan), or anti-phospho Ser967 ASK1 (Cell Signaling Technologies, Boston, MA, USA) antibodies, diluted in 5% milk. Corresponding horseradish peroxidase-conjugated secondary antibodies (Santa Cruz Biotechnology) were used against each primary antibody. Proteins were detected using West-Pico or West-Dura enhanced chemiluminescent detection reagents (Pierce, Rockford, IL, USA) and a Kodak imaging system. Densitometry was performed with Kodak 1D imaging software, and statistical analysis was carried out using the Student's *t*-test.

## Conflict of interest

The authors declare no conflict of interest.

## Acknowledgements

We thank the past and present members of the Fu laboratory for many stimulating discussions, as well as Zhengbin Yao for helpful suggestions. This work was supported by a National Cancer Institute National Research Service Award Grant 5F31CA117057 and a National Science Foundation Facilitating Academic Careers in Engineering and Science Fellowship 0450303 (I6660663) to LMC, an NIH Pharmacological Sciences Training Grant T32 GM008602 to MCP, NIH Grant RO1GM53165 and Emory URC grant to HF, and NIH/NCI Grant PO1CA116676 and USAMRMC05075002 to FRK and HF. HF is a Georgia Research Alliance Distinguished Investigator, and FRK and HF are Georgia Cancer Coalition Distinguished Cancer Scholars.

## References

Aitken A. (2006). 14-3-3 proteins: a historic overview. *Semin Cancer Biol* **16**: 162–172.

Chang HY, Nishitoh H, Yang X, Ichijo H, Baltimore D. (1998). Activation of apoptosis signal-regulating kinase 1 (ASK1) by the adapter protein Daxx. *Science* **281**: 1860–1863.

Cohen P, Klumpp S, Schelling DL. (1989). An improved procedure for identifying and quantitating protein phosphatases in mammalian tissues. *FEBS Lett* **250**: 596–600.

Fu H, Subramanian RR, Masters SC. (2000). 14-3-3 proteins: structure, function, and regulation. *Annu Rev Pharmacol Toxicol* **40**: 617–647.

Gardino AK, Smerdon SJ, Yaffe MB. (2006). Structural determinants of 14-3-3 binding specificities and regulation of subcellular localization of 14-3-3-ligand complexes: a comparison of the X-ray crystal structures of all human 14-3-3 isoforms. *Semin Cancer Biol* **16**: 173–182.

Goldman EH, Chen L, Fu H. (2004). Activation of apoptosis signal-regulating kinase 1 by reactive oxygen species through dephosphorylation at serine 967 and 14-3-3 dissociation. *J Biol Chem* **279**: 10442–10449.

Ichijo H, Nishida E, Irie K, ten Dijke P, Saitoh M, Moriguchi T *et al*. (1997). Induction of apoptosis by ASK1, a mammalian MAPKKK that activates SAPK/JNK and p38 signaling pathways. *Science* **275**: 90–94.

Imoto K, Kukidome D, Nishikawa T, Matsuhisa T, Sonoda K, Fujisawa K *et al*. (2006). Impact of mitochondrial reactive oxygen species and apoptosis signal-regulating kinase 1 on insulin signaling. *Diabetes* **55**: 1197–1204.

Iriyama T, Takeda K, Nakamura H, Morimoto Y, Kuroiwa T, Mizukami J *et al*. (2009). ASK1 and ASK2 differentially regulate the counteracting roles of apoptosis and inflammation in tumorigenesis. *Embo J* **28**: 843–853.

Izumiya Y, Kim S, Izumi Y, Yoshida K, Yoshiyama M, Matsuzawa A *et al*. (2003). Apoptosis signal-regulating kinase 1 plays a pivotal role in angiotensin II-induced cardiac hypertrophy and remodeling. *Circ Res* **93**: 874–883.

Kyriakis JM, Avruch J. (2001). Mammalian mitogen-activated protein kinase signal transduction pathways activated by stress and inflammation. *Physiol Rev* **81**: 807–869.

Mackintosh C. (2004). Dynamic interactions between 14-3-3 proteins and phosphoproteins regulate diverse cellular processes. *Biochem J* **381**: 329–342.

Matsuzawa A, Saegusa K, Noguchi T, Sadamitsu C, Nishitoh H, Nagai S *et al*. (2005). ROS-dependent activation of the TRAF6-ASK1-p38 pathway is selectively required for TLR4-mediated innate immunity. *Nat Immunol* **6**: 587–592.

Min W, Lin Y, Tang S, Yu L, Zhang H, Wan T *et al*. (2008). AIP1 recruits phosphatase PP2A to ASK1 in tumor necrosis factor-induced ASK1-JNK activation. *Circ Res* **102**: 840–848.

Morrison DK. (2009). The 14-3-3 proteins: integrators of diverse signaling cues that impact cell fate and cancer development. *Trends Cell Biol* **19**: 16–23.

Muslin AJ, Lau JM. (2005). Differential functions of 14-3-3 isoforms in vertebrate development. *Curr Top Dev Biol* **65**: 211–228.

Muslin AJ, Tanner JW, Allen PM, Shaw AS. (1996). Interaction of 14-3-3 with signaling proteins is mediated by the recognition of phosphoserine. *Cell* **84**: 889–897.

Nishitoh H, Matsuzawa A, Tobiume K, Saegusa K, Takeda K, Inoue K *et al*. (2002). ASK1 is essential for endoplasmic reticulum stress-induced neuronal cell death triggered by expanded polyglutamine repeats. *Genes Dev* **16**: 1345–1355.

Osaka N, Takahashi T, Murakami S, Matsuzawa A, Noguchi T, Fujiwara T *et al*. (2007). ASK1-dependent recruitment and activation of macrophages induce hair growth in skin wounds. *J Cell Biol* **176**: 903–909.

Petosa C, Masters SC, Bankston LA, Pohl J, Wang B, Fu H *et al*. (1998). 14-3-3zeta binds a phosphorylated Raf peptide and an unphosphorylated peptide via its conserved amphipathic groove. *J Biol Chem* **273**: 16305–16310.

Subramanian RR, Zhang H, Wang H, Ichijo H, Miyashita T, Fu H. (2004). Interaction of apoptosis signal-regulating kinase 1 with isoforms of 14-3-3 proteins. *Exp Cell Res* **294**: 581–591.

Takeda K, Noguchi T, Naguro I, Ichijo H. (2008). Apoptosis signal-regulating kinase 1 in stress and immune response. *Annu Rev Pharmacol Toxicol* **48**: 199–225.

Takeda K, Shimozono R, Noguchi T, Umeda T, Morimoto Y, Naguro I *et al*. (2007). Apoptosis signal-regulating kinase (ASK) 2 functions as a mitogen-activated protein kinase kinase kinase in a heteromeric complex with ASK1. *J Biol Chem* **282**: 7522–7531.

Thorson JA, Yu LW, Hsu AL, Shih NY, Graves PR, Tanner JW *et al*. (1998). 14-3-3 proteins are required for maintenance of Raf-1 phosphorylation and kinase activity. *Mol Cell Biol* **18**: 5229–5238.

Wang B, Yang H, Liu YC, Jelinek T, Zhang L, Ruoslahti E *et al*. (1999). Isolation of high-affinity peptide antagonists of 14-3-3 proteins by phage display. *Biochemistry* **38**: 12499–12504.

Wang H, Zhang L, Liddington R, Fu H. (1998a). Mutations in the hydrophobic surface of an amphipathic groove of 14-3-3zeta disrupt its interaction with Raf-1 kinase. *J Biol Chem* **273**: 16297–16304.

Wang XS, Diener K, Jannuzzi D, Trollinger D, Tan TH, Lichenstein H *et al*. (1996). Molecular cloning and characterization of a novel protein kinase with a catalytic domain homologous to mitogen-activated protein kinase kinase kinase. *J Biol Chem* **271**: 31607–31611.

Wang XS, Diener K, Tan TH, Yao Z. (1998b). MAPKKK6, a novel mitogen-activated protein kinase kinase kinase, that associates with MAPKKK5. *Biochem Biophys Res Commun* **253**: 33–37.

Winter-Vann AM, Johnson GL. (2007). Integrated activation of MAP3Ks balances cell fate in response to stress. *J Cell Biochem* **102**: 848–858.

Yaffe MB. (2002). How do 14-3-3 proteins work?—Gatekeeper phosphorylation and the molecular anvil hypothesis. *FEBS Lett* **513**: 53–57.

Yaffe MB, Rittinger K, Volinia S, Caron PR, Aitken A, Leffers H *et al*. (1997). The structural basis for 14-3-3: phosphopeptide binding specificity. *Cell* **91**: 961–971.

Zhang L, Chen J, Fu H. (1999a). Suppression of apoptosis signal-regulating kinase 1-induced cell death by 14-3-3 proteins. *Proc Natl Acad Sci USA* **96**: 8511–8515.

Zhang L, Wang H, Masters SC, Wang B, Barbieri JT, Fu H. (1999b). Residues of 14-3-3 zeta required for activation of exoenzyme S of Pseudomonas aeruginosa. *Biochemistry* **38**: 12159–12164.

Zhang R, He X, Liu W, Lu M, Hsieh JT, Min W. (2003). AIP1 mediates TNF-alpha-induced ASK1 activation by facilitating dissociation of ASK1 from its inhibitor 14-3-3. *J Clin Invest* **111**: 1933–1943.

Supplementary Information accompanies the paper on the Oncogene website (http://www.nature.com/onc)

# Baseline Vascular Endothelial Growth Factor Concentration as a Potential Predictive Marker of Benefit from Vandetanib in Non–Small Cell Lung Cancer

Emer O. Hanrahan,[1] Anderson J. Ryan,[2] Helen Mann,[2] Sarah J. Kennedy,[2] Peter Langmuir,[3] Ronald B. Natale,[4] Roy S. Herbst,[1] Bruce E. Johnson,[5] and John V. Heymach[1]

**Abstract**

**Purpose:** Vandetanib [vascular endothelial growth factor (VEGF) receptor/epidermal growth factor receptor/RET inhibitor] has shown improvements in progression-free survival (PFS) in advanced non-small cell lung cancer in three randomized phase II studies: vandetanib versus gefitinib (study 3), docetaxel ± vandetanib (study 6), and carboplatin-paclitaxel and/or vandetanib (study 7). In study 7, vandetanib monotherapy was inferior to carboplatin-paclitaxel. We performed an exploratory retrospective analysis of the relationship between baseline circulating VEGF concentrations and PFS.

**Experimental Design:** Mean baseline VEGF levels were determined by ELISA from two baseline samples of plasma (163 of 168 patients, study 3; 65 of 127, study 6) or serum (144 of 181, study 7). High baseline VEGF values were above the immunoassay reference range for healthy subjects; low baseline VEGF values were within the range.

**Results:** Patients with low baseline VEGF had a lower risk of disease progression with vandetanib versus gefitinib [hazard ratio (HR), 0.55; 95% confidence interval (95% CI), 0.35-0.86; $P = 0.01$] or vandetanib 100 mg/d + docetaxel versus docetaxel (HR, 0.25; 95% CI, 0.09-0.68; $P = 0.01$). High VEGF patients had a similar risk of disease progression with vandetanib monotherapy versus gefitinib (HR, 1.03; 95% CI, 0.60-1.75; $P = 0.92$) or vandetanib 100 mg/d + docetaxel versus docetaxel (HR, 0.95; 95% CI, 0.25-3.61; $P = 0.94$). In study 7, low VEGF patients had a similar risk of disease progression with vandetanib monotherapy 300 mg/d versus carboplatin-paclitaxel (HR, 0.80; 95% CI, 0.41-1.56; $P = 0.51$); high VEGF patients progressed more quickly (HR, 1.60; 95% CI, 0.81-3.15; $P = 0.17$).

**Conclusions:** These analyses suggest that low baseline circulating VEGF may be predictive of PFS advantage in patients with advanced non-small cell lung cancer receiving vandetanib versus gefitinib or vandetanib + docetaxel versus docetaxel. Moreover, patients with low VEGF levels may have a similar outcome with either vandetanib monotherapy or carboplatin-paclitaxel.

Angiogenesis is the process of new blood vessel formation from existing vessels. Generally, tumors cannot grow beyond 1 to 2 $mm^3$ without developing a vascular supply (1, 2). In normal physiologic processes, angiogenesis is closely controlled by the balance of proangiogenic and antiangiogenic factors, but this equilibrium is disrupted in the malignant state by the release of proangiogenic factors from the tumor and its stromal cells (3, 4). Vascular endothelial growth factor (VEGF), an up-regulated, critical proangiogenic factor in tumors, promotes endothelial cell growth, survival, and migration and mediates vessel permeability, thereby facilitating tumor progression and metastatic spread (5–7). Agents targeting the VEGF signaling pathway are

**Authors' Affiliations:** [1]The University of Texas M. D. Anderson Cancer Center, Houston, Texas; [2]AstraZeneca, Macclesfield, United Kingdom; [3]AstraZeneca, Wilmington, Delaware; [4]Cedars-Sinai Cancer Center, Los Angeles, California; and [5]Dana-Farber Cancer Institute, Boston, Massachusetts

Received 10/4/08; revised 1/23/09; accepted 2/9/09; published online 5/15/09.

**Grant support:** Damon Runyan Cancer Research Foundation grant CI 24-04 and American Society for Clinical Oncology Career Development Award (J.V. Heymach) and American Society for Clinical Oncology Young Investigator Award (E.O. Hanrahan). This study, including the editorial assistance provided by John Matthew (Mudskipper Bioscience), was supported financially by AstraZeneca.

The costs of publication of this article were defrayed in part by the payment of page charges. This article must therefore be hereby marked *advertisement* in accordance with 18 U.S.C. Section 1734 solely to indicate this fact.

**Note:** Supplementary data for this article are available at Clinical Cancer Research Online (http://clincancerres.aacrjournals.org/).

J.V. Heymach is a Damon Runyan-Lilly Clinical Investigator.

**Trademark statement:** ZACTIMA and IRESSA are trademarks of the AstraZeneca group of companies.

**Requests for reprints:** John V. Heymach, Department of Thoracic/Head and Neck Medical Oncology and Cancer Biology, University of Texas M. D. Anderson Cancer Center, Unit 432, 1515 Holcombe Boulevard, Houston, TX 77030. Phone: 713-792-6363; Fax: 713-792-1220; E-mail: jheymach@mdanderson.org.

© 2009 American Association for Cancer Research.

doi:10.1158/1078-0432.CCR-08-2568

### Translational Relevance

There is a critical need for biomarkers for identifying patients likely to respond to angiogenesis inhibitors. We describe our analysis of circulating vascular endothelial growth factor (VEGF) levels from three randomized, phase II clinical studies of vandetanib (oral VEGF/epidermal growth factor receptor inhibitor) for advanced non-small cell lung cancer. Our findings have several potentially important clinical implications. Low baseline VEGF levels may identify a subset of patients who can obtain equivalent progression-free survival benefit with first-line vandetanib as with carboplatin/paclitaxel chemotherapy and could thereby be spared upfront chemotherapy. Patients with low baseline VEGF may derive greater benefit from the addition of vandetanib to second-line docetaxel chemotherapy than with docetaxel alone. Patients with low baseline VEGF who are being considered for second/third-line treatment with an epidermal growth factor receptor inhibitor may derive greater progression-free survival benefit if treated with vandetanib monotherapy. Based on these results, VEGF is being evaluated as a predictive biomarker in four phase III trials with vandetanib for non-small cell lung cancer.

now in clinical use for a variety of advanced solid tumors. These include bevacizumab, an anti-VEGF monoclonal antibody, for non-small cell lung cancer (NSCLC), colorectal and breast cancers, and sunitinib and sorafenib, multitargeted receptor tyrosine kinase inhibitors (TKI) with activity against VEGF receptors (VEGFR), for the treatment of renal cell carcinoma (8–13). Many other VEGFR TKIs are currently in clinical development (14).

Vandetanib (ZACTIMA) is a once-daily oral receptor TKI with activity against VEGFR-2, epidermal growth factor receptor (EGFR), and RET. It has shown improvements in progression-free survival (PFS) in advanced NSCLC in three randomized phase II trials (Table 1), 6474IL/0003, 0006, and 0007 (hereafter called studies 3, 6, and 7, respectively), and is now being further evaluated in the phase III setting. In study 3, there was an improvement in PFS with vandetanib 300 mg/d compared with gefitinib (IRESSA) 250 mg/d (15). Study 6 compared docetaxel alone or in combination with vandetanib at either 100 or 300 mg/d (16). PFS was superior with docetaxel + vandetanib 100 mg/d versus docetaxel alone. In study 7, combining vandetanib 300 mg/d with carboplatin-paclitaxel produced a greater PFS benefit than carboplatin-paclitaxel alone (17). In this study, the vandetanib 300 mg/d monotherapy arm was inferior to carboplatin-paclitaxel alone. Nevertheless, the disease control rate with vandetanib monotherapy was 26% (partial response or stable disease for at least 12 weeks), and a subset of patients (11%) remained on single-agent vandetanib for at least 6 months.

Whereas these phase II results show the potential of vandetanib therapy in NSCLC, the identification of pretreatment biomarkers that may predict which patients are most likely to derive the greatest benefit from vandetanib or other inhibitors of VEGF signaling is of considerable interest. Circulating VEGF levels have been shown previously to be both a prognostic marker in cancer(18) and a pharmacodynamic marker of VEGFR-2 inhibition (11, 19–21).We hypothesized that circulating VEGF levels have the potential to be a predictive marker of clinical benefit in patients with advanced NSCLC treated with vandetanib. We therefore performed exploratory analyses of pretreatment blood samples from patients enrolled in studies 3, 6, and 7 to determine if VEGF concentrations might be predictive of benefit from vandetanib monotherapy or vandetanib in combination with docetaxel or carboplatin-paclitaxel chemotherapy.

## Materials and Methods

Data from three separate randomized phase II trials of vandetanib in advanced NSCLC are included in this analysis: studies 3, 6, and 7. The design and results of these trials are described in detail elsewhere and are briefly outlined here and summarized in Table 1 (15–17).

***Study designs and treatments administered.*** In study 3, 168 patients with advanced NSCLC who had progressed despite first- or second-line platinum-based therapy were randomized 1:1 to receive continuous oral dosing with vandetanib 300 mg/d or gefitinib 250 mg/d (Table 1). The primary objective was to determine if vandetanib prolonged PFS relative to gefitinib. On disease progression, eligible patients had the option of switching to the alternative therapy.

In study 6, 127 patients with locally advanced or metastatic NSCLC who had progressed following first-line platinum-based chemotherapy were randomized 1:1:1 to one of three treatment arms: docetaxel (75 mg/m$^2$ intravenously every 21 days) + placebo, docetaxel + vandetanib 100 mg/d, or docetaxel + vandetanib 300 mg/d. The primary objective was to determine whether vandetanib (100 or 300 mg) + docetaxel prolonged PFS compared with placebo + docetaxel.

In study 7, 181 patients with previously untreated, locally advanced, metastatic, or recurrent NSCLC were randomized 2:1:1 to one of three treatment arms: vandetanib 300 mg/d, carboplatin-paclitaxel (carboplatin, AUC 6 mg/mL min; paclitaxel, 200 mg/m$^2$; intravenously every 21 days) + placebo, or carboplatin-paclitaxel + vandetanib 300 mg/d. The primary objective was to determine whether vandetanib ± carboplatin-paclitaxel prolonged PFS compared with carboplatin-paclitaxel alone.

Tumor response and disease progression were determined by Response Evaluation Criteria in Solid Tumors in all three trials, which were approved by all relevant institutional ethical committees or review bodies, and conducted in accordance with the Declaration of Helsinki, Good Clinical Practice, and the AstraZeneca policy on Bioethics. Each patient provided written informed consent.

***Plasma and serum collection and preparation.*** Patients in studies 3 and 6 provided two baseline blood samples taken at least 24 h apart (on day 1 and usually within 7 days before commencing treatment) and which were taken into tubes containing EDTA anticoagulant. Within 30 min of collection, blood samples were centrifuged at 1,000 to 1,500 × *g* for 10 min. Plasma was frozen and stored at −70°C to −80°C. In study 7, serum was prepared from two baseline blood samples taken at least 24 h apart (on day 1 and usually within 7 days before commencing treatment). Blood samples were allowed to coagulate for 30 to 60 min and then centrifuged for 10 to 15 min at 1,000 × *g*. Serum was frozen and stored at −70°C to −80°C.

***Measurement of VEGF concentration.*** Plasma or serum samples were thawed on ice and the VEGF concentration was determined using ELISA (R&D Systems). The VEGF standard curve ranged from 0 to 2,000 pg/mL and the lower limit of detection was 31 pg/mL. Each sample was analyzed in duplicate, and samples were analyzed in batches to minimize interassay variability.

*Statistical methods.* Summary statistics of baseline VEGF values were obtained for each study and each treatment group to determine the distribution of baseline VEGF values. VEGF values from two samples provided by each patient were used to obtain baseline and reproducibility measurements of the VEGF values. Where two pretreatment samples were obtained, the mean of the two VEGF values was used as the baseline measure. Where one pretreatment sample was available, this single VEGF value was used as the baseline measure. The variability between the two baseline VEGF values obtained for each patient was investigated through estimating intersubject and intrasubject components of variation using an ANOVA model fitted to the log-transformed baseline VEGF value, with patient included as a random effect.

An evaluation of different cutoff points of baseline VEGF values to predict PFS was done using a Cox proportional hazards regression model. PFS is defined as the time from randomization until progression or death in the absence of progression if death is <3 months from the last evaluable Response Evaluation Criteria in Solid Tumors assessment. Separate models were fitted for each study and different cutoff points were used to dichotomize patients into "high" and "low" VEGF subgroups. The high and low VEGF subgroups reported in this study were defined using the upper limits of VEGF concentrations reported in healthy volunteers. The VEGF concentrations in samples from 37 healthy volunteers have been reported to range from 62 to 707 pg/mL in serum and from nondetectable to 115 pg/mL in EDTA plasma (R&D Systems Human VEGF Immunoassay). Therefore, in studies 3 and 6, high and low plasma VEGF levels were defined as concentrations >115 and ≤115 pg/mL, respectively; in study 7, high and low serum VEGF levels were defined as concentrations >707 and ≤707 pg/mL, respectively.

The fitted models allowed for the effect of treatment and included terms for gender, histology, and previous response to therapy (study 3) and tumor stage and number of organs involved (studies 6 and 7). From the fitted models, hazard ratio (HR), 95% confidence interval (95% CI), and two-sided *P* value for the following five comparisons were calculated for all patients in the study and the low and high VEGF subgroups: vandetanib 300 mg versus gefitinib 250 mg (study 3), docetaxel with vandetanib 100 mg/d versus docetaxel and placebo (study 6), docetaxel with vandetanib 300 mg/d versus docetaxel and placebo (study 6), carboplatin-paclitaxel with vandetanib 300 mg/d versus carboplatin-paclitaxel and placebo (study 7), and vandetanib 300 mg/d versus carboplatin-paclitaxel and placebo (study 7). Comparisons were only between the treatment arms in each clinical study (that is, comparisons across different clinical studies were not done). A similar analysis was done using the endpoint of overall survival (OS). OS is defined as the number of days from randomization until death by any cause.

The treatment-by-VEGF interaction was investigated by assessing the difference between the log likelihoods for the full model for PFS (including all covariates, dichotomized VEGF value, and an interaction between treatment and baseline VEGF) and a reduced model for PFS (excluding the interaction). The change in $-2 \times$ log likelihood was calculated to determine whether the inclusion of the interaction term significantly improves the fit of the model; hence, the interaction is significant. *P* value(s) for the improvement of model fit are presented.

All of the phase II clinical studies were powered for the PFS primary endpoint. The VEGF analysis is therefore exploratory and multiple comparisons have been conducted, for which no adjustments have been made.

## Results

***Patient characteristics and baseline VEGF levels.*** Baseline VEGF plasma concentrations were available from the following patients: 82 of 83 (99%) in the vandetanib arm and 81 of 85 (95%) in the gefitinib arm (study 3), 24 of 41 (59%) in the

**Table 1.** Study designs

| | Study 3 | Study 6 | Study 7 |
|---|---|---|---|
| Study design | Two-arm, randomized phase II<br>Second/third-line treatment for advanced NSCLC; previous platinum-based therapy | Three-arm, randomized phase II<br>Second-line treatment for advanced NSCLC; post-failure of platinum-based therapy | Three-arm, randomized phase II<br>First-line treatment for stage IIIB/IV NSCLC |
| Treatment arms | 1: Gefitinib 250 mg/d, orally | 1: Docetaxel 75 mg/m$^2$ every 21 d + placebo | 1: Carboplatin AUC 6 + paclitaxel 200 mg/m$^2$ every 21 d (carboplatin-paclitaxel) |
| | 2: Vandetanib 300 mg/d, orally | 2: Docetaxel 75 mg/m$^2$ every 21 d + vandetanib 100 mg/d, orally<br>3: Docetaxel 75 mg/m$^2$ every 21 d + vandetanib 300 mg/d, orally | 2: Carboplatin-paclitaxel + vandetanib 300 mg/d, orally<br>3: Vandetanib 300 mg/d, orally |
| Primary endpoint | PFS | PFS | PFS |
| PFS result | Primary endpoint was met | Primary endpoint was met for arm 2 | Primary endpoint was met for arm 2 |
| | Superior PFS with vandetanib | Superior PFS with docetaxel + vandetanib 100 mg compared with docetaxel + placebo | Superior PFS with carboplatin-paclitaxel + vandetanib 300 mg compared with carboplatin-paclitaxel + placebo |
| | HR, 0.69; *P* = 0.013 (one-sided) and 0.025 (two-sided) | HR, 0.64; *P* = 0.037 (one-sided) and 0.074 (two-sided) | HR, 0.76; *P* = 0.098 (one-sided) and 0.197 (two-sided)<br>Arm 3 was stopped at an interim analysis (HR for PFS vs carboplatin-paclitaxel was >1.33)* |
| OS result | Trial had switchover design to other treatment, so OS result may be confounded | No significant difference | No significant difference |

*The disease control rate with vandetanib monotherapy was 26% (partial response or stable disease for at least 12 wk) and a subset of patients (11%) remained on single-agent vandetanib for at least 6 mo.

**Table 2.** Summary of PFS data

| | Group | PFS | | | | |
|---|---|---|---|---|---|---|
| | | Patients (*n*) | Events (*n*) | HR (two-sided 95% CI) | Two-sided *P* | $P_{interaction}$ (VEGF × treatment) |
| Study 3 | | | | | | |
| Vandetanib 300 mg/d versus gefitinib 250 mg/d | All patients | 168 | 152 | 0.69 (0.50-0.96) | 0.03 | |
| | All patients with VEGF value | 163 | 147 | 0.70 (0.50-0.97) | 0.03 | |
| | Low VEGF group | 93 | 84 | 0.55 (0.35-0.86) | 0.01 | |
| | High VEGF group | 70 | 63 | 1.03 (0.60-1.75) | 0.92 | 0.08 |
| Study 6 | | | | | | |
| Vandetanib 100 mg/d + docetaxel versus placebo + docetaxel | All patients | 83 | 64 | 0.64 (0.39-1.05) | 0.07 | |
| | All patients with VEGF value | 44 | 32 | 0.38 (0.18-0.81) | 0.01 | |
| | Low VEGF group | 29 | 20 | 0.25 (0.09-0.68) | 0.01 | |
| | High VEGF group | 15 | 12 | 0.95 (0.25-3.61) | 0.94 | 0.09 |
| Vandetanib 300 mg/d + docetaxel versus placebo + docetaxel | All patients | 85 | 65 | 0.83 (0.50-1.37) | 0.46 | |
| | All patients with VEGF value | 45 | 32 | 0.59 (0.29-1.21) | 0.15 | |
| | Low VEGF group | 29 | 22 | 0.66 (0.28-1.54) | 0.33 | |
| | High VEGF group | 16 | 10 | 0.53 (0.13-2.20) | 0.38 | 0.71 |
| Study 7 | | | | | | |
| Vandetanib 300 mg/d + carboplatin-paclitaxel versus placebo + carboplatin-paclitaxel | All patients | 108 | 92 | 0.76 (0.50-1.15) | 0.20 | |
| | All patients with VEGF value | 86 | 75 | 0.75 (0.47-1.19) | 0.22 | |
| | Low VEGF group | 50 | 45 | 0.72 (0.39-1.33) | 0.29 | |
| | High VEGF group | 36 | 30 | 0.47 (0.20-1.07) | 0.07 | 0.09 |
| Vandetanib 300 mg/d versus placebo + carboplatin-paclitaxel | All patients | 113 | 98 | 1.30 (0.85-1.98) | 0.23 | |
| | All patients with VEGF value | 91 | 79 | 1.27 (0.80-2.01) | 0.31 | |
| | Low VEGF group | 45 | 37 | 0.80 (0.41-1.56) | 0.51 | |
| | High VEGF group | 46 | 42 | 1.60 (0.81-3.15) | 0.17 | 0.92 |

docetaxel arm, 20 of 42 (48%) in the docetaxel + vandetanib 100 mg/d arm, and 21 of 44 (48%) in the docetaxel + vandetanib 300 mg/d arm (study 6). Baseline serum VEGF concentrations were available for 44 of 56 (79%) patients in the carboplatin-paclitaxel + vandetanib arm and 42 of 52 (81%) in the carboplatin-paclitaxel arm (study 7). Because the vandetanib monotherapy arm in study 7 was closed at interim analysis, the subgroup of patients included in the statistical analysis of the vandetanib monotherapy arm were all patients concurrently randomized to receive either vandetanib monotherapy or carboplatin-paclitaxel up until the date when the last monotherapy patient was enrolled (August 15, 2005). For this subgroup, baseline serum VEGF concentrations were available for 58 of 73 (79%) patients in the vandetanib monotherapy arm and 33 of 40 (83%) patients in the carboplatin-paclitaxel arm. The numbers of patients in the high and low VEGF groups for each of the five comparisons between treatment arms in this analysis are shown in Table 2. The pretreatment VEGF concentrations are shown in Fig. 1 and Table 3. The intrapatient variability between the two baseline VEGF measurements taken from samples drawn on different days was low to moderate (coefficient of variation values of 36%, 55%, and 60% for studies 7, 3, and 6, respectively; Supplementary Table S1).

The patient characteristics are shown in Supplementary Table S2. There were no apparent differences between the VEGF subgroups (low or high) and the whole study population in terms of the following characteristics: treatment arm, age, performance status, and smoking status (all studies) and gender, histology, and disease stage (studies 3 and 7). In study 6, there were significant differences between the proportion of males and females in the high baseline VEGF group (33% and 67%, respectively) and the whole study group (57% and 43%, respectively) and in the proportion of patients with stage IIIB disease (14%) in the low VEGF group compared with the whole study group (26%). Study 6 also had a larger proportion of patients with adenocarcinoma (66%) and a smaller proportion of patients with squamous cell carcinoma (14%) in the low baseline VEGF group than in the whole study (50% and 29%, respectively). In addition, compared with the overall population in study 6, patients with an available baseline sample had a lower HR for benefit with vandetanib + docetaxel versus docetaxel (e.g., PFS HR of 0.64 for overall population versus 0.38 for those with baseline value in vandetanib 100 mg/d arm; Table 2; Supplementary Table S3).

***Relationship between baseline VEGF levels and patient outcomes with vandetanib monotherapy.*** Study 3: Patients in the low baseline plasma VEGF group receiving vandetanib 300 mg/d had a superior PFS compared with those receiving gefitinib 250 mg/d (HR, 0.55; 95% CI, 0.35-0.86; two-sided $P$ = 0.01; Figs. 2 and 3A; Table 2). In contrast, patients with high

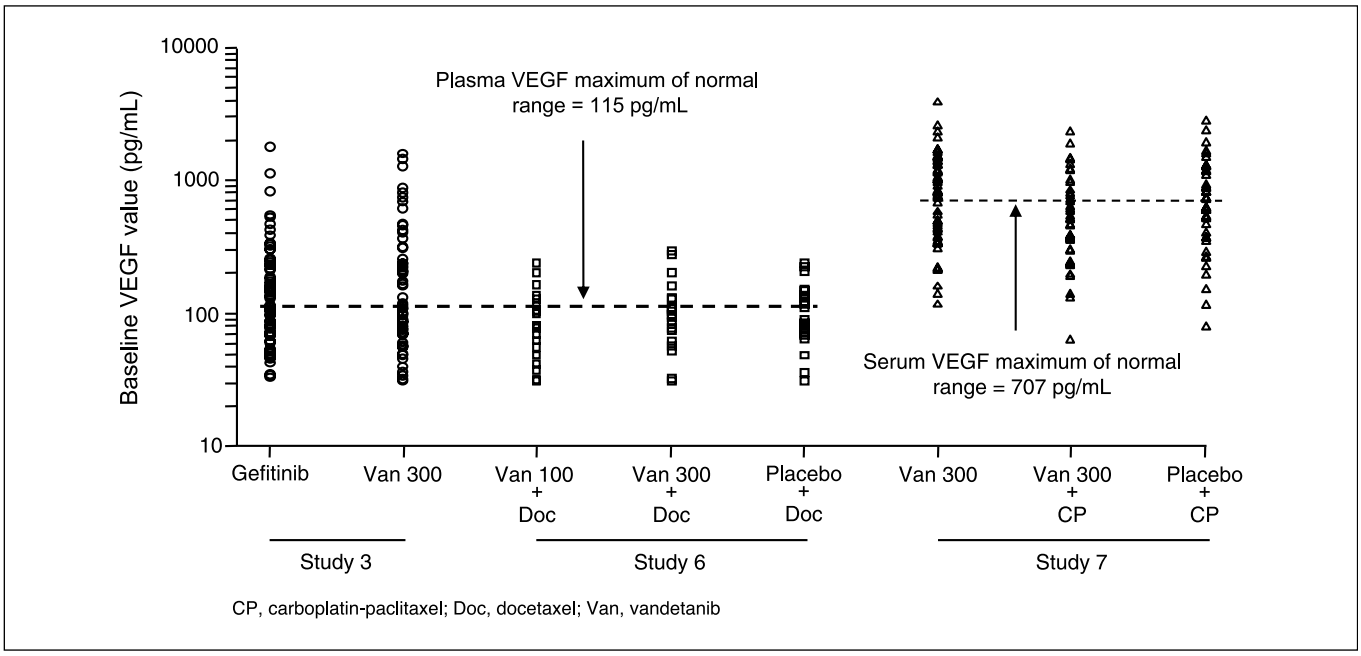


**Fig. 1.** Baseline VEGF values by treatment group.

baseline plasma VEGF had similar PFS when treated with either vandetanib or gefitinib (HR, 1.03; 95% CI, 0.60-1.75; $P = 0.92$; treatment-by-factor interaction test for VEGF, $P = 0.08$). Although a similar analysis was done for survival, the two-part design of the study, which allowed eligible patients the option to switch to the alternative treatment regimen in part B (following disease progression), confounds the interpretation of this analysis (Fig. 3B; Supplementary Table S3).

The finding that patients with low VEGF may derive differential PFS benefit from vandetanib compared with gefitinib was further explored to determine if the specific cutoff value for defining low or high baseline VEGF affected the overall findings. Across a broad range of cutoff points for VEGF, including the median and mean values of VEGF, the findings were similar (Fig. 4). The low baseline VEGF group consistently had a HR of <1, and the high baseline VEGF group consistently had a HR greater than that of the low VEGF group.

Study 7: The vandetanib monotherapy arm was closed at interim analysis because PFS met the criterion for discontinuation (HR > 1.33 versus carboplatin-paclitaxel); hence, the subgroup

**Table 3.** Baseline VEGF values by treatment group

| Study | Treatment arm | Patients providing baseline samples (*n*) | VEGF (pg/mL)* | | | | | |
|---|---|---|---|---|---|---|---|---|
| | | | Arithmetic mean | Geometric mean | Maximum | Minimum† | Median | Interquartile range |
| 3 | Vandetanib 300 mg | 81 | 180 | 121 | 1,678 | 31 | 107 | 138 |
| | Gefitinib 250 mg | 82 | 226 | 120 | 1,595 | 31 | 88 | 164 |
| 6 | Docetaxel + placebo | 24 | 103 | 86 | 240 | 31 | 88 | 79 |
| | Docetaxel + vandetanib 300 mg | 20 | 96 | 81 | 238 | 31 | 82 | 69 |
| | Docetaxel + vandetanib 100 mg | 21 | 108 | 89 | 296 | 31 | 86 | 66 |
| 7 | Carboplatin-paclitaxel + placebo | 42 | 827 | 630 | 2,781 | 80 | 674 | 788 |
| | Carboplatin-paclitaxel + vandetanib 300 mg | 44 | 664 | 511 | 2,315 | 64 | 512 | 500 |
| | Vandetanib 300 mg | 58 | 914 | 703 | 3,870 | 117 | 768 | 864 |

*VEGF levels in studies 3 and 6 are from plasma. VEGF levels in study 7 are from serum.
†The limit of VEGF quantification in the ELISA assay was 31 pg/mL. Samples at or below the limit of detection were ascribed a level of 31 pg/mL.

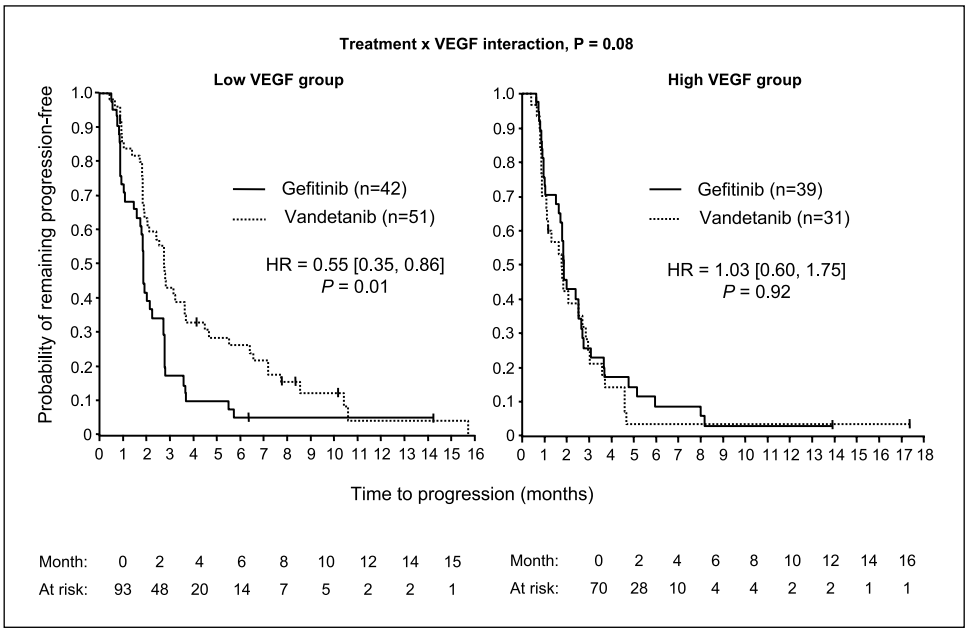


**Fig. 2.** Kaplan-Meier analysis for patients treated with vandetanib or gefitinib (study 3) with low or high baseline VEGF.

of patients included in this analysis were those patients concurrently randomized to receive vandetanib monotherapy ($n = 73$) or carboplatin-paclitaxel ($n = 40$) up to the date when the last monotherapy patient was enrolled. Among chemotherapy-naive NSCLC patients with low baseline serum VEGF, there was no significant difference in PFS between those initially treated with vandetanib 300 mg/d monotherapy or carboplatin-paclitaxel chemotherapy, but there was a trend toward superior PFS with vandetanib (HR, 0.80; 95% CI, 0.41-1.56; $P = 0.51$; Fig. 3A; Table 2). Patients with a high baseline serum VEGF tended to have an inferior PFS when treated with vandetanib 300 mg/d compared with carboplatin-paclitaxel (HR, 1.60; 95% CI, 0.81-3.15; $P = 0.17$; treatment-by-factor interaction test for VEGF, $P = 0.09$). These findings for low and high serum VEGF subgroups held across a broad range of cutoff values for VEGF, including the median and mean values of VEGF (data not shown).

Patients with a high baseline serum VEGF also trended toward having an inferior OS when treated with vandetanib 300 mg/d monotherapy compared with carboplatin-paclitaxel (HR, 1.40; 95% CI, 0.58-3.37; $P = 0.46$) in contrast to patients with a low baseline serum VEGF value (HR, 0.68; 95% CI, 0.29-1.60; $P = 0.38$; Fig. 3B; Supplementary Table S3).

***Relationship between baseline VEGF levels and patient outcomes with combination therapy.*** Study 6: Patients in the low baseline plasma VEGF group receiving docetaxel with vandetanib 100 mg/d had a superior PFS compared with those receiving docetaxel with placebo (HR, 0.25; 95% CI, 0.09-0.68; $P = 0.01$; Fig. 3C; Table 2; treatment-by-factor interaction test for VEGF, $P = 0.14$). However, there was no significant difference in PFS among patients with low baseline plasma VEGF who received docetaxel + vandetanib 300 mg/d versus docetaxel with placebo (HR, 0.66; 95% CI, 0.28-1.54; $P = 0.33$). Among patients with high baseline plasma VEGF, there was no evidence of differences in PFS between the three treatment arms.

Among patients with high baseline plasma VEGF, there were also no significant differences in OS between the three treatment arms (Fig. 3D). However, there was evidence of superior OS for patients with low baseline plasma VEGF who received either vandetanib 100 mg/d (HR, 0.10; 95% CI, 0.03-0.31; $P < 0.001$) or vandetanib 300 mg/d (HR, 0.27; 95% CI, 0.10-0.69; $P = 0.01$) + docetaxel compared with docetaxel + placebo (Fig. 3D; Supplementary Table S3). A similar relationship between the dichotomous VEGF grouping and clinical outcomes of PFS and OS was observed using a median cutoff value but could not be shown across a broad range of cutoff points due to insufficient baseline VEGF data.

Study 7: Among patients with low baseline VEGF, there was no significant difference in PFS between those treated with vandetanib 300 mg/d + carboplatin-paclitaxel compared with carboplatin-paclitaxel (HR, 0.72; 95% CI, 0.39-1.33; $P = 0.29$; Fig. 3C; Table 2). There was a trend for patients with a high baseline serum VEGF to have superior PFS when treated with vandetanib 300 mg/d + carboplatin-paclitaxel compared with carboplatin-paclitaxel (HR, 0.47; 95% CI, 0.20-1.07; $P = 0.07$; treatment-by-factor interaction test for VEGF, $P = 0.92$). This finding was similar when the baseline VEGF median value was used as a cutoff to define the low and high VEGF groups. However, these findings were not consistent across a broad range of cutoff values for baseline VEGF. Similar results were obtained for OS between treatment arms of the high and low baseline serum VEGF groups (Fig. 3D; Supplementary Table S3).

## Discussion

In this exploratory retrospective analysis of pretreatment plasma or serum VEGF concentrations among the participants in three randomized phase II studies, we have evaluated baseline circulating VEGF level as a potential predictive marker for clinical benefit from vandetanib treatment either as a monotherapy or in combination with chemotherapy for advanced NSCLC. From the study 3 results, we have shown that patients with advanced NSCLC and a low baseline plasma VEGF concentration had a significantly superior PFS when treated with vandetanib monotherapy compared with gefitinib monotherapy

(HR, 0.55; $P = 0.01$). In contrast, patients with a high baseline concentration of VEGF had a similar risk of tumor progression when treated with either vandetanib or gefitinib (HR, 1.03; $P = 0.92$). Due to the two-part crossover design of this study, it is not possible to make any definitive conclusions about the effect of therapy on OS. In addition, NSCLC patients with low baseline serum VEGF treated in the first-line setting in study 7 appeared to derive similar benefit in terms of both PFS and OS from either vandetanib monotherapy or carboplatin-paclitaxel doublet chemotherapy, an established standard of care, whereas patients with high VEGF had a shorter PFS with vandetanib. This suggests that determining pretreatment circulating VEGF concentrations may have the potential to identify patients who could derive equivalent benefit from front-line targeted therapy with vandetanib monotherapy as from standard carboplatin-paclitaxel doublet chemotherapy.

Baseline VEGF levels may also have the potential to identify patients most likely to benefit from the addition of vandetanib to chemotherapy, particularly for vandetanib 100 mg/d + docetaxel compared with docetaxel alone in the second-line treatment of NSCLC. In this setting, patients with low baseline plasma VEGF treated with vandetanib 100 mg/d + docetaxel

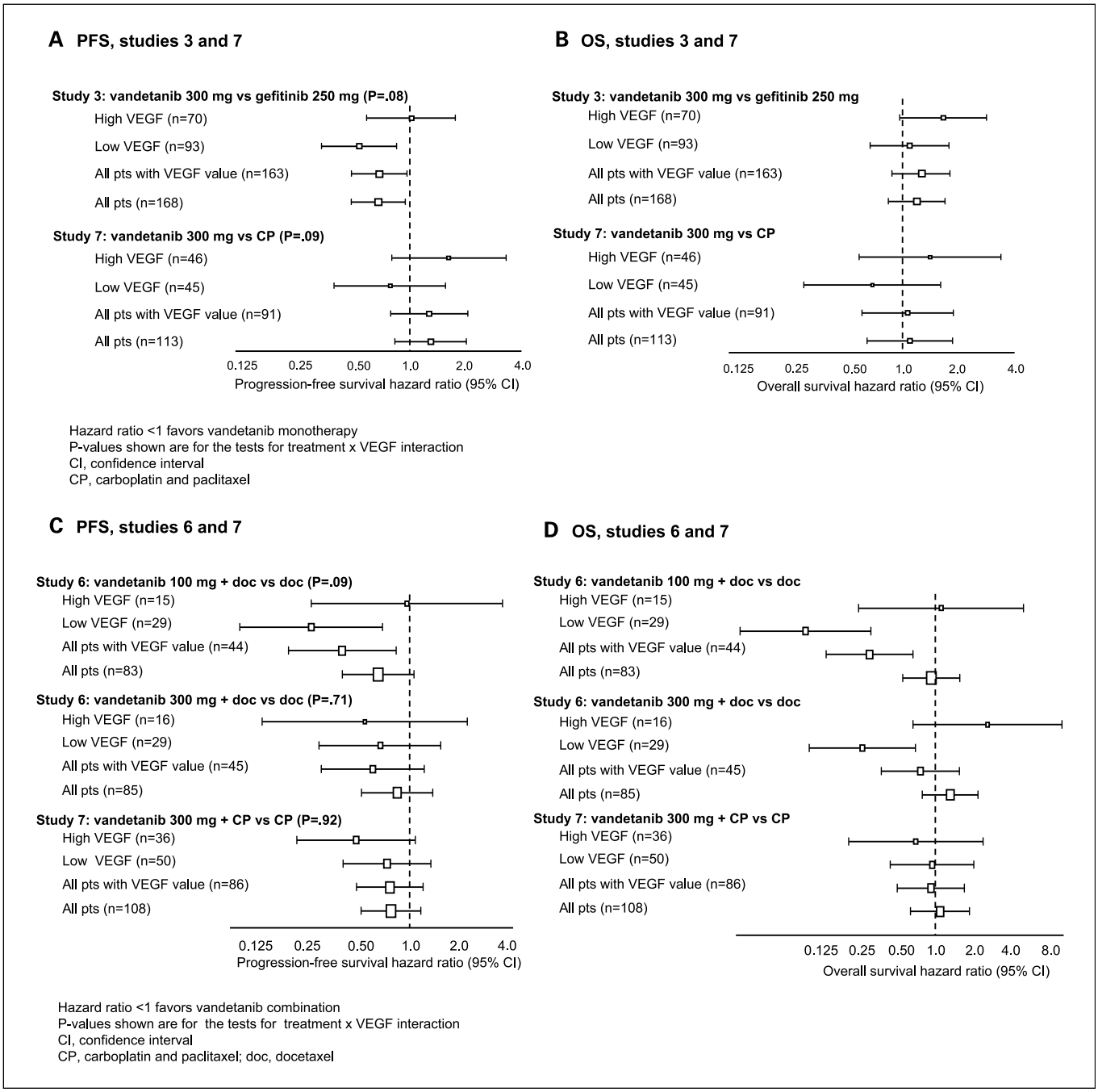


**Fig. 3.** PFS and OS for patients with low or high baseline VEGF treated with vandetanib monotherapy (studies 3 and 7) or vandetanib combination therapy (studies 6 and 7).

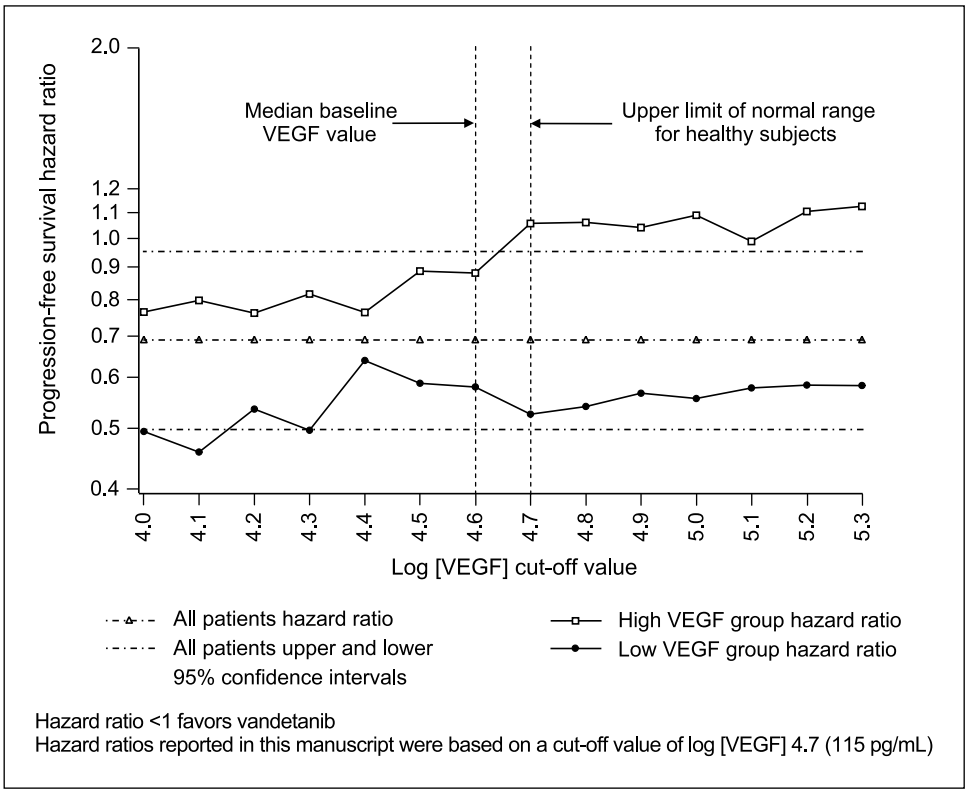


**Fig. 4.** Exploration of different cutoff points to dichotomize patients into low or high baseline VEGF groups for study 3 (PFS).

appeared to have superior PFS and OS outcomes compared with those treated with docetaxel alone, whereas patients with high baseline VEGF had similar treatment outcomes in both arms. The results were more complex for vandetanib 300 mg/d in combination with chemotherapy. For vandetanib 300 mg/d in combination with docetaxel versus docetaxel alone, there was a superior OS, but not PFS, outcome for previously treated NSCLC patients with low baseline VEGF. For vandetanib 300 mg/d in combination with carboplatin-paclitaxel versus carboplatin-paclitaxel alone, there was some evidence that previously untreated patients with high levels of pretreatment serum VEGF may have gained greater benefit in terms of both PFS and OS. One possible explanation for these observations is that the predictive value of VEGF may depend, at least in part, on the vandetanib dose. This reflects the observed clinical trial results with vandetanib in combination with chemotherapy. In studies 6 and 7, the addition of vandetanib 300 mg/d to docetaxel and carboplatin-paclitaxel, respectively, yielded modest PFS benefits compared with chemotherapy alone (HR, 0.83 and 0.76, respectively), and the greatest PFS benefit was seen when vandetanib 100 mg/d was added to docetaxel (HR, 0.64; refs. 16, 17). As shown in four randomized phase III studies, the addition of EGFR TKIs to chemotherapy for NSCLC does not improve outcome (22–25). It is thought that EGFR TKIs induce $G_1$ cell cycle arrest and thereby reduce the efficacy of cell cycle-dependent cytotoxic agents (26). It has been theorized that the EGFR inhibitory capacity of vandetanib predominates at higher doses, thereby limiting the benefit of adding this agent at the 300 mg/d dose to chemotherapy (16). At the lower 100 mg/d dose, there may be less EGFR inhibitory effect, such that the anti-VEGFR effects of vandetanib and the cytotoxic effects of chemotherapy can predominate (16). This theory is in keeping with our findings that VEGF levels may only be associated with outcome when the lower dose of vandetanib is combined with chemotherapy.

We defined "high" and "low" VEGF levels as being either above or below, respectively, the upper limit of normal reported in analyses of blood by ELISA from healthy subjects (R&D Systems Human VEGF Immunoassay). Although our findings were similar across a range of cutoff values for high versus low VEGF, including the median VEGF concentration in all three studies, we chose to present the data using this predefined, fixed cutoff point rather than the median VEGF level. Our rationale for this was that a fixed cutoff point for VEGF level could be more easily applied to clinical practice than the median concentration, which would be expected to vary between different groups of patients, if circulating VEGF level is validated as a predictive biomarker and becomes incorporated into future clinical decision-making processes.

Increased circulating VEGF concentration in patients with NSCLC and other solid tumors has been shown to correlate with poor prognosis (18, 27), and although VEGF levels in blood correlated with VEGF expression in tumor tissue from patients with colorectal cancer (28), this was not the case in NSCLC or breast cancer (29, 30). The origin of circulating VEGF measured by ELISA in plasma (studies 3 and 6) or serum (study 7) in the present analyses has not been determined but may include contributions from both tumor and nontumor tissues (31). In addition, platelet disruption, particularly during the preparation of serum, is likely to contribute to the overall levels of circulating VEGF measured in the present study (32), although whether platelet-derived VEGF originates from tumor or other tissues remains to be determined (33). However, irrespective of the origin of plasma or serum VEGF, it was unanticipated that our analyses showed that low,

rather than high, circulating VEGF levels before treatment appeared to be predictive of clinical benefit from vandetanib monotherapy. One potential explanation is that, in patients with high VEGF levels, vandetanib is unable to achieve an adequate degree of VEGFR inhibition and blockade of tumor angiogenesis; alternatively, high VEGF may be associated with high levels of other angiogenic factors, such as basic fibroblast growth factor and interleukin-8, which are able to sustain angiogenesis even in the presence of VEGFR blockade. Consistent with our findings, baseline plasma VEGF levels were recently reported to be lower in Japanese NSCLC patients who experienced clinical benefit from vandetanib than those who did not in a phase II trial (34). However, because all patients received vandetanib, it was not possible to determine whether baseline plasma VEGF was a prognostic or predictive biomarker. However, because all patients received vandetanib, it was not possible to determine whether baseline plasma VEGF was a prognostic or predictive biomarker in this setting.

A blood-based predictive biomarker has many practical and safety advantages over tissue- or imaging-based predictive biomarkers. Although there is considerable debate about whether serum or plasma is the better medium in which to assess factors such as VEGF (18), both plasma VEGF concentrations from studies 3 and 6 and serum VEGF concentrations from study 7, as determined by ELISA, were predictive in our analyses. We did not have both plasma and serum suitable for analysis by ELISA from the participants in these randomized trials of vandetanib, so we cannot draw any conclusions about the relative benefits of each of these types of blood sample in assessing circulating VEGF.

With regards to future potential clinical application of blood-based biomarkers, it may be most practical to identify a single factor that can predict benefit from VEGFR TKIs, such as VEGF, but in reality it is likely that baseline levels of other circulating angiogenic factors or cytokines also have predictive values in identifying patients who will benefit most from these therapies. Therefore, a limitation of the current work is that VEGF was the only angiogenic biomarker measured across all three clinical studies. For example, low baseline plasma intercellular adhesion molecule-1 predicted a greater PFS benefit from the addition of bevacizumab to carboplatin-paclitaxel compared with carboplatin-paclitaxel alone in the randomized phase III Eastern Cooperative Oncology Group 4599 trial (35). In squamous cell carcinoma of the head and neck treated with chemoradiation, baseline levels and coordinate changes in multiple cytokines, including VEGF, were associated with poor outcomes (36). This suggests that VEGF may be one of several circulating factors that alone, or in combination with other cytokines or angiogenic factors, may be prognostic or predictive of clinical benefit following treatment with vandetanib or other VEGFR signaling inhibitors. Our preliminary data using multiplex beads to assess >30 factors from the plasma of patients in trial 7 is consistent with this possibility, as several other factors were found to potentially be predictive of vandetanib benefit (37).

Several other phase II and III studies of VEGF signaling inhibitors in a variety of solid tumor types have considered the predictive value of pretreatment circulating VEGF levels, although the findings have been somewhat inconsistent (18, 35, 38–41). The addition of bevacizumab, a monoclonal antibody targeting VEGF, to bolus 5-fluorouracil and irinotecan as first-line treatment for metastatic colorectal cancer significantly improved PFS and OS, but survival benefit was unrelated to pretreatment plasma VEGF concentration (38). Similarly, in the Eastern Cooperative Oncology Group 4599 trial of carboplatin-paclitaxel with or without bevacizumab in NSCLC, high baseline plasma VEGF was associated with a greater response rate with the use of bevacizumab but not with improved survival (35). Patients with renal cell carcinoma treated second-line with sorafenib showed a significant improvement in PFS relative to placebo, but baseline plasma VEGF was not predictive of PFS benefit from sorafenib (39). In a randomized phase II trial, the addition of bevacizumab to first-line chemotherapy with gemcitabine and cisplatin for inoperable malignant mesothelioma did not improve outcome, but on subset analyses, patients with low pretreatment VEGF plasma concentrations derived PFS and OS benefits from the use of bevacizumab, whereas patients with high plasma VEGF levels did not benefit from bevacizumab (40). These inconsistent reports regarding the predictive value of VEGF may in part arise due to the small patient numbers in such retrospective analyses. It is also conceivable that baseline VEGF levels are not a general predictive factor for benefit from VEGF signaling inhibitors, but rather baseline VEGF may be predictive in only certain tumor types and/or with only some agents. For example, if high VEGF levels counterbalance the effects of vandetanib, VEGF levels may not be predictive of benefit from a more potent VEGFR TKI.

In our analysis, the association between low baseline VEGF and benefit from vandetanib, either as monotherapy or at the 100 mg/d dose combined with chemotherapy, was generally consistent across all three clinical trials. However, no definitive conclusions about the role of VEGF as a predictive biomarker for benefit from vandetanib can be drawn from these data. The *P* values for the interaction tests did not reach statistical significance, although they trended toward significance where associations between low VEGF and treatment outcome were found (study 3, $P = 0.08$; study 7, vandetanib versus carboplatin-paclitaxel, $P = 0.09$; study 6, vandetanib 100 mg/d, $P = 0.14$). These analyses of VEGF are exploratory; therefore, the clinical studies were not powered for these interaction tests. The numbers of patients in studies 3, 6, and 7 are modest, and there is the potential for case selection bias in study 6 because VEGF data were available for only half of the study's participants. Nevertheless, our data suggest that baseline circulating VEGF may be a potential predictive biomarker for benefit from vandetanib and that further study of VEGF in large phase III trials is warranted. If our findings are validated, they could have several potentially important clinical implications. Firstly, low baseline circulating VEGF levels may identify a subset of patients with advanced NSCLC who can receive oral vandetanib as a first-line treatment rather than intravenous administration of carboplatin-paclitaxel doublet chemotherapy. In the second-line setting, advanced NSCLC patients with low baseline VEGF levels may derive greater PFS benefit from the addition of vandetanib 100 mg/d to docetaxel chemotherapy rather than with docetaxel alone. Furthermore, patients with a low baseline VEGF levels who are being considered for treatment with a selective EGFR inhibitor in the second/third-line setting may derive greater PFS benefit if treated with vandetanib monotherapy.

Based on the findings in this exploratory analysis, baseline VEGF will be evaluated as a potential predictive biomarker of clinical benefit with vandetanib in four ongoing phase III trials

in advanced NSCLC: (*a*) second/third-line erlotinib versus vandetanib 300 mg/d, (*b*) second-line docetaxel ± vandetanib 100 mg/d, (*c*) second-line pemetrexed ± vandetanib 100 mg/d, and (*d*) second/third-line placebo versus vandetanib in patients who have progressed on prior treatment with an EGFR TKI (42).

## Disclosure of Potential Conflicts of Interest

A.J. Ryan, H. Mann, S.J. Kennedy, P. Langmuir, employment, AstraZeneca. J.V. Heymach, R.B. Natale, R.S. Herbst, commercial research funding, consultant, AstraZeneca. B.E. Johnson, consultant, Genzyme. R.S. Herbst, honoraria, AstraZeneca.

## References


1. Folkman J. Tumor angiogenesis: therapeutic implications. N Engl J Med 1971;285:1182–6.
2. Folkman J. What is the evidence that tumors are angiogenesis dependent? J Natl Cancer Inst 1990;82:4–6.
3. Hanahan D, Folkman J. Patterns and emerging mechanisms of the angiogenic switch during tumorigenesis. Cell 1996;86:353–64.
4. Herbst RS, Onn A, Sandler A. Angiogenesis and lung cancer: prognostic and therapeutic implications. J Clin Oncol 2005;23:3243–56.
5. Hicklin DJ, Ellis LM. Role of the vascular endothelial growth factor pathway in tumor growth and angiogenesis. J Clin Oncol 2005;23:1011–27.
6. Dvorak HF. Vascular permeability factor/vascular endothelial growth factor: a critical cytokine in tumor angiogenesis and a potential target for diagnosis and therapy. J Clin Oncol 2002; 20:4368–80.
7. Nagy JA, Vasile E, Feng D, et al. Vascular permeability factor/vascular endothelial growth factor induces lymphangiogenesis as well as angiogenesis. J Exp Med 2002;196:1497–506.
8. Miller K, Wang M, Gralow J, et al. Paclitaxel plus bevacizumab versus paclitaxel alone for metastatic breast cancer. N Engl J Med 2007; 357:2666–76.
9. Sandler A, Gray R, Perry MC, et al. Paclitaxel-carboplatin alone or with bevacizumab for non-small-cell lung cancer. N Engl J Med 2006;355: 2542–50.
10. Hurwitz H, Fehrenbacher L, Novotny W, et al. Bevacizumab plus irinotecan, fluorouracil, and leucovorin for metastatic colorectal cancer. N Engl J Med 2004;350:2335–42.
11. Motzer RJ, Michaelson MD, Redman BG, et al. Activity of SU11248, a multitargeted inhibitor of vascular endothelial growth factor receptor and platelet-derived growth factor receptor, in patients with metastatic renal cell carcinoma. J Clin Oncol 2006;24:16–24.
12. Motzer RJ, Hutson TE, Tomczak P, et al. Sunitinib versus interferon α in metastatic renal-cell carcinoma. N Engl J Med 2007;356:115–24.
13. Escudier B, Eisen T, Stadler WM, et al. Sorafenib in advanced clear-cell renal-cell carcinoma. N Engl J Med 2007;356:125–34.
14. Morabito A, De Maio E, Di Maio M, Normanno N, Perrone F. Tyrosine kinase inhibitors of vascular endothelial growth factor receptors in clinical trials: current status and future directions. Oncologist 2006;11:753–64.
15. Natale R, Bodkin D, Govindan R, et al. Vandetanib versus gefitinib in patients with advanced NSCLC: results from a two-part, double-blind, randomized phase II trial. J Clin Oncol [Epub ahead of print] 2009.
16. Heymach JV, Johnson BE, Prager D, et al. Randomized, placebo-controlled phase II study of vandetanib plus docetaxel in previously treated non small-cell lung cancer. J Clin Oncol 2007;25: 4270–7.
17. Heymach JV, Paz-Ares L, De Braud F, et al. Randomized phase II study of vandetanib alone or with paclitaxel and carboplatin as first-line treatment for advanced non-small-cell lung cancer. J Clin Oncol 2008;26:5407–15.
18. Longo R, Gasparini G. Challenges for patient selection with VEGF inhibitors. Cancer Chemother Pharmacol 2007;60:151–70.
19. Bocci G, Man S, Green SK, et al. Increased plasma vascular endothelial growth factor (VEGF) as a surrogate marker for optimal therapeutic dosing of VEGF receptor-2 monoclonal antibodies. Cancer Res 2004;64:6616–25.
20. Ebos JM, Lee CR, Christensen JG, Mutsaers AJ, Kerbel RS. Multiple circulating proangiogenic factors induced by sunitinib malate are tumor-independent and correlate with antitumor efficacy. Proc Natl Acad Sci U S A 2007;104: 17069–74.
21. Drevs J, Zirrgiebel U, Schmidt-Gersbach CI, et al. Soluble markers for the assessment of biological activity with PTK787/ZK 222584 (PTK/ZK), a vascular endothelial growth factor receptor (VEGFR) tyrosine kinase inhibitor in patients with advanced colorectal cancer from two phase I trials. Ann Oncol 2005;16:558–65.
22. Herbst RS, Prager D, Hermann R, et al. TRIBUTE: a phase III trial of erlotinib hydrochloride (OSI-774) combined with carboplatin and paclitaxel chemotherapy in advanced non-small-cell lung cancer. J Clin Oncol 2005;23:5892–9.
23. Herbst RS, Giaccone G, Schiller JH, et al. Gefitinib in combination with paclitaxel and carboplatin in advanced non-small-cell lung cancer: a phase III trial-INTACT 2. J Clin Oncol 2004;22: 785–94.
24. Gatzemeier UPA, Szczesna A, Kaukel E, et al, for the TALENT Study Investigators. Results of a phase III trial of erlotinib (OSI-774) combined with cisplatin and gemcitabine (GC) chemotherapy in advanced non-small cell lung cancer (NSCLC). J Clin Oncol 2004;22:7010.
25. Giaccone G, Herbst RS, Manegold C, et al. Gefitinib in combination with gemcitabine and cisplatin in advanced non-small-cell lung cancer: a phase III trial-INTACT 1. J Clin Oncol 2004;22: 777–84.
26. Davies AM, Ho C, Lara PN, Jr., Mack P, Gumerlock PH, Gandara DR. Pharmacodynamic separation of epidermal growth factor receptor tyrosine kinase inhibitors and chemotherapy in non-small-cell lung cancer. Clin Lung Cancer 2006;7: 385–8.
27. Bremnes RM, Camps C, Sirera R. Angiogenesis in non-small cell lung cancer: the prognostic impact of neoangiogenesis and the cytokines VEGF and bFGF in tumours and blood. Lung Cancer 2006;51:143–58.
28. Minagawa N, Nakayama Y, Hirata K, et al. Correlation of plasma level and immunohistochemical expression of vascular endothelial growth factor in patients with advanced colorectal cancer. Anticancer Res 2002;22:2957–63.
29. Imoto H, Osaki T, Taga S, Ohgami A, Ichiyoshi Y, Yasumoto K. Vascular endothelial growth factor expression in non-small-cell lung cancer: prognostic significance in squamous cell carcinoma. J Thorac Cardiovasc Surg 1998;115: 1007–14.
30. Garvin S, Dabrosin C. *In vivo* measurement of tumor estradiol and vascular endothelial growth factor in breast cancer patients. BMC Cancer 2008;8:73.
31. Kut C, Mac Gabhann F, Popel AS. Where is VEGF in the body? A meta-analysis of VEGF distribution in cancer. Br J Cancer 2007;97: 978–85.
32. Wynendaele W, Derua R, Hoylaerts MF, et al. Vascular endothelial growth factor measured in platelet poor plasma allows optimal separation between cancer patients and volunteers: a key to study an angiogenic marker *in vivo*? Ann Oncol 1999;10:965–71.
33. Salgado R, Benoy I, Bogers J, et al. Platelets and vascular endothelial growth factor (VEGF): a morphological and functional study. Angiogenesis 2001;4:37–43.
34. Kiura K, Nakagawa K, Shinkai T, et al. A randomized, double-blind, phase IIa dose-finding study of vandetanib (ZD6474) in Japanese patients with non-small cell lung cancer. J Thorac Oncol 2008;3:386–93.
35. Dowlati A, Gray R, Sandler AB, Schiller JH, Johnson DH. Cell adhesion molecules, vascular endothelial growth factor, and basic fibroblast growth factor in patients with non-small cell lung cancer treated with chemotherapy with or without bevacizumab—an Eastern Cooperative Oncology Group Study. Clin Cancer Res 2008; 14:1407–12.
36. Allen C, Duffy S, Teknos T, et al. Nuclear factor-κB-related serum factors as longitudinal biomarkers of response and survival in advanced oropharyngeal carcinoma. Clin Cancer Res 2007;13:3182–90.
37. Hanrahan EO, Lin HY, Du DZ, et al. Correlative analyses of plasma cytokine/angiogenic factor (C/AF) profile, gender and outcome in a randomized, three-arm, phase II trial of first-line vandetanib (VAN) and/or carboplatin plus paclitaxel (CP) for advanced non-small cell lung cancer (NSCLC). J Clin Oncol 2007 ASCO Annu Meet Proc 2007;25:7593.
38. Holden SN, Ryan E, Kearns A, Holmgren E, Hurwitz H. Benefit from bevacizumab (BV) is independent of pretreatment plasma vascular endothelial growth factor-A (pl-VEGF) in patients (pts) with metastatic colorectal cancer (mCRC). J Clin Oncol 2005 ASCO Annu Meet Proc 2005; 23:3555.
39. Bukowski RM, Eisen T, Szczylik C, et al. Final results of the randomized phase III trial of sorafenib in advanced renal cell carcinoma: survival and biomarker analysis. J Clin Oncol 2007 ASCO Annu Meet Proc 2007;25:5023.
40. Karrison T, Kindler HL, Gandara DR, et al. Final analysis of a multi-center, double-blind, placebo-controlled, randomized phase II trial of gemcitabine/cisplatin (GC) plus bevacizumab (B) or placebo (P) in patients (pts) with malignant mesothelioma (MM). J Clin Oncol 2007 ASCO Annu Meet Proc 2007;25:7526.
41. Burstein HJ, Chen YH, Parker LM, et al. VEGF as a marker for outcome among advanced breast cancer patients receiving anti-VEGF therapy with bevacizumab and vinorelbine chemotherapy. Clin Cancer Res 2008;14:7871–7.
42. Hanrahan EO, Heymach JV. Vascular endothelial growth factor receptor tyrosine kinase inhibitors vandetanib (ZD6474) and AZD2171 in lung cancer. Clin Cancer Res 2007;13:s4617–22.

**Stromal EGFR contributes to VEGF inhibitor resistance in murine models of human NSCLC**

Tina Cascone[1,4], Matthew H. Herynk[1], Li Xu[1], Zhiqiang Du[1], Humam Kadara[1], Monique B. Nilsson[1], Carol J. Oborn[2], Yun-Yong Park[3], Ju-Seog Lee[3], Fortunato Ciardiello[4], Robert R. Langley[2] and John V. Heymach[1,2].

[1]Department of Thoracic/Head and Neck Medical Oncology; [2]Cancer Biology; [3]Systems Biology; The University of Texas M. D. Anderson Cancer Center, Houston, TX, 77030 USA;

[4]Division of Medical Oncology, 'F. Magrassi - A. Lanzara' Department of Clinical and Experimental Medicine, Second University of Naples, Naples, Italy

**Corresponding Author:** John V. Heymach

Departments of Thoracic/Head and Neck Medical Oncology and Cancer Biology

The University of Texas M. D. Anderson Cancer Center, Unit 432

1515 Holcombe Blvd, 77030 Houston, TX

Phone: 713-792-6363

Fax: 713-792-1220

Email: jheymach@mdanderson.org

**Abstract**

The mechanisms by which tumors develop resistance to angiogenesis inhibitors, and the relative contributions of tumor cells and stroma to resistance, have not been established. We developed human NSCLC xenograft models of resistance to the VEGF inhibitor bevacizumab in mice and, using species-specific profiling, investigated tumor cell and stromal mechanisms of resistance. Mouse- and human-specific profiling demonstrated that gene expression changes associated with acquired resistance occurred predominantly in stromal (mouse) and not tumor (human) cells. Components of the EGFR and FGFR2 pathways were significantly upregulated in stroma, but not in tumor cells. Increased phosphoEGFR was detected on pericytes of xenografts that acquired resistance and on endothelium of tumors with primary resistance. Acquired resistance was associated with a pattern of pericyte-covered, normalized revascularization, whereas tortuous, uncovered vessels were observed in primary resistance. Dual targeting of VEGF and EGFR pathways with bevacizumab and erlotinib, or the VEGFR/EGFR inhibitor vandetanib, reduced pericyte coverage and delayed resistance. These findings demonstrate that alterations in tumor stromal pathways, including EGFR and FGFR2, are associated with, and may contribute to VEGF inhibitor resistance and that targeting these pathways may improve efficacy. Understanding stromal signaling may be critical for developing biomarkers for angiogenesis inhibitors and improving combination regimens.

## INTRODUCTION

Tumor growth and metastatic spread are dependent on the acquisition of a vascular supply, which occurs at least in part through angiogenesis (1-3). This process is regulated by the balance of pro- and anti-angiogenic factors (4). Therapeutic approaches to targeting tumor vasculature have focused largely on vascular endothelial growth factor (VEGF), the prototypical pro-angiogenic factor that stimulates endothelial cells to proliferate, migrate, and produce proteases necessary for the formation of new vasculature networks (5-9). Strategies to inhibit VEGF-induced angiogenesis have been developed, including anti-VEGF monoclonal antibodies, such as bevacizumab (Avastin; Genentech, South San Francisco, CA) (10, 11), and VEGF receptor (VEGFR) tyrosine kinase inhibitors (TKIs) (12).

Phase III trials have shown that the addition of bevacizumab (BV) to standard therapy prolonged progression-free or overall survival, and improved objective tumor responses, in patients with advanced malignancies, including non-small cell lung caner (NSCLC) (13). Despite this initial benefit however, therapeutic resistance inevitably emerges in most patients. In patients with colorectal cancer, we observed that acquired resistance was associated with a rise in circulating proangiogenic factors in plasma including basic fibroblast growth factor (bFGF), hepatocyte growth factor (HGF) placental growth factor (PlGF), stromal-derived factor-1, (SDF1) as well as factors associated with myeloid recruitment (*e.g.* macrophage chemoattractant protein-3 (14). Preclinical studies of therapeutic resistance to angiogenesis inhibitors have described compensatory mechanisms

acquired from tumors in the face of anti-angiogenic therapy, including a hypoxia-induced upregulation of pro-angiogenic molecules, such as FGF family members, in tumors with acquired resistance to VEGFR pathway inhibitors (15). Genetic alterations in tumor cells, such as p53 loss, may also promote resistance to hypoxia-induced apoptosis, resulting in a decreased vascular dependence (16). Incomplete target inhibition following treatment with VEGFR antagonists has been described in orthotopic models of pancreatic cancer as well as in patients (17, 18). Moreover, while showing potent antitumor activity in mouse models of pancreatic neuroendocrine carcinoma and glioblastoma, VEGF pathway inhibitors concomitantly may also increase invasiveness and metastatic potential (19).

Collectively, these findings emphasize the adaptive nature of tumor cells to anti-angiogenic therapies, whereas the contribution of stromal cells remains unclear. In this study, we specifically investigated stromal changes associated with resistance to anti-VEGF therapy in two human NSCLC xenograft models of acquired and primary resistance to BV. We performed mouse- (stroma) and human (tumor cell)-specific gene expression profiling to further validate the role of specific stromal molecules involved in resistance. Our results demonstrate that acquired or primary resistance to VEGF inhibition is associated with distinct patterns of vascularization in NSCLC xenografts. The vast majority of gene expression changes observed in resistant tumors occurred in tumor stroma and not in tumor cells themselves, suggesting stromal changes are likely to play a role in the resistant phenotype. Among factors known to regulate angiogenesis,

overexpression of stromal EGFR and FGFR2 signaling pathways was observed in resistant tumors and blockade of the EGFR pathway reversed the increased pericyte coverage observed in vessels of resistant tumors. The results suggest that stromal mechanisms, including an upregulation of EGFR pathway, can contribute to the resistant phenotype, and that targeting these pathways may delay tumor growth and the onset of resistance.

## RESULTS

### H1975 and A549 Xenografts Exhibit Acquired and Primary Resistance to Anti-angiogenic Therapy

To investigate the mechanisms by which NSCLC xenografts develop resistance to VEGF blockade, we injected male nude mice with either H1975 or A549 human NSCLC adenocarcinoma cells. These models were selected because in prior studies (20) we observed that A549 xenograft tumors were relatively insensitive to VEGF signaling inhibitors including BV (primary resistance), whereas H1975 initially experienced significant tumor shrinkage typically lasting for more than one month. Furthermore, the tumor cells contain two common alterations associated with EGFR TKI resistance: a T790M EGFR mutation (H1975 model) (21) and KRas mutation (A549) (22). Approximately 3 weeks after tumor cell injection, mice bearing tumors with a mean volume of ~270 $mm^3$ were randomized to receive either vehicle (control) or BV, as described in detail in the Materials and Methods section. Animals were treated for 2 weeks (short-term treatment) or until mice were sacrificed due to tumor burden. Tumors were

considered to be resistant when they tripled in volume (progression) compared with the pre-treatment tumor size and progression-free survival (PFS) was measured as the time from initiation of treatment until tumor progression. In H1975 tumors, 2 weeks of BV inhibited tumor growth by 77% compared to controls (Figure 1A) whereas in A549 xenografts the drug produced only a 16% reduction in tumor growth compared with vehicle-treated tumors (Figure 1B).

The individual tumor growth curves shown in Figure 1C&D illustrate the growth kinetics of H1975 and A549 xenografts treated with vehicle and BV for a longer term until progression. All H1975 vehicle-treated xenografts progressed within 31 days of the onset of treatment, showing a median PFS of 7 days. In contrast, 67% of xenografts receiving BV developed resistance, and the median PFS was 138 days, ($p<0.001$, log-rank test) (Figure 1C). A549 tumors were less responsive to BV, showing a median PFS of 35 days compared with 22 days of vehicle-treated tumors ($p=0.16$), (Figure 1D). Collectively, these results show that H1975 tumors are initially responsive to BV therapy but acquire resistance after prolonged treatment with the drug, whereas A549 tumors demonstrate primary resistance.

**Acquired Resistance to BV Is Associated With Sustained Inhibition of VEGFR2 Activation**

To determine whether acquired resistance to BV was due to increased VEGFR2 signaling, potentially through increased expression of murine VEGF or other mechanism to bypass blockade of human VEGF by this agent, we evaluated the

phosphorylation status of VEGFR2 in vehicle-treated and BV-resistant tumors using immunofluorescence (IF) staining. In control H1975 tumors, p-VEGFR2 was readily detected on $CD31^+$ tumor-associated endothelial cells (ECs), but it was inhibited on vessels of BV-sensitive tumors (short-term treatment) and this result was sustained when tumors progressed while receiving BV therapy (Figure 2A). To evaluate changes in stromal (defined here as non-tumor cells derived from the host) and tumor-derived VEGF in H1975 BV-resistant tumors, we quantified mouse and human VEGFA mRNA expression by quantitative real-time PCR (qRT-PCR). We observed no change in mouse *Vegfa* mRNA expression in resistant xenografts compared with controls, whereas human *VEGFA* mRNA levels were increased in resistant tumors compared with controls ($p<0.05$, Figure 2B), despite this ligand increase, VEGFR2 phosphorylation remained suppressed during BV treatment in resistant tumors.

We assessed whether the tumor growth inhibition observed in H1975 xenografts after short-term treatment with BV was associated with increased endothelial cell apoptosis. We performed double IF staining for CD31 (red) and TUNEL positivity (green) to identify apoptotic cells, (Figure 2C). The percentage of apoptotic ECs was significantly increased following 2 weeks of BV treatment compared to control xenografts ($p<0.01$). However, at time of progression, H1975 xenografts showed a significant decrease in endothelial cell apoptosis compared with short-term treatment ($p<0.05$) to levels comparable to control tumors (Figure 2D). Thus, endothelial cell apoptosis increased while tumors were initially responding to VEGF signaling blockade and returned to levels comparable with controls in

tumors that acquired BV-resistance. Furthermore, the percentage of total apoptotic ($TUNEL^+$) cells showed a trend toward increase in H1975 BV-sensitive xenografts (BV 2 weeks) compared with controls (p=0.06), but not in tumors that progressed compared with controls (see Supplemental Figure 1A - B).

**Stromal and Tumor Cell Gene Expression Changes in H1975 BV-Resistant Xenografts**

To identify changes in stromal and tumor gene expression associated with acquired resistance to anti-VEGF therapy, we performed RNA microarray analyses comparing H1975 control and BV-resistant xenografts (N=3 samples each group) using Illumina mouse (WG-6 v2) and human (WG-6 v3)-specific expression arrays. Probes in these arrays have been shown to minimize cross-species reactivity (Eun Sung Park, unpublished data). We found that a larger number of stromal mouse genes (1385) were significantly modulated in BV-resistant (BV progression) vs. control xenografts (vehicle progression) compared to human tumor genes (98), according to the statistic criteria described in Materials and Methods. We observed significant changes in the expression of genes involved in angiogenesis, lymphangiogenesis and hypoxia signaling pathway between BV-resistant and control xenografts. Both *Egfr* and *Fgfr2* genes were upregulated in the stromal compartment, but not in tumor cells, of H1975 BV-resistant tumors compared with controls, as well as stromal molecules and ligands associated with these signaling pathways (e.g., *Epgn, Areg, Fgf13, Fgfbp1*) (Figure 3A, see Supplemental Table 1). Among human angiogenic

genes, *CA9* (hypoxia-regulated gene) was significantly upregulated in BV-resistant tumors (Figure 3A, see Supplemental Table 2).

We next sought to identify genes predicted to be important in the phenotype of acquired resistance to the anti-angiogenic effect of BV through both their modulation in expression and molecular interactions. Functional gene-interaction network analyses of gene features differentially expressed between the mouse stroma of BV-resistant and vehicle-treated H1975 xenografts using Ingenuity Pathways Analysis (IPA) revealed the significant modulation in the predicted function of a gene neighborhood and interaction network surrounding *Egfr,* based on the number of focus genes and nodes of interaction ($p<0.001$; Figure 3B). In addition, the modulated gene network associated with *Egfr* gene expression included down-regulated pro-apoptotic genes, such as the BH3-only family member protein, *Bax* and the apoptotic peptidase activating factor 1 (*Apaf1*). Genes with pro-survival functions were up-regulated, such as the heat shock protein *Dnajb1.*

Next, to validate the changes in expression of the significantly modulated network-hub gene, *Egfr*, we assessed the human and mouse mRNA levels using qRT-PCR. We observed a 2.5 fold increase in mouse *Egfr* mRNA levels in H1975 resistant xenografts compared with controls ($p<0.05$), whereas human EGFR mRNA levels were not significantly different than controls (Figure 3C). We also validated the stromal expression of Fgfr2, which we noted to be upregulated in BV-resistant H1975 tumors in the microarray analysis. A significant increase in

mouse *Fgfr2* mRNA expression, but not human FGFR2, was observed in H1975 resistant xenografts compared with controls ($p<0.05$, Figure 3D).

**EGFR Is Activated on Stromal Cells of H1975 and A549 BV-Resistant Tumors**

Given our observation that *Egfr* mRNA is increased in BV-resistant tumors, we next evaluated EGFR protein expression in H1975 tumors by IF staining using antibodies directed against CD31 (red) and total EGFR (green) (see Supplemental Figure 2A). We observed an increase in $EGFR^{+}$ staining in H1975 BV-resistant tumors (BV progression) compared with controls (vehicle progression). Quantification of EGFR staining by laser scanning cytometry (LSC) analysis indicated a nearly 10-fold increase in the percentage of total EGFR-expressing cells in H1975 BV-resistant compared with control tumors ($p<0.01$, Figure 4A). We also evaluated EGF protein expression changes by immunohistochemistry (IHC) in H1975 vehicle-and BV-treated xenografts at progression and noticed increased expression of the EGFR ligand in resistant tumors vs. controls (see Supplemental Figure 2B).

We next evaluated the EGFR activation status in H1975 and A549 xenografts following treatments with vehicle and BV at time of progression. Confocal microscopy was performed to analyze specimens stained with antibodies directed to CD31 (red) and p-EGFR (green). As shown in Figure 4B, BV resistance was associated with a marked increase in p-EGFR in both H1975 and A549 tumors compared with controls; however, notable differences in the

staining pattern were observed between the two xenograft models. In H1975, p-EGFR was increased on the vascular supporting cells (VSCs) of resistant tumors compared with controls ($p<0.01$, Figure 4C, left), whereas, p-EGFR expression was increased on $CD31^+$ ECs in A549 BV-resistant xenografts compared with controls ($p<0.05$, Figure 4C, right).

To identify the population of VSCs expressing p-EGFR in H1975 BV-resistant tumors, we performed IF staining for p-EGFR (red) and desmin (green), a marker for pericytes (Figure 4D). We found p-EGFR expression to be significantly increased on $desmin^+$ cells (pericytes) of BV-resistant H1975 xenografts compared with controls ($p<0.01$, Figure 4E). Taken together our results suggest that increased stromal EGFR is associated with BV resistance, and that multiple stromal cell types can express EGFR.

**bFGF/FGFR2 Overexpression in H1975 Xenografts Resistant to BV Therapy**

Based on our observation that mouse *Fgfr2* gene expression was increased in the stromal compartment of BV-resistant H1975 tumors, we performed immunofluorescent co-localization studies on H1975 vehicle and BV-treated xenografts at progression (n=4, each group) using CD31 (red) and FGFR2 (green) antibodies (Figure 5A). We observed a significant increase in total FGFR2 expression in resistant tumors compared with controls ($p<0.001$; Figure 5B). Furthermore, to assess changes in the FGFR2 ligand, we next measured the plasma concentration (pg/mL) and the expression levels of basic FGF (bFGF). We found a 1.5 fold increase in the levels of the circulating cytokine in

BV-resistant tumors compared with controls (p=0.058; Figure 5C). The immunohistochemical analysis of H1975 vehicle and BV-treated xenografts at progression (n=4, each group) suggested that BV-resistance is associated with increased expression of bFGF compared with controls (Figure 5D).

**Resistance to BV is Associated with Tumor Revascularization and Morphological Changes in the Vasculature**

Because the primary mechanism of action of BV is directed against blood vessels, we quantified the microvascular density (MVD) of H1975 and A549 xenografts. We noted a 3-fold MVD reduction in H1975 tumors treated with BV for 2 weeks compared with controls ($p<0.01$, see Supplemental Figure 3 - Figure 6B, left). Vessel density of A549 tumors treated for 2 weeks showed a trend towards a decrease compared with controls (see Supplemental Figure 3 - Figure 6B, right). To determine whether the vascular effects observed after 2 weeks of BV therapy persisted in tumors receiving BV long-term treatment, we quantified the MVD in BV resistant H1975 and A549 tumors. We found that primary and acquired resistance was associated with distinct patterns of tumor vascularization. In H1975 BV-treated xenografts, MVD was significantly higher at progression compared with short-term treatment ($p<0.01$), returning to levels comparable with vehicle-treated controls (Figure 6A, upper panel – Figure 6B, left panel). In A549 xenografts, there was a significant increase in MVD of BV-treated xenografts at progression compared with controls ($p<0.05$) (Figure 6A, lower panel – Figure 6B, right panel). Taken together, these data suggest that BV

therapy has a dramatic initial anti-angiogenic effect on sensitive H1975 xenografts, but that this effect is lost after continued exposure to the drug, and that therapeutic resistance is associated with revascularization at levels comparable with, or higher than, those in vehicle-treated controls.

Previous results have demonstrated that anti-angiogenic therapy can alter the morphology of the tumor-associated vasculature (23-26). To evaluate the tumor vascularization in greater detail, we assessed vascular tortuosity in vehicle and BV-treated H1975 and A549 xenografts. We found that short-term administration of BV led to a modest, but not statistically significant, reduction in the vessel tortuosity of H1975 tumors (Figure 6A upper panel – Figure 6C, left panel). However, as these tumors developed BV resistance, we noted a 4-fold reduction in vascular tortuosity compared with controls ($p<0.01$), with larger vessels and a greater degree of pericyte coverage (termed “normalized revascularization”). In contrast, we observed that in A549 xenografts with primary resistance to BV, tumor vascularization was associated with smaller, more tortuous vessels with reduced pericyte coverage compared with controls ($p<0.05$; Figure 6A, lower panel – Figure 6C, right panel) (termed “sprouting vascularization”), demonstrating that in these models, acquired and primary resistance is associated with different patterns of tumor vascularization.

**Dual Blockade of EGFR and VEGFR2 Signaling Pathways Delays Tumor Growth of NSCLC Xenografts**

To elucidate whether targeting functioning stromal signaling pathways in BV-resistant tumors can abrogate therapeutic resistance, we targeted EGFR using either the EGFR TKI erlotinib in combination with BV, or the dual VEGFR/EGFR inhibitor vandetanib. Both A549 and H1975 cells are known to be resistant to erlotinib and vandetanib *in vitro*, which is thought to be due to the presence of a KRAS mutation and a secondary EGFR mutation (T790M), respectively (20-22). Consistent with previous results, erlotinib did not inhibit H1975 tumor growth compared with vehicle (Figure 6D), as five (5/6) xenografts progressed, with a median PFS of 12 days. One xenograft progressed while receiving erlotinib plus BV therapy; vandetanib caused tumor growth inhibition in all the xenografts and only two of these progressed. The median PFS in the vandetanib group was 211 days, whereas it was not reached in erlotinib + BV group.

In A549 xenografts, treatment with erlotinib resulted in median PFS values of 53 days, compared with 22 days for vehicle-treated controls ($p=0.12$, log-rank test; Figure 6E). Two tumors progressed on erlotinib plus BV treatment over the course of the experiment (median PFS not reached), and the addition of the EGFR TKI erlotinib to BV significantly delayed the onset of resistance compared with BV alone ($p<0.05$, log-rank test). Only one tumor progressed while receiving vandetanib after 102 days of treatment ($p<0.05$, vandetanib vs. BV). These findings indicate that EGFR inhibition not only reduced the number of NSCLC

xenografts that progressed on therapy compared with BV alone, but also delayed the onset of resistance to VEGF signalling inhibition.

Given the aforementioned EGFR expression in pericytes in the H1975 model, we examined whether targeting EGFR would impact vessel maturation and pericyte coverage. Multicolor IF staining was performed using antibodies directed to CD31 (red) and desmin (green) and pericyte coverage was quantified. In H1975 BV-resistant xenografts, the percentage of blood vessels surrounded by pericytes was 50% higher compared with control tumors ($p<0.01$). However, pericyte coverage was significantly reduced in tumors receiving long-term treatment with erlotinib plus BV or vandetanib ($p<0.01$), which likely induced an inhibition of the EGFR pathway activation on the pericytes (Figure 6F). In contrast, A549 xenografts that progressed on BV therapy had significantly fewer blood vessels supported by pericytes compared with controls ($p<0.05$); nevertheless, long-term administration of erlotinib plus BV or vandetanib also decreased the pericyte coverage in this model compared with controls ($p<0.05$; see Supplemental Figure 4), providing further support for the role of EGFR in tumor stroma.

## Discussion

Early reports examining the effects of anti-angiogenic therapies raised the hopes that these agents may significantly slow or stop tumor growth, and that therapeutic resistance to these agents would be less likely to occur in part because the target was diploid and not prone to the same genetic instability as tumor cells (27, 28). However, both preclinical studies and clinical experience in lung cancer and other solid tumors (13, 15, 29-33) indicate that the vast majority of solid tumors either have primary (de novo) resistance, or will eventually acquire resistance, to the effects of antiangiogenic agents. Although to date most studies of therapeutic resistance to anticancer drugs have focused on the role of tumor cells, recent studies have suggested that host factors, including tumor stroma, may play a role as well (32, 34-38)

In this study, we used mouse- and human-specific profiling of human NSCLC xenografts in mice to investigate stromal and tumor cell alterations occurring in tumors with primary and acquired resistance to BV. This analysis revealed that modulation of angiogenesis-related genes during the development of the resistant phenotype in this model occurs predominantly in the stromal, and not tumor cell, compartment. We validated that two stromal genes, *Egfr* and *Fgfr2* become upregulated during the resistant phase and, moreover, demonstrated that therapeutic inhibition of the EGFR signaling in BV-resistant tumors significantly blocked stromal changes associated with acquired resistance, including increased pericyte coverage, and delayed the onset of resistance.

We studied tumor growth in two human NSCLC xenografts models in mice: H1975, which were initially inhibited by BV but subsequently and sporadically acquired resistance at times ranging from one to six months, and A549, which were not significantly inhibited from the onset of treatment. Human NSCLC cells were used to facilitate species-specific profiling to separately assess tumor and stroma gene expression. These particular models were chosen because of their differences in initial responsiveness to BV and the known resistance of the tumor cells to EGFR blockade (20) which allowed us to assess the impact of stromal EGFR blockade.

We observed that in the acquired resistance model (H1975) BV treatment was initially associated with tumor growth inhibition, a marked reduction in tumor MVD and an increase in tumor endothelial apoptosis after two weeks. These observations are consistent with data from earlier preclinical and clinical reports involving multiple tumor types (23, 24, 26, 39-42). Acquired resistance, however, was associated with a marked increase in overall MVD to levels similar to those of untreated tumors. Furthermore, resistance was not associated with increased phosphoVEGFR2. Consistent with this result, previous reports showed continuing molecular efficacy of the VEGFR2 signaling blockade during the angiogenic evasion phase in a model of pancreatic neuroendocrine tumors (15). Our findings, therefore, provide evidence that VEGFR2-independent mechanisms were contributing to the observed changes in the tumor vasculature. In fact, the vasculature of tumors with acquired resistance had a further, dramatic reduction in vessel tortuosity compared to controls, with greater pericyte

coverage and reduced endothelial apoptosis (“normalized revascularization”). Different patterns of vascular changes were observed in the A549 primary resistance model, with increased MVD at progression associated with greater vessel tortuosity and decreased pericyte coverage (“sprouting vascularization”). Studies have shown that the number of pericytes associated with the tumor vasculature has important clinical implications in that it can determine the efficacy of therapy (43, 44). Pericytes play key roles in maintenance of cancer vasculature by producing survival signaling and may provide a protective mechanism against antiangiogenic therapies. Our findings provide evidence that pericytes may play an important role in the acquisition of resistance in tumors that initially responded to VEGF blockade.

Gene expression analysis showed that among the differentially modulated genes of tumor cells and tumor stroma associated with acquired resistance there is, upregulation of *Egfr* and *Fgfr2,*, as well as other members of these signaling pathways, such as *epiregulin (Epgn), Amphiregulin (Areg), Fgf13*, and *Fgfbp1*. A functional gene-interaction network analyses highlighted the EGFR pathway as a major set of interacting genes that were altered in resistant tumors. Alterations in the stromal EGFR and FGFR2 pathways in tumors with acquired resistance were then validated by qRT-PCR using species-specific probes, and further investigation revealed that in resistant tumors, increased activated EGFR was localized almost exclusively on VSCs consistent with pericytes. No significant phospho-EGFR was detectable on VSCs of control tumors. The dual inhibition of VEGFR/EGFR pathways reduced pericyte coverage of tumor vessels and

delayed tumor progression compared with BV alone. A trend towards longer PFS was observed with dual inhibition compared to BV alone as well. Interestingly, primary resistance in A549 xenografts, which was associated with a pattern of “sprouting vascularization”, also had increased phosphoEGFR immunoreactivity compared with controls but in this model it was localized almost exclusively to tumor endothelium, not VSCs. As expected, dual VEGFR/EGFR inhibition did not reduce pericyte coverage in this model, but did significantly delay the emergence of resistance compared with BV alone. These findings demonstrate that increases in stromal EGFR signaling are associated with tumor progression in two different models of BV resistance and that targeting the EGFR pathway is able to reverse changes associated with resistance (e.g. pericyte coverage) and delay the emergence of resistance. It also highlights that a signaling pathway may play different roles in tumor stroma depending on the cellular context.

Studies examining the EGFR distribution on endothelium suggest that it is restricted to blood vessels supplying pathologic tissues (45), where it activates angiogenic programs (46). Others have reported that EGFR is activated on endothelium when tumor cells express EGFR ligands, such as transforming growth factor alpha (TGF$\alpha$) or EGF (47, 48). We localized p-EGFR to the blood vessels of primary resistant A549 xenografts and to the vascular supporting pericytes of H1975 xenografts that acquired BV-resistance. Consistent with this observation, a recent study found that the EGFR TKI gefitinib significantly suppressed tumor-associated pericyte function (49). We also found that EGFR blockade decreased pericyte coverage in this model. To our knowledge, this is

the first evidence demonstrating a potential role for EGFR signaling in pericytes or other stromal cells in resistance to VEGF pathway inhibitors or other antiangiogenic agents.

A recent study has identified a role for PDGF-C expressed by tumor associated fibroblasts in VEGF inhibitor resistance (38) and in attenuating tumor response to anti-VEGF treatment in a model of glioblastoma (50). Somewhat surprisingly, we did not observe upregulation of any PDGF receptors (PDGFR) or ligands. In contrast, we observed a modest but statistically significant *downregulation* of stromal genes encoding PDGF-A, PDGF-B and PDGFR-β. Given the role of the PDGF family in multiple tumor processes, including pericyte recruitment and function (51, 52), it appears that pericyte-expressed EGFR may play a complimentary or compensatory role in the increased pericyte coverage observed in the acquired resistance model.

Activation of FGF/FGFR pathway has been shown to be a critical regulator of the "angiogenic switch" (53) and to be upregulated in response to anti-angiogenic therapy (15). We observed an approximately 6-fold increase in stromal *Fgfr2* gene expression in tumors with acquired resistance and, consistent with this finding, an increase in the number of FGFR2-expressing cells in these tumors. This immunoreactivity appeared to be largely, but not exclusively, on tumor endothelium. This suggests that the FGFR2 pathway may promote VEGF-independent endothelial survival as previously observed in other preclinical models (54, 55) although we cannot rule out the possibility that it plays a role in other non-endothelial stromal cells. Circulating levels of the FGFR2 ligand bFGF

were also elevated in the plasma of mice with BV-resistant tumors. This observation is notable in light of our recent observation that acquired resistance to chemotherapy and BV in colorectal cancer patients is associated with an increase in circulating bFGF (14), suggesting that similar mechanisms may be occurring in cancer patients.

Other genes differentially expressed in tumors with acquired resistance included *Thrombospondin 2* (*Thbs2*), a potent negative regulator of angiogenesis (56) and *Bax*, a pro-apoptotic member of the Bcl-2 family of proteins (57), which were both downregulated in resistant tumors. Recent studies have shown Amphiregulin to be involved in resistance to targeted therapy in NSCLC cells by promoting BAX inhibition (58). Consistent with these observations, our results showed an upregulation of *Areg* gene accompanied by downregulation of *Bax* in the stromal compartment of BV resistant tumors compared with controls.

The mechanisms underlying regulation of tumor stromal genes altered in resistant tumors remains to be established and are likely to differ in the various stromal cell types. Expression of many of the genes, including *FGFR2* (59) and *EGFR* family members and *thromobspondin-2* (as well as tumor cell *carbonic anhydrase-9*), are known to be regulated by hypoxia or to correlate with expression of hypoxia inducible factor 1 alpha (HIF1$\alpha$), as reviewed in (60). One possible explanation is that BV therapy initially triggers a significant decrease in tumor MVD and an increase in tumor hypoxia (61), triggering upregulation of hypoxia-dependent pathways. It is worth noting, however, that BV resistance was not associated with significant increases in many stromal genes known to be

upregulated by hypoxia, and many of the genes upregulated in BV resistance are not known to be hypoxia-regulated. Hypoxia is likely, therefore, to be only one of many factors- both host- and tumor cell dependent- that are likely to be impacting the tumor and its microenvironment in resistant tumors.

To date, studies of therapeutic resistance have almost exclusively focused on mechanisms involving tumor cells. Our findings provide evidence that there are substantial changes in tumor stroma associated with resistance in our models, and in fact a far greater number of stromal genes than tumor cell genes were significantly different in tumors with acquired resistance compared with vehicle controls. Pathway analysis implicated EGFR as a central pathway upregulated in resistant stroma. EGFR localization differed in the two models: in pericytes of highly “normalized” vessels (acquired resistance) and tumor endothelium (primary resistance). As expected, the addition of EGFR blockade reduced pericyte coverage in the acquired resistance model, and delayed the emergence of resistance.

Murine xenograft models such as those used in this study have several limitations, such as absence of an intact immune system, and it is likely that different types of tumors, or tumors growing in locations (e.g. lung), may employ different mechanisms. Nevertheless, taken as a whole, these findings have important scientific and clinical implications. They demonstrate that stromal mechanisms can play a role- perhaps, in some cases a dominant role- in impacting the responsiveness of a tumor. In this regard, it is worth noting that stromal cells typically comprise a minority of cells in a tumor, and that detecting

stromal-specific changes associated with resistance (for example, endothelial phosphoEGFR) requires methodologies different than those in typical clinical use. The results also highlight a previously unappreciated role for stromal EGFR in therapeutic resistance, and illustrate that EGFR may play different roles in stroma depending on the cellular context. Effects on stromal cells may therefore contribute to the clinical benefit observed in patients treated with EGFR inhibitors even when tumors were negative for EGFR by IHC (62) or FISH (63), or did not contain activating mutations (64). Finally, they suggest that approaches targeting stromal resistance pathways may enhance the efficacy of regimens containing VEGF inhibitors. It is worth noting, however, that while combinations of VEGF and EGFR pathway inhibition have shown promise in NSCLC (65, 66), therapeutic resistance nevertheless continues to emerge, indicating that additional resistance mechanisms remain to be uncovered.

## Materials and Methods

### *In Vivo* Studies

All animal studies reported were approved from the local committee for animal care. To generate tumor xenografts, A549 and H1975 tumor cells ($2.0 \times 10^6$) were injected in 100 μl of HBSS into the subcutaneous flank of 4 to 8 weeks old male athymic nude mice (NCI-nu). Body weights and tumor volumes were recorded twice weekly. Tumor volumes ($mm^3$) were calculated as = $\pi/6(a)^2(b)$, where *a* is the smaller measurement of the tumor and *b* is the larger one. When the tumor volumes reached an average of approximately 270 $mm^3$, mice were

randomly assigned to one of six treatment groups: (a) control intraperitoneal (i.p.) injection of vehicle (PBS) twice weekly; (b) i.p. injection of BV (10 mg/kg) twice weekly; (c) control, oral (p.o.) administration of vehicle daily; (d) erlotinib (100 mg/kg) p.o. daily; (e) erlotinib p.o. daily plus BV i.p. twice weekly; (f) vandetanib (50 mg/kg) p.o. daily. Tumors were sacrificed due to tumor burden. Tumors were excised and one portion was fixed in formalin and embedded in paraffin; another portion was embedded in OCT (Miles, Inc., Elkhart, IN) and rapidly frozen in liquid nitrogen. Additional tumor sections for molecular studies were snap-frozen in liquid nitrogen. Staining with hematoxylin and eosin (H&E) was used to confirm the presence of tumor in each sample included in the analysis. For short-term treatment studies, tumor-bearing animals were treated for 2 weeks with vehicle and BV and then sacrificed. Tumor tissues were collected for immunohistochemical studies.

**RNA Microarray Analysis**

Total RNA was extracted from snap-frozen tissues using the *mir*Vana™ miRNA Isolation Kit (Ambion, Austin, TX) and 1 µg of total RNA was amplified using the Illumina® TotalPrep RNA Amplification Kit (Ambion) according to the manufacturer's instructions. Labeled cRNA was hybridized on mouseWG-6 v2 and human WG-6v3 Expression BeadChips (Illumina®, San Diego, CA) for analysis of murine and human transcriptomes. Signal intensities determined by streptavidin-Cy3 fluorescence were scanned with a Sherlock_1000 Array Scanner (Ambion). Data were analyzed using the BRB-ArrayTools Version 3.7.0

Beta platform developed by Dr. Richard Simon [http://linus.nci.nih.gov./BRB-ArrayTools.html]. A log base 2 transformation was applied to the data set prior to data normalization. A median array was selected as the reference array for normalization and statistical significance was set using a $p<0.01$. To evaluate the expression of genes involved in response to hypoxia, lymphangiogenesis and angiogenesis in BV-resistant xenografts compared with controls, a gene list of 269 genes used in previous publications and associated with and involved in these processes and was compared (67). Genes differentially expressed between groups were determined applying univariate t-test with estimation of the false discovery rate (FDR). Genes were determined using selection criteria of a $p<0.005$ and a fold-change ≥1.5.

**Determination of Microvessel Density (MVD), vessel tortuosity and pericyte coverage of tumor-associated blood vessels**

Tumor MVD was determined as previously described (68). In brief, we examined tumors microscopically to identify hot spots by low magnification (x100), and the mean MVD was quantified as the total number of $CD31^+$ structures observed in a minimum of five microscopic fields at higher power of vision per tumor (x200). For each group, tumors from four different mice receiving short- and long-term treatment were used. As previously described (69), the tortuosity (T) of blood vessel was defined as $T = (L/S)-1$, where L is the length of the vessel of interest and S is the straight-line distance between its endpoints. The vessel length (L)

was evaluated in 4 samples for each treatment group by tracing along the midline of the blood vessels that showed up in a longitudinal cut within an image (100x) and the number of pixels was converted into distance in millimeters with Image J v1.34 software (NIH).

To determine the extent of pericyte coverage on the tumor vasculature, tumor sections were stained for CD31 (red) and desmin (green) as described above. Five fields in each tumor were randomly identified at original magnification x200, and those blood vessels that were at least 50% covered by green-desmin positive cells were considered to be positive for pericyte coverage.

**Standard Methods**

Reagents, tumor cell lines and conditions, and standard techniques for qRT-PCR, IHC, confocal microscopy and LSC are described in the Supplemental Data.

**Plasma bFGF Concentration Analysis**

Basic FGF levels were measured in the plasma of tumor-bearing animals by multiplex bead assay (BioRad, Hercules, CA; Millipore, Billerica, MA) in a 96-well plate according to the manufacturer's protocol. The concentrations were calculated based on a standard curve derived by performing six serial dilutions of

a protein standard in assay diluent. Plasma samples were tested in duplicate and the mean value used for analysis.

**Statistics**

Statistical significance was tested using GraphPad Prism 5 software (GraphPad Software Inc., San Diego, CA). For comparison between two groups, Student's t test and log-rank test were used. A p value $< 0.05$ on two-tailed testing was considered significant.

**Supplemental Data**

The Supplemental Data include Supplemental Experimental Procedures, 2 supplemental tables and 4 supplemental figures.

**ACKNOWLEDGMENTS**

This study was supported in part by the Department of Defense BATTLE W81XWH-06-1-0303, Department of Defense PROSPECT award W81XWH-07-1-03060, the University of Texas Southwestern Medical Center, The University of Texas M. D. Anderson Cancer Center Lung SPORE NIH grant P50 CA070907, and research support from AstraZeneca Cross Alliance. J.V. Heymach is a Damon Runyon-Lilly Clinical Investigator supported in part by Damon Runyon

Cancer Research Foundation grant CI 24-04 and is also supported by the Physician Scientist Program at M. D. Anderson Cancer Center. We gratefully acknowledge Dr. Michael Worley for editing the manuscript, Drs. Anderson Ryan, Juliane Jürgensmeier, and Lee Ellis for helpful scientific discussions, and AstraZeneca (Macclesfield, United Kingdom) for providing vandetanib. Research in the laboratory of Fortunato Ciardiello is supported by a grant from the Associazione Italiana per la Ricerca sul Cancro (AIRC).

## References


1. Folkman, J., and Shing, Y. 1992. Angiogenesis. *J Biol Chem* 267:10931-10934.
2. Folkman, J. 1971. Tumor angiogenesis: therapeutic implications. *N Engl J Med* 285:1182-1186.
3. Carmeliet, P., and Jain, R.K. 2000. Angiogenesis in cancer and other diseases. *Nature* 407:249-257.
4. Hanahan, D., and Folkman, J. 1996. Patterns and emerging mechanisms of the angiogenic switch during tumorigenesis. *Cell* 86:353-364.
5. Ferrara, N., Gerber, H.P., and LeCouter, J. 2003. The biology of VEGF and its receptors. *Nat Med* 9:669-676.
6. Ferrara, N., and Davis-Smyth, T. 1997. The biology of vascular endothelial growth factor. *Endocr Rev* 18:4-25.
7. Ellis, L.M., and Hicklin, D.J. 2008. VEGF-targeted therapy: mechanisms of anti-tumour activity. *Nat Rev Cancer* 8:579-591.
8. Kerbel, R.S. 2008. Tumor angiogenesis. *N Engl J Med* 358:2039-2049.
9. Jain, R.K., di Tomaso, E., Duda, D.G., Loeffler, J.S., Sorensen, A.G., and Batchelor, T.T. 2007. Angiogenesis in brain tumours. *Nat Rev Neurosci* 8:610-622.
10. Ferrara, N., Hillan, K.J., Gerber, H.P., and Novotny, W. 2004. Discovery and development of bevacizumab, an anti-VEGF antibody for treating cancer. *Nat Rev Drug Discov* 3:391-400.
11. Dvorak, H.F. 2002. Vascular permeability factor/vascular endothelial growth factor: a critical cytokine in tumor angiogenesis and a potential target for diagnosis and therapy. *J Clin Oncol* 20:4368-4380.
12. Nilsson, M., and Heymach, J.V. 2006. Vascular endothelial growth factor (VEGF) pathway. *J Thorac Oncol* 1:768-770.
13. Sandler, A., Gray, R., Perry, M.C., Brahmer, J., Schiller, J.H., Dowlati, A., Lilenbaum, R., and Johnson, D.H. 2006. Paclitaxel-carboplatin alone or with bevacizumab for non-small-cell lung cancer. *N Engl J Med* 355:2542-2550.
14. Kopetz, S., Hoff, P.M., Morris, J.S., Wolff, R.A., Eng, C., Glover, K.Y., Adinin, R., Overman, M.J., Valero, V., Wen, S., et al. Phase II Trial of Infusional Fluorouracil, Irinotecan, and Bevacizumab for Metastatic Colorectal Cancer: Efficacy and Circulating Angiogenic Biomarkers Associated With Therapeutic Resistance. *J Clin Oncol* 28:453-459.
15. Casanovas, O., Hicklin, D.J., Bergers, G., and Hanahan, D. 2005. Drug resistance by evasion of antiangiogenic targeting of VEGF signaling in late-stage pancreatic islet tumors. *Cancer Cell* 8:299-309.
16. Yu, J.L., Rak, J.W., Coomber, B.L., Hicklin, D.J., and Kerbel, R.S. 2002. Effect of p53 status on tumor response to antiangiogenic therapy. *Science* 295:1526-1528.
17. Davis, D.W., Takamori, R., Raut, C.P., Xiong, H.Q., Herbst, R.S., Stadler, W.M., Heymach, J.V., Demetri, G.D., Rashid, A., Shen, Y., et al. 2005. Pharmacodynamic analysis of target inhibition and endothelial cell death in tumors treated with the vascular endothelial growth factor receptor antagonists SU5416 or SU6668. *Clin Cancer Res* 11:678-689.

18. Heymach, J.V., Desai, J., Manola, J., Davis, D.W., McConkey, D.J., Harmon, D., Ryan, D.P., Goss, G., Quigley, T., Van Den Abbeele, A.D., et al. 2004. Phase II Study of the Antiangiogenic Agent SU5416 in Patients with Advanced Soft Tissue Sarcomas. *Clin Cancer Res* 10:5732-5740.
19. Paez-Ribes, M., Allen, E., Hudock, J., Takeda, T., Okuyama, H., Vinals, F., Inoue, M., Bergers, G., Hanahan, D., and Casanovas, O. 2009. Antiangiogenic therapy elicits malignant progression of tumors to increased local invasion and distant metastasis. *Cancer Cell* 15:220-231.
20. Naumov, G.N., Nilsson, M.B., Cascone, T., Briggs, A., Straume, O., Akslen, L.A., Lifshits, E., Byers, L.A., Xu, L., Wu, H.K., et al. 2009. Combined Vascular Endothelial Growth Factor Receptor and Epidermal Growth Factor Receptor (EGFR) Blockade Inhibits Tumor Growth in Xenograft Models of EGFR Inhibitor Resistance. *Clin Cancer Res* 15:3484-3494.
21. Kobayashi, S., Boggon, T.J., Dayaram, T., Janne, P.A., Kocher, O., Meyerson, M., Johnson, B.E., Eck, M.J., Tenen, D.G., and Halmos, B. 2005. EGFR mutation and resistance of non-small-cell lung cancer to gefitinib. *N Engl J Med* 352:786-792.
22. Pao, W., Wang, T.Y., Riely, G.J., Miller, V.A., Pan, Q., Ladanyi, M., Zakowski, M.F., Heelan, R.T., Kris, M.G., and Varmus, H.E. 2005. KRAS mutations and primary resistance of lung adenocarcinomas to gefitinib or erlotinib. *PLoS Med* 2:e17.
23. Jain, R.K. 2005. Normalization of tumor vasculature: an emerging concept in antiangiogenic therapy. *Science* 307:58-62.
24. Batchelor, T.T., Sorensen, A.G., di Tomaso, E., Zhang, W.T., Duda, D.G., Cohen, K.S., Kozak, K.R., Cahill, D.P., Chen, P.J., Zhu, M., et al. 2007. AZD2171, a pan-VEGF receptor tyrosine kinase inhibitor, normalizes tumor vasculature and alleviates edema in glioblastoma patients. *Cancer Cell* 11:83-95.
25. Greenberg, J.I., and Cheresh, D.A. 2009. VEGF as an inhibitor of tumor vessel maturation: implications for cancer therapy. *Expert Opin Biol Ther* 9:1347-1356.
26. Jain, R.K. 2001. Normalizing tumor vasculature with anti-angiogenic therapy: A new paradigm for combination therapy. *Nat Med* 7:987-989.
27. Boehm, T., Folkman, J., Browder, T., and O'Reilly, M.S. 1997. Antiangiogenic therapy of experimental cancer does not induce acquired drug resistance. *Nature* 390:404-407.
28. Kerbel, R.S. 1991. Inhibition of tumor angiogenesis as a strategy to circumvent acquired resistance to anti-cancer therapeutic agents. *Bioessays* 13:31-36.
29. Heymach, J.V., Paz-Ares, L., De Braud, F., Sebastian, M., Stewart, D.J., Eberhardt, W.E., Ranade, A.A., Cohen, G., Trigo, J.M., Sandler, A.B., et al. 2008. Randomized phase II study of vandetanib alone or with paclitaxel and carboplatin as first-line treatment for advanced non-small-cell lung cancer. *J Clin Oncol* 26:5407-5415.
30. Broxterman, H.J., Lankelma, J., and Hoekman, K. 2003. Resistance to cytotoxic and anti-angiogenic anticancer agents: similarities and differences. *Drug Resist Updat* 6:111-127.
31. Kerbel, R.S., Yu, J., Tran, J., Man, S., Viloria-Petit, A., Klement, G., Coomber, B.L., and Rak, J. 2001. Possible mechanisms of acquired resistance to anti-

angiogenic drugs: implications for the use of combination therapy approaches. *Cancer Metastasis Rev* 20:79-86.

32. Ellis, L.M., and Hicklin, D.J. 2008. Pathways mediating resistance to vascular endothelial growth factor-targeted therapy. *Clin Cancer Res* 14:6371-6375.
33. Heymach, J.V., Sledge, G.W., and Jain, R.K. 2010. Tumor Angiogenesis. In *Holland-Frei Cancer Medicine 8*. W.K. Hong, R.C. Bast Jr., W.N. Hait, D.W. Kufe, R.E. Pollock, R.R. Weichselbaum, J.F. Holland, and E. Frei III, editors. Hamilton: BC Decker.
34. Ferrara, N. 2009. Pathways mediating VEGF-independent tumor angiogenesis. *Cytokine Growth Factor Rev*.
35. Crawford, Y., and Ferrara, N. 2009. Tumor and stromal pathways mediating refractoriness/resistance to anti-angiogenic therapies. *Trends Pharmacol Sci* 30:624-630.
36. Ebos, J.M., Lee, C.R., and Kerbel, R.S. 2009. Tumor and host-mediated pathways of resistance and disease progression in response to antiangiogenic therapy. *Clin Cancer Res* 15:5020-5025.
37. Shojaei, F., Wu, X., Malik, A.K., Zhong, C., Baldwin, M.E., Schanz, S., Fuh, G., Gerber, H.P., and Ferrara, N. 2007. Tumor refractoriness to anti-VEGF treatment is mediated by CD11b+Gr1+ myeloid cells. *Nat Biotechnol* 25:911-920.
38. Crawford, Y., Kasman, I., Yu, L., Zhong, C., Wu, X., Modrusan, Z., Kaminker, J., and Ferrara, N. 2009. PDGF-C mediates the angiogenic and tumorigenic properties of fibroblasts associated with tumors refractory to anti-VEGF treatment. *Cancer Cell* 15:21-34.
39. Roland, C.L., Dineen, S.P., Lynn, K.D., Sullivan, L.A., Dellinger, M.T., Sadegh, L., Sullivan, J.P., Shames, D.S., and Brekken, R.A. 2009. Inhibition of vascular endothelial growth factor reduces angiogenesis and modulates immune cell infiltration of orthotopic breast cancer xenografts. *Mol Cancer Ther* 8:1761-1771.
40. Kim, K.J., Li, B., Winer, J., Armanini, M., Gillett, N., Phillips, H.S., and Ferrara, N. 1993. Inhibition of vascular endothelial growth factor-induced angiogenesis suppresses tumour growth in vivo. *Nature* 362:841-844.
41. Willett, C.G., Boucher, Y., di Tomaso, E., Duda, D.G., Munn, L.L., Tong, R.T., Chung, D.C., Sahani, D.V., Kalva, S.P., Kozin, S.V., et al. 2004. Direct evidence that the VEGF-specific antibody bevacizumab has antivascular effects in human rectal cancer. *Nat Med* 10:145-147.
42. Tong, R.T., Boucher, Y., Kozin, S.V., Winkler, F., Hicklin, D.J., and Jain, R.K. 2004. Vascular normalization by vascular endothelial growth factor receptor 2 blockade induces a pressure gradient across the vasculature and improves drug penetration in tumors. *Cancer Res* 64:3731-3736.
43. Lu, C., Thaker, P.H., Lin, Y.G., Spannuth, W., Landen, C.N., Merritt, W.M., Jennings, N.B., Langley, R.R., Gershenson, D.M., Yancopoulos, G.D., et al. 2008. Impact of vessel maturation on antiangiogenic therapy in ovarian cancer. *Am J Obstet Gynecol* 198:477 e471-479; discussion 477 e479-410.
44. Bergers, G., Song, S., Meyer-Morse, N., Bergsland, E., and Hanahan, D. 2003. Benefits of targeting both pericytes and endothelial cells in the tumor vasculature with kinase inhibitors. *J Clin Invest* 111:1287-1295.

45. Amin, D.N., Hida, K., Bielenberg, D.R., and Klagsbrun, M. 2006. Tumor endothelial cells express epidermal growth factor receptor (EGFR) but not ErbB3 and are responsive to EGF and to EGFR kinase inhibitors. *Cancer Res* 66:2173-2180.
46. Cheng, H., Langley, R.R., Wu, Q., Wu, W., Feng, J., Tsan, R., Fan, D., and Fidler, I.J. 2005. Construction of a novel constitutively active chimeric EGFR to identify new targets for therapy. *Neoplasia* 7:1065-1072.
47. Wu, W., O'Reilly, M.S., Langley, R.R., Tsan, R.Z., Baker, C.H., Bekele, N., Tang, X.M., Onn, A., Fidler, I.J., and Herbst, R.S. 2007. Expression of epidermal growth factor (EGF)/transforming growth factor-alpha by human lung cancer cells determines their response to EGF receptor tyrosine kinase inhibition in the lungs of mice. *Mol Cancer Ther* 6:2652-2663.
48. Kuwai, T., Nakamura, T., Sasaki, T., Kim, S.J., Fan, D., Villares, G.J., Zigler, M., Wang, H., Bar-Eli, M., Kerbel, R.S., et al. 2008. Phosphorylated epidermal growth factor receptor on tumor-associated endothelial cells is a primary target for therapy with tyrosine kinase inhibitors. *Neoplasia* 10:489-500.
49. Iivanainen, E., Lauttia, S., Zhang, N., Tvorogov, D., Kulmala, J., Grenman, R., Salven, P., and Elenius, K. 2009. The EGFR inhibitor gefitinib suppresses recruitment of pericytes and bone marrow-derived perivascular cells into tumor vessels. *Microvasc Res* 78:278-285.
50. di Tomaso, E., London, N., Fuja, D., Logie, J., Tyrrell, J.A., Kamoun, W., Munn, L.L., and Jain, R.K. 2009. PDGF-C induces maturation of blood vessels in a model of glioblastoma and attenuates the response to anti-VEGF treatment. *PLoS One* 4:e5123.
51. Pietras, K., Pahler, J., Bergers, G., and Hanahan, D. 2008. Functions of paracrine PDGF signaling in the proangiogenic tumor stroma revealed by pharmacological targeting. *PLoS Med* 5:e19.
52. Ostman, A., and Heldin, C.H. 2007. PDGF receptors as targets in tumor treatment. *Adv Cancer Res* 97:247-274.
53. Kandel, J., Bossy-Wetzel, E., Radvanyi, F., Klagsbrun, M., Folkman, J., and Hanahan, D. 1991. Neovascularization is associated with a switch to the export of bFGF in the multistep development of fibrosarcoma. *Cell* 66:1095-1104.
54. Paris, F., Fuks, Z., Kang, A., Capodieci, P., Juan, G., Ehleiter, D., Haimovitz-Friedman, A., Cordon-Cardo, C., and Kolesnick, R. 2001. Endothelial apoptosis as the primary lesion initiating intestinal radiation damage in mice. *Science* 293:293-297.
55. Karsan, A., Yee, E., Poirier, G.G., Zhou, P., Craig, R., and Harlan, J.M. 1997. Fibroblast growth factor-2 inhibits endothelial cell apoptosis by Bcl-2-dependent and independent mechanisms. *Am J Pathol* 151:1775-1784.
56. Zhang, X., and Lawler, J. 2007. Thrombospondin-based antiangiogenic therapy. *Microvasc Res* 74:90-99.
57. Wei, M.C., Zong, W.X., Cheng, E.H., Lindsten, T., Panoutsakopoulou, V., Ross, A.J., Roth, K.A., MacGregor, G.R., Thompson, C.B., and Korsmeyer, S.J. 2001. Proapoptotic BAX and BAK: a requisite gateway to mitochondrial dysfunction and death. *Science* 292:727-730.

58. Busser, B., Sancey, L., Josserand, V., Niang, C., Favrot, M.C., Coll, J.L., and Hurbin, A. 2009. Amphiregulin Promotes BAX Inhibition and Resistance to Gefitinib in Non-small-cell Lung Cancers. *Mol Ther*.
59. Giatromanolaki, A., Koukourakis, M.I., Sivridis, E., Turley, H., Talks, K., Pezzella, F., Gatter, K.C., and Harris, A.L. 2001. Relation of hypoxia inducible factor 1 alpha and 2 alpha in operable non-small cell lung cancer to angiogenic/molecular profile of tumours and survival. *Br J Cancer* 85:881-890.
60. Semenza, G.L. 2003. Targeting HIF-1 for cancer therapy. *Nat Rev Cancer* 3:721-732.
61. Franco, M., Man, S., Chen, L., Emmenegger, U., Shaked, Y., Cheung, A.M., Brown, A.S., Hicklin, D.J., Foster, F.S., and Kerbel, R.S. 2006. Targeted anti-vascular endothelial growth factor receptor-2 therapy leads to short-term and long-term impairment of vascular function and increase in tumor hypoxia. *Cancer Res* 66:3639-3648.
62. Chung, K.Y., Shia, J., Kemeny, N.E., Shah, M., Schwartz, G.K., Tse, A., Hamilton, A., Pan, D., Schrag, D., Schwartz, L., et al. 2005. Cetuximab shows activity in colorectal cancer patients with tumors that do not express the epidermal growth factor receptor by immunohistochemistry. *J Clin Oncol* 23:1803-1810.
63. Italiano, A., Follana, P., Caroli, F.X., Badetti, J.L., Benchimol, D., Garnier, G., Gugenheim, J., Haudebourg, J., Keslair, F., Lesbats, G., et al. 2008. Cetuximab shows activity in colorectal cancer patients with tumors for which FISH analysis does not detect an increase in EGFR gene copy number. *Ann Surg Oncol* 15:649-654.
64. Tsao, M.S., Sakurada, A., Cutz, J.C., Zhu, C.Q., Kamel-Reid, S., Squire, J., Lorimer, I., Zhang, T., Liu, N., Daneshmand, M., et al. 2005. Erlotinib in lung cancer - molecular and clinical predictors of outcome. *N Engl J Med* 353:133-144.
65. Natale, R.B., Bodkin, D., Govindan, R., Sleckman, B.G., Rizvi, N.A., Capo, A., Germonpre, P., Eberhardt, W.E., Stockman, P.K., Kennedy, S.J., et al. 2009. Vandetanib Versus Gefitinib in Patients With Advanced Non-Small-Cell Lung Cancer: Results From a Two-Part, Double-Blind, Randomized Phase II Study. *J Clin Oncol* 27:2523-2529.
66. Herbst, R.S., O'Neill, V.J., Fehrenbacher, L., Belani, C.P., Bonomi, P.D., Hart, L., Melnyk, O., Ramies, D., Lin, M., and Sandler, A. 2007. Phase II study of efficacy and safety of bevacizumab in combination with chemotherapy or erlotinib compared with chemotherapy alone for treatment of recurrent or refractory non small-cell lung cancer. *J Clin Oncol* 25:4743-4750.
67. Van den Eynden, G.G., Van Laere, S.J., Van der Auwera, I., Gilles, L., Burn, J.L., Colpaert, C., van Dam, P., Van Marck, E.A., Dirix, L.Y., and Vermeulen, P.B. 2007. Differential expression of hypoxia and (lymph)angiogenesis-related genes at different metastatic sites in breast cancer. *Clin Exp Metastasis* 24:13-23.
68. Weidner, N., Semple, J.P., Welch, W.R., and Folkman, J. 1991. Tumor angiogenesis and metastasis--correlation in invasive breast carcinoma. *N Engl J Med* 324:1-8.
69. Stockmann, C., Doedens, A., Weidemann, A., Zhang, N., Takeda, N., Greenberg, J.I., Cheresh, D.A., and Johnson, R.S. 2008. Deletion of vascular endothelial growth factor in myeloid cells accelerates tumorigenesis. *Nature* 456:814-818.

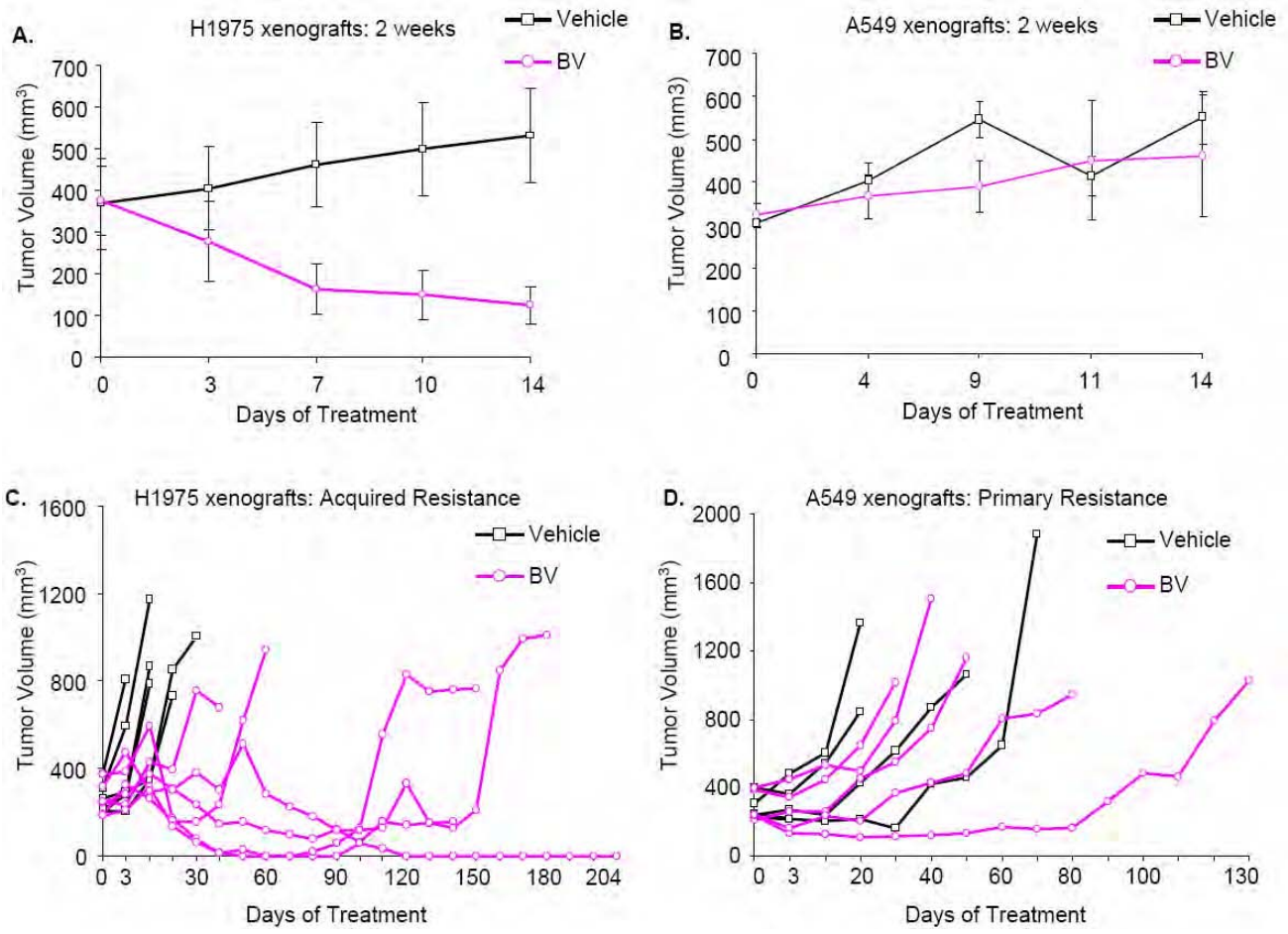


**Figure 1. H1975 and A549 NSCLC Xenografts Show Acquired and Primary Resistance to BV**

**A, B.** Tumor growth curves of H1975 xenografts receiving vehicle (control) and BV (n=5) for 2 weeks (short-term treatment).

**C, D**. Individual tumor growth curves of H1975 (A) and A549 (B) vehicle- and BV-treated xenografts. Vehicle- and BV-treated tumors are shown in black and pink, respectively. The median PFS in H1975 BV-resistant xenografts was 138 days compared with 7 days in the control group ($p<0.001$ BV vs. vehicle, log-rank test); in A549 BV-resistant tumors the median PFS was 35 days compared with 22 days in controls ($p=0.16$ BV vs. vehicle, log-rank test).

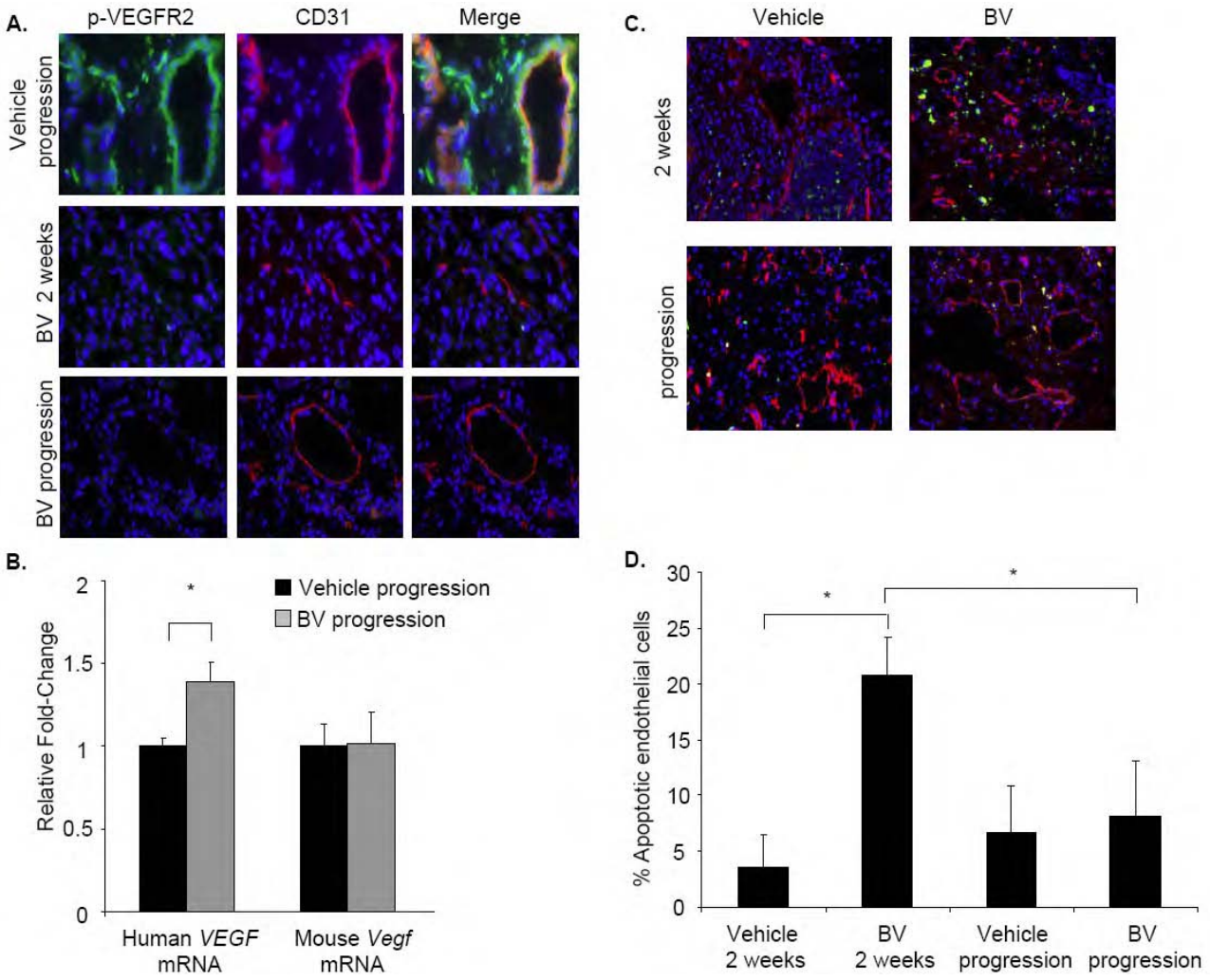


**Figure 2. BV Resistance Is Associated with Sustained p-VEGFR2 Inhibition and Decreased Endothelial Cell Apoptosis**

**A**. Representative IF staining of H1975 vehicle and BV-treated tumors for 2 weeks and at progression show p-VEGFR-2 (green) and $CD31^+$ cells (red). Blue shows the nuclei.

**B.** Human and mouse *VEGFA* mRNA expression in H1975 vehicle- and BV-treated tumors at progression using qRT-PCR (n=4, each group). Human *GAPDH* and mouse tubulin were used as housekeeping controls for human and mouse mRNA, respectively. Data were normalized relative to mRNA levels in vehicle-progression samples and are graphed as relative fold change ± SEM, *p<0.05 (t-test).

**C.** Representative immunofluorescent images of CD31 (red) and TUNEL (green) staining in H1975 xenografts after 2 weeks and at progression with vehicle and BV. Blue shows the nuclei.

**D.** Percentage of apoptotic ECs quantified by IF staining, labeling the endothelial marker CD31 and using the terminal TUNEL kit to identify apoptotic cells. The percentage of $CD31^+$ and $TUNEL^+$ cells was counted in a minimum of 5 microscopic fields (200×) in each of minimum 3 tumor samples per each group. Data are graphed as the percentage ± SEM, *p<0.05 (t-test).

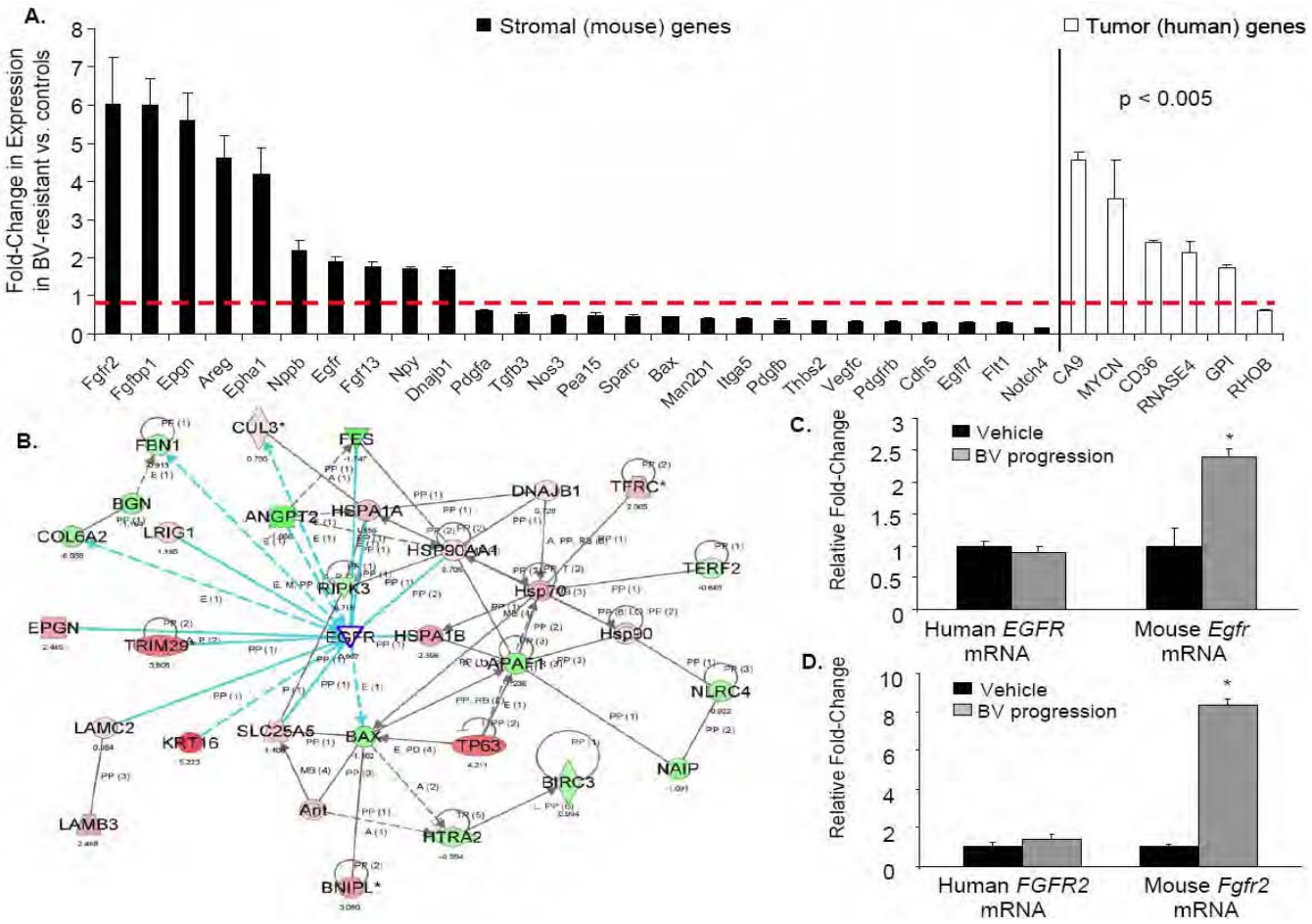


**Figure 3. BV Resistance Is Associated with Increased Expression of Stromal Genes Involved in Angiogenesis**

**A.** Stromal and human angiogenic genes differentially regulated in H1975 BV-resistant xenografts compared with vehicle-controls (n=3, each group). Two-sample t-test ($p<0.005$) with random variance model was applied. Exact permutation p-values for significant genes were computed based on 10 available permutations. Data are graphed as differences in fold change ± SEM of genes in BV-resistant tumors vs. controls. The dashed red line defines the fold change of gene expression at 1, indicating no changes in the expression of a specific gene in BV-resistant tumors vs. controls. **B.** Functional pathway analysis of selected genes and their interaction nodes in a gene network significantly modulated between the BV-resistant and control xenografts mouse stroma. The network score was calculated by the inverse log of the p-value and indicates the likelihood of focus genes in a network being found together than due to chance. The selected genes (*Egfr*, *Bax* and *Dnajb1*) and their interaction segments are highlighted by a blue border. Gene expression variation by at least 1.5-fold is depicted by color (red, upregulated; green, down-regulated; grey, no significant change). **C, D.** Human and mouse *EGFR* (C) and *FGFR2* (D) mRNA expression in H1975 vehicle- and BV- progression xenografts (n=4, each group) using qRT-PCR. Human *GAPDH* and mouse tubulin were used as housekeeping controls for human and mouse mRNA, respectively. Data are normalized relative to mRNA levels in vehicle-progression samples and graphed as relative fold change ± SEM, *$p<0.05$ (t-test).

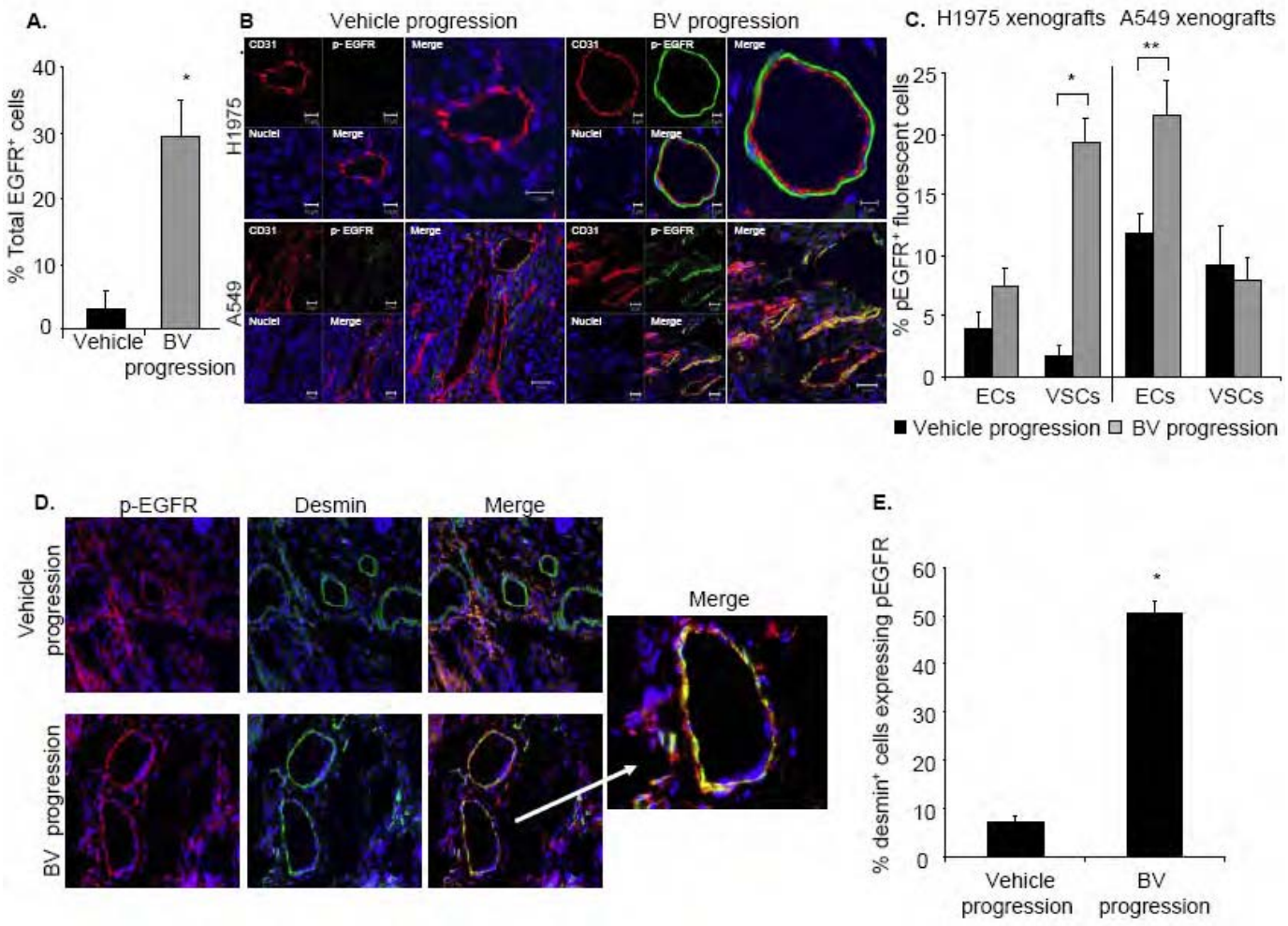


**Figure 4. BV Resistance Is Associated with Increased EGFR Activation on the Vascular Supporting Cells and the Tumor Vasculature**

**A.** Quantification of EGFR-expressing cells in H1975 tumors following vehicle and BV treatment at progression (n=4, each group), using LCS. Data are graphed as the mean ± SEM, *p<0.01 (t-test). **B.** Representative IF staining of CD31 (red) and p-EGFR (green) using confocal microscopy in vehicle- and BV-treated H1975 (top panel) and A549 xenografts (lower panel) at progression (n=4, each group in both xenograft models). **C.** Quantification of vascular supporting cells (VSCs) and endothelial cells ($CD31^+$, ECs) expressing p-EGFR in H1975 and A549 vehicle- and BV-treated tumors at progression (n=4, each group in both the xenograft models). Phospho-$EGFR^+$ cells were counted in a minimum of 5 random microscopic fields for each tumor sample at 200× magnification. Data are graphed as percentage ± SEM, *p<0.01, **p<0.05 (t-test). **D.** Representative immunofluorescent images of p-EGFR (red) and desmin (green) positive staining in H1975 vehicle- and BV-treated H1975 xenografts at progression. The white arrow shows the overlapping of p-EGFR and desmin in BV-resistant H1975 tumors at higher magnification (400×). **E.** Quantification of $desmin^+$ cells expressing p-EGFR in H1975 vehicle- and BV-treated H1975 tumors at progression. Phospho-$EGFR^+$ cells were counted in a minimum of 5 random microscopic fields for each tumor sample at 200× (n=4, each group). Data are graphed as percentage ± SEM, *p<0.01, (t-test).

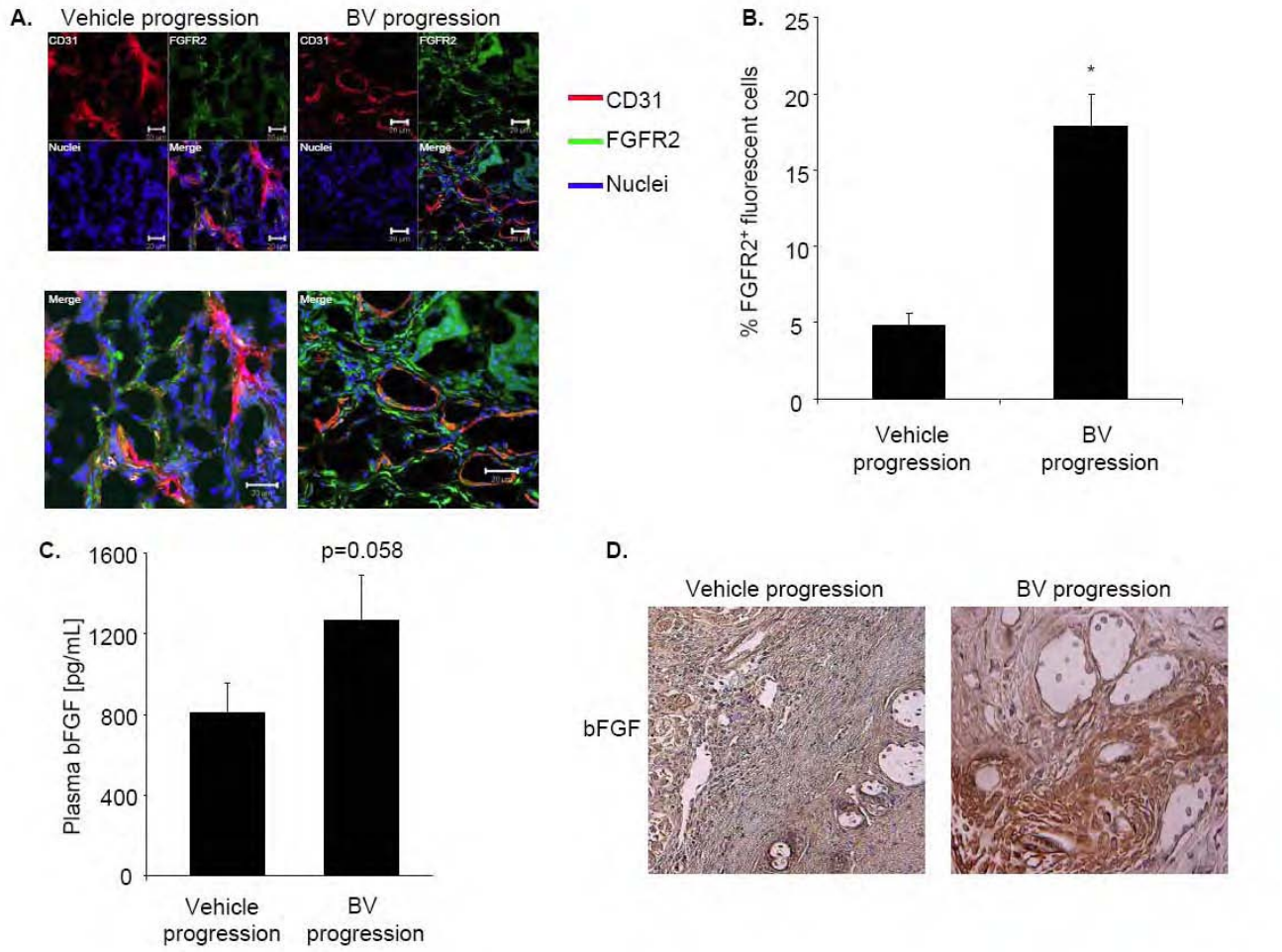


**Figure 5. Increase in Stromal FGFR2 Expression in H1975 BV-Resistant Xenografts**

**A.** Representative immunofluorescent images of CD31 (red) and FGFR2 (green) staining in H1975 vehicle- and BV-treated H1975 xenografts at progression, using confocal microscopy (200×).

**B.** Quantification of $FGFR2^+$ cells (green) counted in 5 random microscopic fields (200×; n=4, each group). Data are graphed as the percentage ± SEM, *p<0.01 (t-test).

**C.** Basic FGF (bFGF) levels (pg/mL) were measured in the plasma of vehicle- and BV-treated H1975 xenografts at progression, by multiplex bead assay. Data are graphed as the mean ± SEM, p=0.058 (t-test).

**D.** Representative IHC staining of bFGF in vehicle- and BV-treated H1975 tumors at time of progression (n=4, per each group).

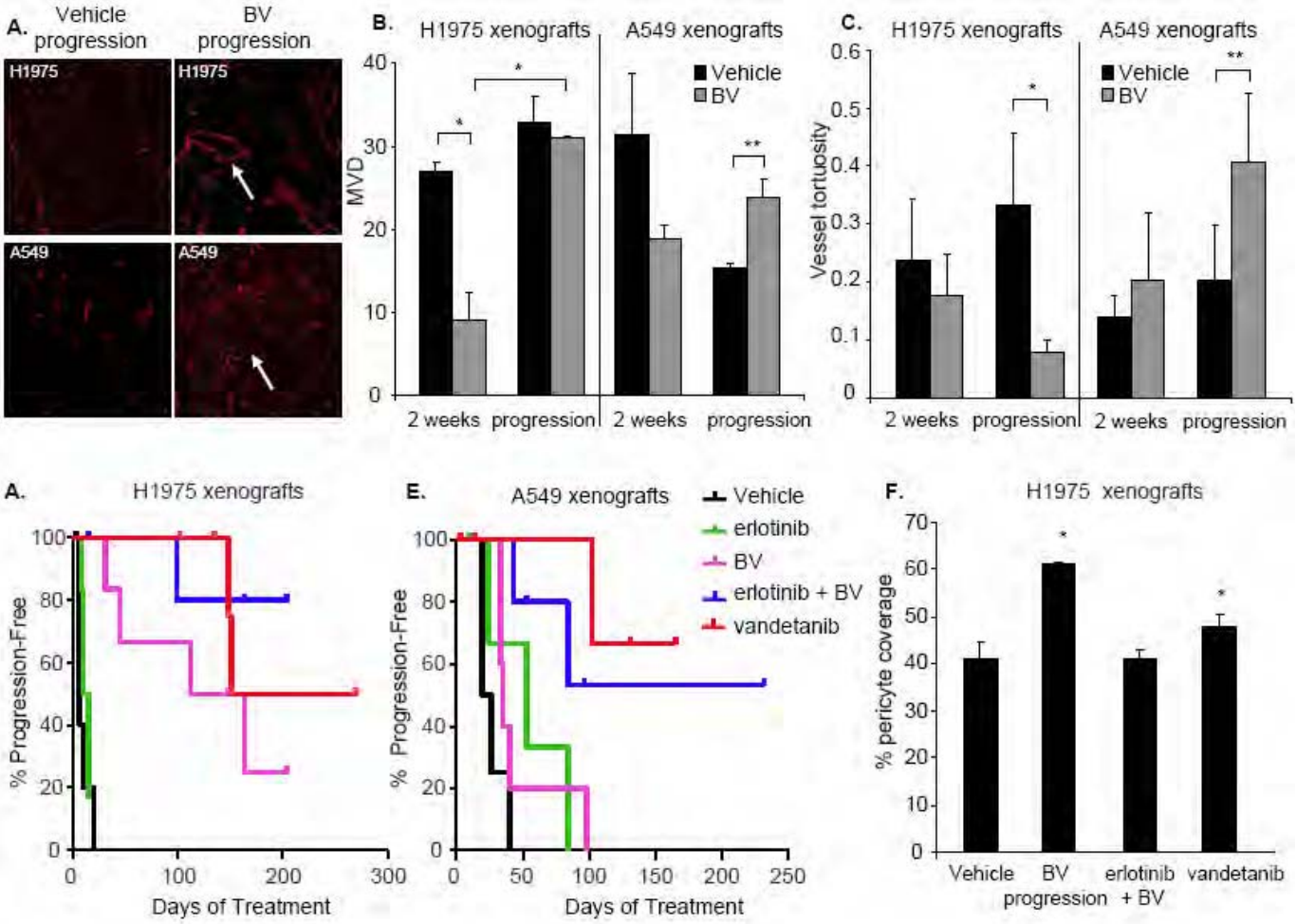


**Figure 6. Altered patterns of tumor vascular density, tortuosity, and pericyte coverage in BV-resistant tumors, and impact of combined EGFR/VEGFR inhibition**

**A.** $CD31^+$ staining (red) showing representative images of vasculature in H1975 (upper panel) and A549 (lower panel) tumors after short-term (2 weeks) treatment with BV and at progression.

**B, C.** Quantification of MVD (B) and tumor vessel tortuosity (C) in the same tumors. CD31+ vessels were counted in 5 microscopic fields in each of 4 samples per each group at 200×., shown as mean ± SEM, * $p<0.01$, ** $p<0.05$ (t-test).

**D, E.** Kaplan-Meier plots of PFS in H1975 (D) and A549 xenografts (E). H1975 xenografts: BV vs. vehicle $p<0.01$; BV vs. erlotinib $p<0.01$; erlotinib + BV vs. BV $p=0.24$, erlotinib + BV vs. vehicle $p<0.01$; vandetanib vs. BV $p=0.295$; vandetanib vs. vehicle $p<0.01$ (log-rank test). A549 xenografts: BV vs. vehicle $p = 0.16$; BV vs. erlotinib $p = 0.99$; erlotinib + BV vs. BV $p = 0.044$; erlotinib + BV vs. vehicle $p<0.01$ vandetanib vs. BV $p = 0.012$; vandetanib vs. vehicle $p = 0.015$ (log-rank test).

**F**. Pericyte coverage in H1975 xenografts. The percentage of $CD31^+$ vessels with at least 50% coverage of associated $desmin^+$ cells was counted in 5 microscopic fields at 200× in tumors that progressed on the indicated treatment (n=4, vehicle and BV groups; n=2, vandetanib group, and n=1, erlotinib + BV). Data are graphed as percentage ± SEM, *$p<0.05$ (t-test).

**D10.1 - Stromal HGF and VEGFR-1 are associated with acquired resistance to VEGFR tyrosine kinase inhibitors in non-small cell lung cancer (NSCLC)**
**Oral**
**Novel Therapeutics and Modalities**

T. Cascone, M. Herynk, D. Du, H. Kadara, E. Hanrahan, M. Nilsson, H.Y. Lin, J..J. Lee, Y.-Y. Park, J.-S. Lee, J.V. Heymach; Houston, TX/US

**Body**

Background: Tyrosine kinase inhbitors (TKIs) targeting vascular endothelial growth factor/receptor (VEGF/VEGFR) pathway, such as cediranib (AZD2171) and the dual VEGFR-2/EGFR inhibitor vandetanib (ZD6474) have demonstrated clinical benefit in NSCLC and other solid tumors. Unfortunately, while a subset of patients initially responds to these agents, therapeutic resistance inevitably emerges. The mechanisms underlying resistance are not well understood, but may include incomplete inhibition of VEGFR or EGFR activation, bypass of these pathways through redundant expression of proangiogenic molecules, a switch in stromal cell dependency from VEGFR activation to alternative signaling pathways or other mechanisms. Therefore, there is a critical need for tumoral and stromal molecular markers able to predict resistance to TKIs such as vandetanib and cediranib in NSCLC.Methods: To generate NSCLC xenograft models with acquired resistance to cediranib and vandetanib, A549 and H 1975 human NSCLC cells were injected in athymic nude mice. Tumors were considered resistant to treatments when their volumes tripled compared to the starting volume and were then sacrificed. A murine specific expression array (mouseWG-6 v2 Expression BeadChip, ILLUMINA) was used to evaluate changes in the stromal microenvironment to develop gene signatures indicative of therapeutic resistance in vandetanib and cediranib-resistant H1975 tumors compared to sensitive tumors (2 weeks of treatment) and vehicle treated controls. Differentially expressed genes between the different treatment groups were selected based on a $p<0.005$ of the univariate t-test and at least a 1.5 fold-change in expression.Results: H1975 NSCLC xenografts initially responded to treatment with vandetanib and 33% of treated tumors developed resistance after a median time to progression of 210 days in the vandetanib-treated group compared to 7 days in the control group ($p<0.001$). In cediranib-treated tumors, 60% of xenografts exhibited resistance after a median time to progression of 250 days following treatment. In A549 xenograft model, treatment with vandetanib induced resistance in only one tumor after 102 days. Cediranib-induced resistance was observed in two xenograft animals after 201 days of treatment. An up-regulation of stromal Hepatocyte growth factor (Hgf) ($p=0.001$) and Vegfr-1 ($p<0.001$) mRNA was observed in cediranib-resistant tumors, as compared to sensitive tumors. In addition, an increase in stromal Hgf mRNA was observed in vandetanib-resistant H1975 tumors ($p<0.001$) relative to sensitive tumors. These interesting data are in accordance with our previous analysis of clinical specimens from patients with stage IIIB/IV NSCLC who participated in a randomized Phase 2 trial that showed HGF as a predictive marker for resistance to vandetanib treatment alone when compared to chemotherapy alone or the combination of both ($p=0.004$).Conclusions: Our preliminary results identify HGF and VEGFR-1 as potential markers associated with acquired resistance to VEGFR TKIs in NSCLC, pointing to the HGF/MET axis and/or VEGFR-1 pathway as crucial therapeutic targets to overcome resistance to anti-angiogenic therapy in NSCLC.

Print this Page


Presentation Abstract

| | |
|---|---|
| Abstract Number: | 376 |
| Presentation Title: | Increased HGF is associated with resistance to VEGFR tyrosine kinase inhibitors (TKIs) in non-small cell lung cancer (NSCLC) |
| Presentation Time: | Sunday, Apr 18, 2010, 2:00 PM - 5:00 PM |
| Location: | Exhibit Hall A-C, Poster Section 13 |
| Poster Section: | 13 |
| Poster Board Number: | 13 |
| Author Block: | Tina Cascone[1], Matthew H. Herynk[1], Li Xu[1], Humam N. Kadara[1], Emer Hanrahan[1], You-Hong Fan[1], Babita Siagal[1], Yun-Yong Park[1], Ju-Seog Lee[1], Robert R. Langley[1], Juliane M. Jurgensmeier[2], Anderson Ryan[2], John V. Heymach[1]. [1]UT M.D. Anderson Cancer Ctr., Houston, TX; [2]AstraZeneca, Macclesfield, United Kingdom |
| Abstract Body: | Emergence of therapeutic resistance to angiogenesis inhibitors, the mechanisms of which are poorly understood, remains a major obstacle in treatment of NSCLC patients. Previously we reported that mechanisms governing resistance to anti-angiogenic therapy may involve both tumor and stromal cells in the tumor microenvironment. In this study we investigated potential mechanisms of resistance to the multi-tyrosine kinase inhibitors cediranib (AZD2171, Recentin®) and vandetanib (ZD6474, Zactima®) using NSCLC xenografts treated either for 2 weeks (sensitive tumors) or until resistance occurred. Quantification of $TUNEL^+$ staining using laser scanning cytometry (LSC) showed increased apoptosis in H1975 xenografts sensitive to cediranib ($p<0.01$) and vandetanib ($p<0.05$) when compared with controls, whereas no changes were noticed at time of resistance. Microvessel density (MVD) was significantly increased in resistant H1975 xenografts compared with controls ($p<0.05$) and sensitive tumors ($p<0.01$), whereas in A549 model, vandetanib-resistance was associated with an angiogenic independent phenotype. To investigate stromal mechanisms of Vascular Endothelial |

Growth Factor Receptor (VEGFR) TKI resistance, we characterized the stromal angiogenic gene expression profiles of H1975 sensitive and resistant tumors using a mouse-specific gene expression array (mouseWG-6 v2 Expression BeadChip, Illumina®). Differentially modulated genes were selected based on a $p<0.005$ of the univariate t-test and at least a 1.5 fold-change in expression and cross-referenced to defined list(s) of angiogenesis-related genes. Stromal *Hgf* (hepatocyte growth factor) was up-regulated in VEGFR TKI-resistant xenografts compared to sensitive tumors. *Hgf* up-regulation was confirmed at the protein level using immunofluorescent staining and confocal microscopy. HGF protein levels were strongly decreased after 2 weeks of treatment with cediranib and vandetanib ($p<0.01$), whereas a significant increase in HGF was observed in resistant xenografts ($p<0.01$). To assess whether HGF upregulation contributes to tumor resistance to TKIs, we implanted HGF-overexpressing and vector control HCC827 NSCLC cells into nude mice. In HCC827-vector control xenografts, cediranib inhibited tumor growth by 93%, whereas a 60% of growth inhibition was observed in HGF-overexpressing tumors. These data agree favorably with our previous analysis of clinical specimens from patients with stage IIIB/IV NSCLC that identified HGF as a predictive marker of resistance to vandetanib treatment alone when compared to chemotherapy or the combination of chemotherapy and vandetanib ($p=0.033$). Our results suggest that HGF up-regulation may resistance to VEGFR pathway inhibition and that the HGF/MET axis may represent a crucial target for NSCLCs that are resistant to anti-angiogenic therapy.

**American Association for Cancer Research**
**615 Chestnut St. 17th Floor**
**Philadelphia, PA 19106**

**Control/Tracking Number:** 10-LB-8642-AACR
**Activity:** Late Breaking
**Current Date/Time:** 2/11/2010 8:04:08 AM

# The BATTLE trial (Biomarker-integrated Approaches of Targeted Therapy for Lung Cancer Elimination): Personalizing therapy for lung cancer

**Short Title:**
Personalized lung cancer therapy

**Author Block:** *Edward S. Kim*, *Roy S. Herbst*, *J Jack Lee*, *George R. Blumenschein Jr.*, *Anne Tsao*, *Christine M. Alden*, *Ximing Tang*, *Suyu Liu*, *David J. Stewart*, *John V. Heymach*, *Hai T. Tran*, *Marshall E. Hicks*, *Jeremy Erasmus Jr.*, *Sanjay Gupta*, *Garth Powis*, *Scott M. Lippman*, *Ignacio I. Wistuba*, *Waun K. Hong*. University of Texas M. D. Anderson Cancer Center, Houston, TX

*Abstract:*
**Background**: Patients (pts) with chemorefractory non-small cell lung cancer (NSCLC) have few options for effective treatment. BATTLE is a hypothesis-driven prospective study that identifies biomarkers (BMs) to predict tumor response and thus may help select personalized therapy for lung cancer pts.
**Methods**: Pts enrolled in this phase II adaptively randomized study required fresh core needle biopsy specimens to test 11 BMs performed in our research lab from 4 NSCLC molecular pathways: *EGFR*, *KRAS*, and *BRAF* mutation (M) (by PCR), *EGFR* and *Cyclin D1* copy number (by FISH), and VEGF, VEGFR, 3 RXR receptors and Cyclin D1 (by IHC). Based on eligibility criteria and tumor BM analyses, pts were adaptively randomized into treatments: erlotinib (E) 150 mg qd; sorafenib (S) 400 mg bid; vandetanib (V) 300 mg qd; E 150 mg + bexarotene (B) 400 mg/m2 qd. Pts with prior E were randomized only between S and V. The primary endpoint was 8-week disease control (DC).
**Results**: From 11/06 to 10/09, 255 pts were randomized to E (59 pts), V (54 pts), EB (37 pts), S (105 pts). Demographics: Median age 62 yrs (26-84); male 54%; ECOG PS 0-1 86%, PS 2 14%; Caucasian 82%, Asian 5%, other 13%; never/former/current smokers 22%/69%/9%; adenocarcinoma 63% squamous cell 18%, NSCLC NOS 19%; prior E 45%, median prior therapies for metastatic NSCLC: 2 (range 1-9); prior brain metastases 33%. 244 pts were evaluable for 8 wk DC. All 11 BMs were assessable in 215 pts. Biopsy sites were lung 55%, liver/adrenal 19%, other 26%. Pneumothorax incidence was 11.5%, and 6.5% of pts had treatment-related grade 3-4 toxicity. *EGFR* status included M in 15%, FISH amplification (A) in 16% and high polysomy in 28%; Other BMs were *KRAS* M in 20%; VEGF/R2 staining in 83%; RXR alpha nuclear staining in 79%; Cyclin D1 staining in 53%. Overall DCR at 8 weeks was 46%, median overall survival (OS) was 9 months, 1 year survival was 39%, and progression-free survival (PFS) was 1.9 months. Better DC was seen with *EGFR* M for E (p=0.04); Cyclin D1 IHC positivity (IHC+) (p=0.011) and *EGFR* FISH A (p=0.006) for E + B; VEGFR2 IHC+ for V (p=0.05); and absence of *EGFR* M (p=0.012) or high polysomy (p=0.048) for S. Pts with both EGFR M and FISH A had 100% DC (n=6) with E and 0% DC (n=6) with S. Pts with *KRAS* M tended to respond better with S (8-wk DC 61%) compared to other three regimens (8-wk DC 32%) (P=0.11). Pts with mutant *KRAS* Cys amino acid (aa) substitution had worse OS (all pts) and PFS (S-treated pts) compared to pts with wild type or all other *KRAS* aa substitutions (p=0.015 and p=0.013).
**Conclusions:** BATTLE is the first completed biopsy-mandated study in pretreated NSCLC. Our pre-specified hypotheses regarding BMs and targeted treatment were confirmed. Identifying proper BMs for a favorable population is a step towards personalizing therapy. BATTLE establishes a new paradigm to investigate BMs and molecularly targeted treatments in lung cancer pts. DoD W81XWH-6-1-0303


**Joint ECCO 15 - 34TH ESMO Multidisciplinary Congress**
**BERLIN, 20 - 24 SEPTEMBER 2009**

This service is sponsored by GSK Oncology
gsk GlaxoSmithKline Oncology

**Abstract P-9174:** **Phase II study of everolimus plus erlotinib in previously treated patients with advanced non-small cell lung cancer (NSCLC)**

**Citation: European Journal of Cancer Supplements, Vol 7 No 2, September 2009, Page 558**

**J.C. Soria**[1], J. Bennouna[2], N. Leighl[3], F. Khuri[4], A.M. Traynor[5], B. Johnson[6], A. Kay[7], N. Blais[8], V. Jehl[9], V. Papadimitrakopoulou[10]

[1]*Institute Gustave Roussy, Medicine, Villejuif, France*
[2]*Centre René Gauducheau, Medical Oncology, Saint Herblain Cédex, France*
[3]*Princess Margaret Hospital, Haematology and Oncology, Toronto, Canada*
[4]*Emory University, Hematology, Atlanta, USA*
[5]*University of Wisconsin Carbone Comprehensive Cancer Center, Haematology, Madison, USA*
[6]*Dana Farber Cancer Institute, Lowe Center for Thoracic Oncology, Boston, USA*
[7]*Novartis Pharmaceuticals Corporation, Oncology, Florham Park, USA*
[8]*CHUM – Campus Notre Dame, Oncology, Montreal, Canada*
[9]*Novartis Pharma AG, Oncology, Basel, Switzerland*
[10]*University of Texas, Thoracic Head and Neck Medical Oncology, Houston, USA*

**Background:** Everolimus (RAD001) is an oral mTOR inhibitor that has been evaluated as monotherapy in a phase II study of NSCLC patients previously treated with platinum-based chemotherapy, with evidence of some activity (ASCO 2007, Abstract 7589). Erlotinib is an oral epidermal growth factor receptor-tyrosine kinase inhibitor that is approved as second-line therapy for advanced/metastatic NSCLC. The present phase I/II study is evaluating the combination of everolimus and erlotinib in patients with advanced NSCLC who had progressed after ≤2 prior chemotherapy regimens (NCT00456833). Phase I results were promising and establish a feasible dose of everolimus in combination with erlotinib (ASCO 2008, Abstract 8051).
**Materials and Methods:** This ongoing, randomized phase II study includes patients with advanced NSCLC whose disease progressed following ≤2 prior chemotherapy regimens. Other inclusion criteria are WHO performance status ≤1 and adequate liver and bone marrow function. Patients are randomized to receive erlotinib 150 mg/day orally or everolimus 5 mg/day plus erlotinib 150 mg/day orally until disease progression or unacceptable toxicity. Survival data will be collected every 2 months following the end of treatment until all patients discontinue from the study. The primary study endpoint is disease control rate (ie, the proportion of patients with stable disease or response at their 3-month evaluation). Other endpoints include overall response, progression-free survival safety, pharmacokinetics, and molecular markers.
**Results:** As of April 2009, 133 patients have been randomized, with 60 patients included in the planned interim analysis. Preliminary safety data suggest no new safety concerns with the combination of everolimus plus erlotinib.
**Conclusion:** The planned interim analysis of this trial is ongoing; full results of the

interim analysis will be presented at the meeting. Results of this study will provide useful data on the efficacy and safety of everolimus in combination with erlotinib in patients with advanced NSCLC who have received prior chemotherapy; there is an urgent need to improve treatment options for these patients.

**Acknowledgment:** This study is supported by Novartis Pharmaceuticals Corporation.

Print Close

**Development and testing of an mRNA expression signature correlated with the presence of *EGFR* mutations in non-small cell lung cancer**

Pierre Saintigny[1], Li Zhang[2], Luc Girard[6], You H. Fan[1], J. Jack Lee[3], Roy S. Herbst[1], Edward S. Kim[1], Kevin Coombes[3], George Blumenschein[1], Anne Tsao[1], David C Lam[7], William L Gerald[8], David G Beer[9], Xi Ming Tang[1], Scott M. Lippman[1], Li Mao[1,10], Waun Ki Hong[5], Ignacio Wistuba[4], John Minna[6], John V. Heymach[1]

**Authors' Affiliations:** Departments of [1]Thoracic/Head&Neck Medical Oncology, [2]Bioinformatics and Computational Biology, [3]Biostatistics and Applied Mathematics, [4]Pathology and the [5]Division of Cancer Medicine at The University of Texas M. D. Anderson Cancer Center, Houston, Texas; [6]The Hamon Center for Therapeutic Oncology Research and Departments of Internal Medicine and Pharmacology, University of Texas Southwestern Medical Center, Dallas, Texas; [7]Department of Medicine and Pathology, University of Hong-Kong, HKSAR; [8]Department of Pathology, Memorial Sloan-Kettering Cancer Center, New York, New York; [9]University of Michigan, Department of Surgery, Ann Arbor, Michigan; [10]Department of Oncology and Diagnostic Sciences, University of Maryland Dental School, Baltimore, Maryland.

**Grant Support:** Department of Defense PROSPECT W81XWH-07-1-03060 and BATTLE W81XWH-06-1-0303 awards, and University of Texas SPORE in Lung Cancer P50CA070907.

**Corresponding author:** John V. Heymach[1]

**Keywords:** non-small-cell lung cancer, adenocarcinoma, EGFR, oncogenic pathway, mutation, gene expression profiling, prediction.

**Abstract**

**Background and aim**: Oncogenically mutated epidermal growth factor receptor (EGFR) is a validated therapeutic target for non-small cell lung cancer (NSCLC) and activation of the EGFR signaling pathway by somatically acquired EGFR mutations is known to play a critical role in lung cancer development. Using multiple tumor datasets, our aims were to develop an EGFR mutation mRNA expression signature from human lung adenocarcinomas to aid in developing personalized medicine for targeting EGFR in NSCLC, to characterize the downstream events of EGFR signaling associated with EGFR mutation, and to determine if mRNA signatures associated with EGFR mutations in NSCLC lines were maintained in tumor specimens. **Material and methods**: We performed lung adenocarcinoma (N = 195) mRNA expression profiling using several microarray platforms and determined the presence of tumor EGFR mutations in by sequencing tumor cDNAs or DNAs and also performed similar studies on 53 NSCLC cell lines. The tumor sets were from University of Hong Kong, University of Michigan Comprehensive Cancer Center, Memorial Sloan Kettering Cancer Center, and The University of Texas M.D. Anderson Cancer Center (BATTLE I trial). In addition, gefitinib and erlotinib drug response phenotypes were performed on the NSCLC lines by *in vitro* testing. Training and testing sets and cross validation were used to test and evaluate the mRNA signature model. **Results**: We developed a 93 gene signature that was consistently associated with EGFR mutation in multiple different datasets including validation in the BATTLE I tumor set of chemotherapy refractory advanced stage NSCLCs. In addition, the EGFR mutation signature of NSCLC lines and tumors were preserved. In leave-one-out cross validation tests using the training set, the misclassification rate was found to be 23%. Prediction accuracy of the signature was further evaluated in 2 independent data sets using receiver operating characteristic curves. The area under the curve was 0.95 (p-value=2.2e-06) for the NSCLC cell lines set of 53 samples, and 0.67 (p-value=0.014) for 100 human tissue samples collected from our recent BATTLE (ES Kim, ASCO 2009) clinical trial in chemotherapy-refractory NSCLC patients. We also found that the

signature was correlated with drug sensitivity to erlotinib (R=-0.52, p-value=3.3e-04) and gefitinib (R=-0.59, p-value=3.2e-05) in the NSCLC cell lines. Furthermore, the signature was found to be associated with survival in the Director's Challenge dataset of 442 adenocarcinomas. Using gene set enrichment analysis (GSEA) we found gene sets associated with endocytosis and vesicle recycling to be upregulated in EGFR mutant tumors, while mitotic-related genes were down regulated. **Conclusion**: We have identified an EGFR mutation signature developed from human adenocarcinomas from previously-untreated NSCLC patients that was significantly associated with EGFR mutations in an independent cohort of chemotherapy-refractory NSCLC patients. This signature also provided prognostic information in resected lung adenocarcinomas. In addition, the gene signature identified in clinical samples was also associated with EGFR TKI response in NSCLC cell lines and identifies genes whose expression are altered in EGFR mutated tumors including those involved in endocytosis and mitosis. These data suggest that an EGFR mutation signature may provide predictive value and biological insights into EGFR inhibitor-responsive in lung adenocarcinomas.

Print this Page


Presentation Abstract

| | |
|---|---|
| Abstract Number: | 1981 |
| Presentation Title: | MYC downregulation and chemoresistance in non-small cell lung cancer (NSCLC): Evidence from the Biomarker-Based Approaches of Targeted Therapy for Lung Cancer Elimination (BATTLE) program |
| Presentation Time: | Monday, Apr 19, 2010, 2:00 PM - 5:00 PM |
| Location: | Exhibit Hall A-C, Poster Section 1 |
| Poster Section: | 1 |
| Poster Board Number: | 4 |
| Author Block: | Pierre Saintigny[1], Lauren A. Byers[1], Li Zhang[1], John S. Yordy[1], Xi M. Tang[1], Luc Girard[2], Wenhua Lang[1], You H. Fan[1], Lin Ji[1], Jack J. Lee[1], Edward S. Kim[1], Waun K. Hong[1], Scott M. Lippman[1], Roy E. Herbst[1], John Minna[2], Ignacio I. Wistuba[1], John V. Heymach[1], Li Mao[1]. [1]UT M.D. Anderson Cancer Ctr., Houston, TX; [2]UT Southwestern Medical Center, Dallas, TX |
| Abstract Body: | Background: Primary or acquired resistance to platinum-based therapy remains an important issue in the treatment of unresectable non-small cell lung cancer (NSCLC). Our objective was to identify factors of resistance to platinum-based therapy. Experimental procedures: Gene expression profiling from the BATTLE program (pretreated resistant tumors stage III/IV, N=32) and a control group from 2 independent publicly available datasets (never treated tumors stage III/IV, N=45) were compared. Gene expression profiling was generated using the same platform (U133 Plus 2.0 Array). Pathway and gene set analyses were used to define networks and pathways associated with resistance. For validation, we used: i-an independent set of 38 never treated NSCLC stage III/IV, ii-a set of 53 NSCLC cell lines tested for cisplatin sensitivity with proteomic profiling generated by Reverse Phase Protein Array (RPPA) technology using 177 well-characterized antibodies, iii-the comparison of two pairs of NSCLC cell lines (H1437, H460) that were made resistant by iterative exposure to cisplatin, and iv-transfection experiments. Results: A total of 3,963 probesets were found to be differentially expressed between |

BATTLE samples and the control group with a p-value < 0.001 (two-tailed t-test). DNA repair gene sets were upregulated in BATTLE samples compared to never treated tumors. Network analysis found that MYC as well as many of its downstream regulated genes were significantly downregulated in BATTLE samples. In particular, a high proportion of MYC target genes associated with apoptosis were downregulated. Using real time PCR, MYC gene expression was significantly lower in 15 BATTLE samples compared with an independent set of 38 never treated stage III/IV NSCLC (p-value=0.01). The proteomic profiling of 53 NSCLC cell lines showed that MYC expression was one of the top proteins associated with sensitivity to cisplatin. An inverse correlation was observed between sensitivity to cisplatine (IC50) and MYC protein expression evaluated by RPPA (total MYC: r=-0.41, p-value=0.003; phosphorylated MYC: r=-0.30, p-value=0.03). MYC gene expression by real time PCR was lower in resistant H1437 and H460 cell lines compared to parental cell lines. Finally, transfection of H226 cell lines with a vector expressing MYC improved sensitivity to cisplatin compared to the control. Conclusion: This is the first gene expression profiling analysis of NSCLC samples pretreated and resistant to chemotherapy included in a prospective clinical trial. MYC down regulation may play an important role in NSCLC resistance to platinum-based chemotherapy. Mechanisms of MYC down regulation should be further explored.

**American Association for Cancer Research**
**615 Chestnut St. 17th Floor**
**Philadelphia, PA 19106**